

# State sum models with defects based on spherical fusion categories

Catherine Meusburger

Department Mathematik  
Friedrich-Alexander-Universität Erlangen-Nürnberg  
Cauerstraße 11, 91058 Erlangen, Germany  
Email: catherine.meusburger@math.uni-erlangen.de

May 13, 2022

## Abstract

We define a Turaev-Viro-Barrett-Westbury state sum model of triangulated 3-manifolds with surface, line and point defects. Surface defects are oriented embedded 2d PL submanifolds and are labeled with bimodule categories over spherical fusion categories with bimodule traces. Line and point defects form directed graphs on these surfaces and labeled with bimodule functors and bimodule natural transformations. The state sum is based on generalised 6j symbols that encode the coherence isomorphisms of the defect data. We prove the triangulation independence of the state sum and show that it can be computed in terms of polygon diagrams that satisfy the cutting and gluing identities for polygon presentations of oriented surfaces. By computing state sums with defect surfaces, we show that they detect the genus of a defect surface and are sensitive to its embedding. We show that defect lines on defect surfaces with trivial defect data define ribbon invariants for the centre of the underlying spherical fusion category.

## Introduction

Turaev-Viro-Barrett-Westbury state sums were introduced in [TV92, BW96] and define invariants of 3-manifolds and topological quantum field theories (TQFTs). They are also of interest from the physics perspective, since they arise in the quantisation of Chern-Simons and BF theories and have applications in topological quantum computing. In particular, it was established by Balsam and Kirillov in [BK12, Kr11] that they are closely related to two condensed matter physics models for topological quantum computers, namely Kitaev's quantum double model [Ki03] and Levin-Wen models [LW05].

Introducing defects in these models is natural in this physics context. Early work on specific line and point defects in Turaev-Viro-Barrett-Westbury state sums by Karowski and Schrader [KS93] and by Barrett et al. [BMG07] was motivated by the wish to introduce observables. In models from condensed matter physics it is also natural to study codimension one defects as domain walls. Introducing defects in these models amounts to labeling distinguished submanifolds with higher categorical data that relates the categorical data outside the defects. The general algebraic data for defects of all codimensions in Levin-Wen models was identified by Kitaev and Kong [KK12] and coincides largely with the defect data in this article.

From the mathematics perspective the introduction of defects in Turaev-Viro-Barrett-Westbury state sums is of interest as a concrete model for defect TQFTs, in which the usual cobordism category is replaced with a decorated cobordism category that involves distinguished submanifolds of various codimensions. A general formalism and concrete examples of defect TQFTs were developed by Carqueville et al. [CRS18, CRS19, CMS20]. However, these are not constructed as state sum models, but from a cobordism category.

State sum models that extend Turaev-Viro TQFTs and involve defect lines decorated by the centre of a spherical fusion category were defined by Turaev and Virelizier [TV10, TV17] and by Balsam and Kirillov in [KB10, B10]. More recently, Fuchs et al. [FSS19] gave a state sum construction for a modular functor with bimodule categories over finite tensor categories and Lee and Yetter [LY20] defined a triangulation independent state sum with defect surfaces. However, the categorical defect data in [LY20] differs from the data in the other publications and should be thought of as additional structure, as pointed out in [LY20].

Thus, a Turaev-Viro-Barrett-Westbury style state sum model with defects of all codimensions labeled by bimodule categories, functors and natural transformations is still missing. In this article we define such a state sum model and prove its triangulation independence. The model generalises the usual Turaev-Viro-Barrett-Westbury state sum, which is obtained by choosing trivial defect data.

## State sum model with defects

We consider three-dimensional PL manifolds  $M$ , possibly with boundary. Defect surfaces are embedded oriented PL surfaces with compact boundary contained in  $\partial M$ . Defect lines and points form directed graphs on these surfaces, whose edges may end on  $\partial M$ .

Regions outside the defects are assigned spherical fusion categories. Oriented defect surfaces are assigned finite semisimple bimodule categories with bimodule traces, oriented defect lines bimodule functors and defect vertices bimodule natural transformations.

Bimodule traces were introduced by Schaumann in [S13, S15], where it was shown that for fixed spherical fusion categories, bimodule categories with bimodule traces, bimodule functors and bimodule natural transformations form a pivotal 2-category. The restriction to finite semisimple bimodule categories with bimodule traces is motivated by the fact that semisimplicity, summation over simple objects and the existence of traces are essential ingredients in the usual Turaev-Viro-Barrett-Westbury state sum. Although the latter can be generalised to pivotal fusion categories, see [TV10, TV17], we stick with the original formulation in terms of spherical fusion categories and 6j symbols and hence require bimodule traces.

The state sum is based on a triangulation of  $M$ , which is required at first to intersect defect surfaces, defect lines and defect vertices transversally and generically. This means each tetrahedron can intersect at most one defect surface, either in a triangle, whose vertices lie on three edges incident at a common vertex, or in a quadrilateral, whose vertices lie on two pairs of opposite edges. Defect vertices must be in the interior of tetrahedra and defect edges must intersect their faces transversally in the interior.

To define the state sum, one labels the edges of the triangulation with simple objects, either in a spherical fusion category, if the edge does not intersect any defect surface, or in the bimodule category at its intersection point with a defect surface. This assigns to each labeled tetrahedron a generalised 6j symbol that is the 6j symbol for a spherical fusion category for a tetrahedron without defects. The state sum is then obtained by taking the product of the generalised 6j symbols of all tetrahedra and the dimensions of the simple objects at the internal edges, summing over all assignments of simple objects and over bases of the morphism spaces for its triangles and rescaling by the dimensions of the spherical fusion categories at the vertices.

## Generalised 6j symbols

The generalised 6j symbol for a tetrahedron depends on the simple objects assigned to its edges and the bimodule functors and natural transformation in its interior. By combining the latter with the morphisms assigned to its boundary triangles one obtains an endomorphism of a simple object in a bimodule category. The generalised 6j symbol is the trace of this endomorphism. It generalises the usual 6j symbols or F-matrices for spherical fusion categories and has a similar algebraic and geometric interpretation.

Just as the 6j symbols for a spherical fusion category encode its associator on its simple objects, the 6j symbols for a bimodule category encode the natural isomorphisms that describe its bimodule category structure. If a tetrahedron also contains defect lines or defect vertices, these coherence isomorphisms are combined with the coherence isomorphisms for the bimodule functors at the defect lines and with the bimodule natural transformations at the defect points.

The 6j symbols for a spherical fusion category relate the geometry of a tetrahedron to the diagrammatic calculus for a spherical fusion category. Their diagrams are obtained by taking the dual graph on the surface of the tetrahedron and labeling its edges and vertices with objects and morphisms in a spherical fusion category. The properties of a spherical fusion category imply that it has the symmetries of a tetrahedron.

Similarly, generalised 6j symbols for defect tetrahedra relate the geometry of a tetrahedron with defects to a diagrammatic calculus for bimodule categories, functors and natural transformations. Their diagrams are obtained by projecting the duals of those edges and triangles that do not intersect the defect surface on the defect surface. This yields a polygon with lines and vertices in its interior labeled by bimodule functors and natural transformations as well as objects and morphisms in spherical fusion categories. The diagrams also involve crossings labeled by coherence isomorphisms of bimodule categories and functors.

We develop a diagrammatic calculus for such polygon diagrams and define their evaluation. For a diagram obtained from a tetrahedron with defects, this is the generalised 6j symbol of the tetrahedron. As the presence of defects reduces the symmetries of a tetrahedron, generalised 6j symbols exhibit fewer symmetries than the 6j symbols of a spherical fusion category. Nevertheless, the associated polygon diagrams can be cut and glued by summing over simple objects and bases of the morphism spaces at their boundary.

**Theorem 1: (Theorem 3.1)** *Evaluations of polygon diagrams are invariant under rotations of the polygon. They satisfy the usual cutting and gluing identities for polygon presentations of oriented surfaces and an additional identity that allows one to cut and glue diagrams for spherical fusion categories in their interior.*

### Triangulation independence

With the cutting and gluing identities for polygon diagrams we prove that the state sum of a 3-ball bisected by a defect disc is the evaluation of the polygon diagram obtained by projecting the dual graph of the boundary triangulation on the defect disc. This is sufficient to establish invariance under bistellar moves that involve only transversal and generic tetrahedra.

To establish triangulation independence, we then refine the triangulations via stellar subdivisions, finite sequences of bistellar moves that involve only generic and transversal tetrahedra. The state sums can then be computed separately for neighbourhoods of the defect surfaces and for the regions between them. The latter are usual Turaev-Viro-Barrett-Westbury state sums. The former are given by polygon diagrams, but with additional summations over boundary labels that glue their sides pairwise. Combining them yields

**Theorem 2: (Theorem 5.16)** *If two transversal and generic triangulations of a 3-manifold with defect surfaces, defect lines and defect points agree at the boundary, their state sums are equal.*

This allows one to extend the definition of the state sum to triangulations that are non-generic or non-transversal in the interior of a 3-manifold via generic transversal subdivisions and establishes full triangulation independence for manifolds without boundaries.

### Examples

To illustrate the formalism and the properties of the state sum we treat a number of examples. We compute the state sum of a defect sphere in a 3-ball for general categorical data. We also compute state sums with defect surfaces of genus  $g \geq 1$ , but only for the simple categorical data underlying Dijkgraaf-Witten models [DW90]. Here, we consider spherical fusion categories  $\text{Vec}_G$  and  $\text{Vec}_{G'}$  of graded vector spaces over finite groups  $G, G'$ , equipped with trivial cocycles, and bimodule categories defined by finite transitive  $G \times G'^{op}$ -sets, also equipped with the trivial cocycle. For this data, it is simple to compute the state sums of a 3-manifold  $M = [0, 1] \times \Sigma$  and of a 3-ball with a defect surface  $\Sigma$  of general genus in the interior. This shows that the state sum detects properties of the bimodule categories labeling the defect surface as well as its genus.

We also compute the state sum for a 3-sphere with an embedded torus labeled by a trivial  $G$ -set and show that it gives the number of conjugacy classes of group homomorphisms from the fundamental group of its complement into  $G$ . This shows that the state sum is sensitive to the embedding of the surface.

Our last examples are framed links or ribbon links. They are realised as defect graphs on trivial defect surfaces that are labeled by a spherical fusion category  $\mathcal{C}$  as a bimodule category over itself. In this case, bimodule functors labeling defect lines and bimodule natural transformations labeling defect vertices correspond to objects and morphisms of the categorical centre  $\mathcal{Z}(\mathcal{C})$ .

In this setting, ribbons or framed links can be realised in two ways. The first is a ribbon diagram on a defect surface, in which line segments are labeled by objects of  $\mathcal{Z}(\mathcal{C})$  and crossings are viewed as defect vertices labeled by braidings. The second is an embedded ribbon link labeled by objects of  $\mathcal{Z}(\mathcal{C})$  without vertices.

We show that in both cases, the state sum is the product of the evaluation of the ribbon link with the usual Turaev-Viro-Barrett-Westbury state sum for the manifold without defects. This reproduces the results by Turaev and Virelizier [TV10, TV17] on ribbon links in graph TQFTs.

### Structure of the article

In Section 1 we introduce the categorical data for the state sum model and summarise the relevant background from the literature.

Section 2 develops the diagrammatic calculus underlying generalised 6j symbols. After recalling diagrams for spherical fusion categories and pivotal 2-categories, we introduce mixed diagrams, in which diagrams for spherical fusion categories overlap with diagrams labeled by bimodule functors and natural transformations. By labeling segments and line endpoints at their boundaries with objects and morphisms in bimodule categories we then obtain the polygon diagrams that are the building blocks of the state sum.

In Section 3 we show that these polygon diagrams satisfy the usual cutting and gluing identities for polygon presentations of surfaces.

The state sum of a triangulated 3-manifold with defect surfaces, defect lines and defect points is introduced in Section 4. After discussing the labeling of defects and of the triangulation with algebraic data, we define the generalised 6j symbol of a tetrahedron with defects. We then introduce the state sum, which reduces to the usual Turaev-Viro Barrett-Westbury state sum in the absence of defects, and show that it can be computed by gluing 3-manifolds with defects.

In Section 5 we establish the triangulation independence of the state sum. We first summarise some background from PL topology and introduce certain neighbourhoods of defect surfaces required for our constructions. We then prove that the state sum of a 3-ball bisected by a defect disc is the evaluation of the polygon diagram obtained by projecting the dual graph of the boundary triangulation on the disc. This implies that the state sum is invariant under bistellar moves that involve only generic transversal tetrahedra. We then prove triangulation independence by refining the triangulation and decomposing it into neighbourhoods of defect surfaces and 3-manifolds without defects.

In Section 6 we compute examples and discuss the results.

# 1 Categorical data

## 1.1 Spherical fusion categories

We work over  $\mathbb{C}$  and follow the conventions of Etingof et al. in [EGNO]. A **multitensor category** is a locally finite,  $\mathbb{C}$ -linear abelian rigid monoidal category  $\mathcal{C}$  with a tensor product  $\otimes : \mathcal{C} \times \mathcal{C} \rightarrow \mathcal{C}$  that is bilinear on the morphisms. A **tensor category** is an indecomposable multitensor category with  $\text{End}_{\mathcal{C}}(e) \cong \mathbb{C}$ , where  $e$  is the tensor unit. A **(multi)fusion category** is a finite semisimple (multi)tensor category.

For all categories  $\mathcal{C}$  we denote by  $\mathcal{C}^{op}$  the opposite category and for all monoidal categories  $\mathcal{C}$  by  $\mathcal{C}^{rev}$  the category  $\mathcal{C}$  with the opposite monoidal structure. We define a **left rigid** monoidal category as a category in which every object  $x$  has a left dual  $x^*$  and evaluation and coevaluation morphisms

$$\text{ev}_x^L : x^* \otimes x \rightarrow e, \quad \text{coev}_x^L : e \rightarrow x \otimes x^* \quad (1)$$

that satisfy the identities

$$(1_x \otimes \text{ev}_x^L) \circ (\text{coev}_x^L \otimes 1_x) = 1_x \quad (\text{ev}_x^L \otimes 1_{x^*}) \circ (1_{x^*} \otimes \text{coev}_x^L) = 1_{x^*}, \quad (2)$$

up to associators and unit constraints. We denote by  $*$  :  $\mathcal{C} \rightarrow \mathcal{C}^{op,rev}$  the induced monoidal functor, see the end of Section 2.10 in [EGNO]. A **pivotal** monoidal category  $\mathcal{C}$  is a left rigid monoidal category  $\mathcal{C}$  with a monoidal isomorphism  $\omega : ** \Rightarrow \text{id}_{\mathcal{C}}$ . Every pivotal category is right rigid with

$$\text{ev}_x^R = \text{ev}_{x^*}^L \circ (\omega_{x^*}^{-1} \otimes 1_{x^*}) : x \otimes x^* \rightarrow e, \quad \text{coev}_x^R = (1_{x^*} \otimes \omega) \circ \text{coev}_{x^*}^L : e \rightarrow x^* \otimes x, \quad (3)$$

and the left and right trace of a morphism  $\alpha \in \text{End}_{\mathcal{C}}(x)$  are given by

$$\text{tr}^L(\alpha) = \text{ev}_x^L \circ (1_{x^*} \otimes \alpha) \circ \text{coev}_x^R, \quad \text{tr}^R(\alpha) = \text{ev}_x^R \circ (\alpha \otimes 1_{x^*}) \circ \text{coev}_x^L. \quad (4)$$

A pivotal category  $\mathcal{C}$  is **spherical** if  $\text{tr}^L(\alpha) = \text{tr}^R(\alpha)$  for all endomorphisms  $\alpha$  in  $\mathcal{C}$ . In this case we write  $\text{tr}(\alpha) = \text{tr}^L(\alpha) = \text{tr}^R(\alpha)$  and  $\dim(x) = \text{tr}(1_x) = \text{tr}(1_{x^*}) = \dim(x^*)$  for all  $\alpha \in \text{End}_{\mathcal{C}}(x)$  and  $x \in \text{Ob}\mathcal{C}$ . The **dimension** of a spherical fusion category  $\mathcal{C}$  is

$$\dim(\mathcal{C}) = \sum_{i \in I} \dim(i)^2, \quad (5)$$

where  $I$  is a set of representatives of the isomorphism classes of simple objects.

**Example 1.1.** [EGNO, Ex. 2.3.6]

Let  $G$  be a finite group and  $\omega : G \times G \times G \rightarrow \mathbb{C}^\times$  a normalised 3-cocycle. The fusion category  $\text{Vec}_G^\omega$  has

- as objects finite-dimensional  $G$ -graded vector spaces  $V = \bigoplus_{g \in G} V_g$ ,
- as morphisms linear maps  $f : V \rightarrow W$  with  $f(V_g) \subset W_g$  for all  $g \in G$ ,
- simple objects  $\delta^g$  for  $g \in G$  with  $(\delta^g)_g = \mathbb{C}$  and  $(\delta^g)_h = 0$  for  $g \neq h$ ,
- the tensor product  $V \otimes W = \bigoplus_{g \in G} (\bigoplus_{hk=g} V_h \otimes W_k)$ ,

- the associator given by  $a_{\delta^g, \delta^h, \delta^k} = \omega(g, h, k) \text{id}_{\delta^{ghk}}$  on the simple objects,
- dual objects  $V^* = \bigoplus_{g \in G} V_{g^{-1}}^*$  with the usual (co)evaluation for finite-dimensional vector spaces,
- pivotal structures that are in bijection with characters  $\kappa : G \rightarrow \mathbb{C}^\times$ .

A pivotal structure is spherical iff  $\kappa(g) \in \{1, -1\}$  for all  $g \in G$ . In particular, the trivial character  $\kappa \equiv 1$  determines a spherical structure on  $\text{Vec}_G^\omega$ , its **standard spherical structure**.

## 1.2 (Bi)module categories, functors and natural transformations

In this section, we summarise background on (bi)module categories, (bi)module functors and (bi)module natural transformations from [EGNO, Ch. 7].

**Definition 1.2.** Let  $\mathcal{C}, \mathcal{D}$  be multitensor categories.

1. A  **$\mathcal{C}$ -left module category** is a locally finite  $\mathbb{C}$ -linear abelian category  $\mathcal{M}$  together with
  - a functor  $\triangleright : \mathcal{C} \times \mathcal{M} \rightarrow \mathcal{M}$  that is  $\mathbb{C}$ -bilinear on the morphisms and exact in the first variable,
  - natural isomorphisms  $c : \triangleright(\otimes \times \text{id}_{\mathcal{M}}) \Rightarrow \triangleright(\text{id}_{\mathcal{C}} \times \triangleright)$  and  $\gamma : e \triangleright - \Rightarrow \text{id}_{\mathcal{M}}$
such that the following diagrams commute for all  $x, y, z \in \text{Ob}\mathcal{C}$  and  $m \in \text{Ob}\mathcal{M}$ :

$$\begin{array}{ccc} ((x \otimes y) \otimes z) \triangleright m & \xrightarrow{c_{x \otimes y, z, m}} & (x \otimes y) \triangleright (z \triangleright m) \xrightarrow{c_{x, y, z \triangleright m}} x \triangleright (y \triangleright (z \triangleright m)) \\ \downarrow a_{x, y, z} \triangleright 1_m & & \nearrow 1_x \triangleright c_{y, z, m} \\ (x \otimes (y \otimes z)) \triangleright m & \xrightarrow{c_{x, y \otimes z, m}} & x \triangleright ((y \otimes z) \triangleright m) \end{array} \quad (6)$$

$$\begin{array}{ccc} (x \otimes e) \triangleright m & \xrightarrow{c_{x, e, m}} & x \triangleright (e \triangleright m) \\ \searrow r_x \triangleright 1_m & & \swarrow 1_x \triangleright \gamma_m \\ & x \triangleright m. & \end{array} \quad (7)$$

2. A  **$\mathcal{D}$ -right module category** is a locally finite  $\mathbb{C}$ -linear abelian category  $\mathcal{M}$  together with
  - a functor  $\triangleleft : \mathcal{M} \times \mathcal{D} \rightarrow \mathcal{M}$  that is  $\mathbb{C}$ -bilinear on the morphisms and exact in the second variable,
  - natural isomorphisms  $d : \triangleleft(\triangleleft \times \text{id}_{\mathcal{D}}) \Rightarrow \triangleleft(\text{id}_{\mathcal{M}} \times \otimes)$  and  $\delta : - \triangleleft e \Rightarrow \text{id}_{\mathcal{M}}$
that make the following diagrams commute for all  $x, y, z \in \text{Ob}\mathcal{D}$  and  $m \in \text{Ob}\mathcal{M}$

$$\begin{array}{ccc} ((m \triangleleft x) \triangleleft y) \triangleleft z & \xrightarrow{d_{m \triangleleft x, y, z}} & (m \triangleleft x) \triangleleft (y \otimes z) \xrightarrow{d_{m, x, y \otimes z}} m \triangleleft (x \otimes (y \otimes z)) \\ \downarrow d_{m, x, y} \triangleleft 1_z & & \nearrow 1_m \triangleleft a_{x, y, z} \\ (m \triangleleft (x \otimes y)) \triangleleft z & \xrightarrow{d_{m, x \otimes y, z}} & m \triangleleft ((x \otimes y) \otimes z) \end{array} \quad (8)$$

$$\begin{array}{ccc} m \triangleleft (e \otimes x) & \xrightarrow{d_{m, e, x}} & (m \triangleleft e) \triangleleft x \\ \searrow 1_m \triangleleft l_x & & \swarrow \delta_m \triangleleft 1_x \\ & m \triangleleft x. & \end{array} \quad (9)$$

3. A  **$(\mathcal{C}, \mathcal{D})$ -bimodule category** is a locally finite  $\mathbb{C}$ -linear abelian category  $\mathcal{M}$  with
  - a  $\mathcal{C}$ -left module category structure  $(\triangleright, c, \gamma)$ ,
  - a  $\mathcal{D}$ -right module category structure  $(\triangleleft, d, \delta)$ ,
  - a natural isomorphism  $b : \triangleleft(\triangleright \times \text{id}_{\mathcal{D}}) \Rightarrow \triangleright(\text{id}_{\mathcal{C}} \times \triangleleft)$
such that the following diagrams commute for all  $x, y \in \text{Ob}\mathcal{C}$ ,  $u, v \in \text{Ob}\mathcal{D}$  and  $m \in \text{Ob}\mathcal{M}$

$$\begin{array}{ccc} ((x \otimes y) \triangleright m) \triangleleft u & \xrightarrow{b_{x \otimes y, m, u}} & (x \otimes y) \triangleright (m \triangleleft u) \xrightarrow{c_{x, y, m \triangleleft u}} x \triangleright (y \triangleright (m \triangleleft u)) \\ \downarrow c_{x, y, m} \triangleleft 1_u & & \nearrow 1_x \triangleright b_{y, m, u} \\ (x \triangleright (y \triangleright m)) \triangleleft u & \xrightarrow{b_{x, y \triangleright m, u}} & x \triangleright ((y \triangleright m) \triangleleft u) \end{array} \quad (10)$$

$$\begin{array}{ccc}
((x \triangleright m) \triangleleft u) \triangleleft v \xrightarrow{d_{x \triangleright m, u, v}} (x \triangleright m) \triangleleft (u \otimes v) \xrightarrow{b_{x, m, u \otimes v}} x \triangleright (m \triangleleft (u \otimes v)) & & (11) \\
\downarrow b_{x, m, u} \triangleleft 1_v & \nearrow 1_x \triangleright d_{y, m, u} & \\
(x \triangleright (m \triangleleft u)) \triangleleft v \xrightarrow{b_{x, m \triangleleft u, v}} x \triangleright ((m \triangleleft u) \triangleleft v). & & 
\end{array}$$

A  $\mathcal{D}$ -right module category can be defined more succinctly as a  $\mathcal{D}^{rev}$ -module category and a  $(\mathcal{C}, \mathcal{D})$ -bimodule category as a  $\mathcal{C} \boxtimes \mathcal{D}^{rev}$ -module category, where  $\boxtimes$  is the Deligne product. We expanded the definitions to set up notation and introduce the relevant diagrams.

**Remark 1.3.** [EGNO, Prop. 7.1.3]

$\mathcal{C}$ -module category structures on  $\mathcal{M}$  correspond bijectively to monoidal functors  $F : \mathcal{C} \rightarrow \text{End}(\mathcal{M})$ . The monoidal functor defined by a  $\mathcal{C}$ -module structure assigns to an object  $x$  in  $\mathcal{C}$  the endofunctor  $x \triangleright - : \mathcal{M} \rightarrow \mathcal{M}$  and to a morphism  $\alpha : x \rightarrow y$  in  $\mathcal{C}$  the natural transformation  $\alpha \triangleright - : x \triangleright - \Rightarrow y \triangleright -$ . The monoidal structure of  $F$  is given by the natural isomorphisms  $\gamma : e \triangleright - \Rightarrow \text{id}_{\mathcal{M}}$  and  $c_{x, y, -} : (x \otimes y) \triangleright - \Rightarrow x \triangleright (y \triangleright -)$ .

**Example 1.4.** Every fusion category  $\mathcal{C}$  is a  $(\mathcal{C}, \mathcal{C})$ -bimodule category with  $\triangleright = \triangleleft = \otimes : \mathcal{C} \times \mathcal{C} \rightarrow \mathcal{C}$  and coherence isomorphisms  $c_{x, y, z} = d_{x, y, z} = b_{x, y, z} = a_{x, y, z} : (x \otimes y) \otimes z \rightarrow x \otimes (y \otimes z)$ .

**Example 1.5.** Any locally finite  $\mathbb{C}$ -linear abelian category  $\mathcal{M}$  is a bimodule category over the fusion category  $\text{Vect}_{\mathbb{C}}$  of finite-dimensional complex vector spaces. This  $\text{Vect}_{\mathbb{C}}$ -module category structure is unique up to bimodule equivalence (cf. Definition 1.8).

**Example 1.6.** For any  $(\mathcal{C}, \mathcal{D})$ -bimodule category  $\mathcal{M}$  over pivotal fusion categories  $\mathcal{C}, \mathcal{D}$  the category  $\mathcal{M}^{op}$  is a  $(\mathcal{D}, \mathcal{C})$ -bimodule category with

$$\triangleleft^{op} = \triangleright(* \times \text{id}_{\mathcal{M}})\tau : \mathcal{M} \times \mathcal{C} \rightarrow \mathcal{M} \qquad \triangleright^{op} = \triangleleft(\text{id}_{\mathcal{M}} \times *)\tau : \mathcal{D} \times \mathcal{M} \rightarrow \mathcal{M}, \quad (12)$$

where  $*$  :  $\mathcal{C} \rightarrow \mathcal{C}^{op, rev}$  is the duality functor and  $\tau$  the flip functor that exchanges the two factors in a cartesian product. The coherence isomorphisms are given by  $c_{x, y, m}^{op} = d_{m, y^*, x^*}$ ,  $d_{x, y, m}^{op} = c_{y^*, x^*, m}$ ,  $b_{x, m, y}^{op} = b_{y^*, m, x^*}$ . We call it the **opposite bimodule category**  $\mathcal{M}^{\#}$ .

**Example 1.7.** [EGNO, Ex. 7.4.10]

Indecomposable semisimple module categories  $\mathcal{M}$  over the fusion category  $\text{Vec}_G := \text{Vec}_G^{\omega=1}$ , up to equivalence, correspond to pairs  $(X, \psi)$  of a finite transitive  $G$ -set  $X \cong G/L$  and an element  $\psi \in H^2(L, \mathbb{C}^{\times})$ .

- The objects of  $\mathcal{M}$  are  $X$ -graded vector spaces.
- The simple objects of  $\mathcal{M}$  are of the form  $\delta^x$  for  $x \in X$ .
- The action functor  $\triangleright : \text{Vec}_G \times \mathcal{M} \rightarrow \mathcal{M}$  is given by  $\delta^g \triangleright \delta^x = \delta^{g \triangleright x}$  on the simple objects.
- The natural isomorphism  $c : \triangleright(\otimes \times \text{id}) \Rightarrow \triangleright(\text{id} \times \triangleright)$  is given by  $\psi \in H^2(L, \mathbb{C}^{\times})$ .

**Definition 1.8.** Let  $\mathcal{C}, \mathcal{D}$  be multitensor categories.

1. A  **$\mathcal{C}$ -module functor**  $F : \mathcal{M} \rightarrow \mathcal{N}$  between  $\mathcal{C}$ -module categories  $\mathcal{M}, \mathcal{N}$  is a  $\mathbb{C}$ -linear right exact functor  $F : \mathcal{M} \rightarrow \mathcal{N}$  together with a natural isomorphism  $s : F \triangleright \Rightarrow \triangleright(\text{id}_{\mathcal{C}} \times F)$  that satisfies the pentagon and the triangle axiom: for all  $x, y \in \text{Ob} \mathcal{C}$  and  $m \in \text{Ob} \mathcal{M}$  the following diagrams commute

$$\begin{array}{ccc}
F((x \otimes y) \triangleright m) \xrightarrow{s_{x \otimes y, m}} (x \otimes y) \triangleright F(m) \xrightarrow{c_{x, y, F(m)}} x \triangleright (y \triangleright F(m)) & & (13) \\
\downarrow F(c_{x, y, m}) & \nearrow 1_x \triangleright s_{y, m} & \\
F(x \triangleright (y \triangleright m)) \xrightarrow{s_{x, y \triangleright m}} x \triangleright F(y \triangleright m) & & 
\end{array}$$

$$\begin{array}{ccc}
F(e \triangleright m) \xrightarrow{s_{e, m}} e \triangleright F(m) & & (14) \\
\searrow F(\gamma_m) & \swarrow \gamma_{F(m)} & \\
& F(m) & 
\end{array}$$

2. A  **$\mathcal{D}$ -right module functor**  $F : \mathcal{M} \rightarrow \mathcal{N}$  between  $\mathcal{D}$ -right module categories  $\mathcal{M}, \mathcal{N}$  is a  $\mathbb{C}$ -linear right exact functor  $F : \mathcal{M} \rightarrow \mathcal{N}$  together with a natural isomorphism  $t : \triangleleft(F \times \text{id}_{\mathcal{D}}) \Rightarrow F \triangleleft$  that satisfies the

pentagon and the triangle axiom: for all  $x, y \in \text{Ob}\mathcal{D}$  and  $m \in \text{Ob}\mathcal{M}$  the following diagrams commute

$$\begin{array}{ccc}
(F(m) \triangleleft x) \triangleleft y & \xrightarrow{d_{F(m),x,y}} & F(m) \triangleleft (x \otimes y) \xrightarrow{t_{m,x \otimes y}} F(m \triangleleft (x \otimes y)) \\
\downarrow t_{m,x} \triangleleft 1_y & & \nearrow F(d_{m,x,y}) \\
F(m \triangleleft x) \triangleleft y & \xrightarrow{t_{m \triangleleft x,y}} & F((m \triangleleft x) \triangleleft y)
\end{array} \quad (15)$$

$$\begin{array}{ccc}
F(m) \triangleleft e & \xrightarrow{t_{m,e}} & F(m \triangleleft e) \\
\searrow \delta_{F(m)} & & \swarrow F(\delta_m) \\
& & F(m).
\end{array} \quad (16)$$

3. A  $(\mathcal{C}, \mathcal{D})$ -bimodule functor between  $(\mathcal{C}, \mathcal{D})$ -bimodule categories  $\mathcal{M}, \mathcal{N}$  is a  $\mathcal{C}$ -linear right exact functor  $F : \mathcal{M} \rightarrow \mathcal{N}$  with a  $\mathcal{C}$ -module functor structure  $s$  and a  $\mathcal{D}$ -right module functor structure  $t$  that satisfy the hexagon axiom: for all  $x \in \text{Ob}\mathcal{C}$ ,  $y \in \text{Ob}\mathcal{D}$  and  $m \in \text{Ob}\mathcal{M}$  the following diagram commutes

$$\begin{array}{ccc}
F(x \triangleright m) \triangleleft y & \xrightarrow{t_{x \triangleright m,y}} & F((x \triangleright m) \triangleleft y) \xrightarrow{F(b_{x,m,y})} F(x \triangleright (m \triangleleft y)) \\
\downarrow s_{x,m} \triangleleft 1_y & & \downarrow s_{x,m} \triangleleft y \\
(x \triangleright F(m)) \triangleleft y & \xrightarrow{b_{x,F(m),y}} & x \triangleright (F(m) \triangleleft y) \xrightarrow{1_{x \triangleright t_{m,y}}} x \triangleright F(m \triangleleft y).
\end{array} \quad (17)$$

An equivalence of (bi)module categories is a (bi)module functor that is an equivalence of categories.

**Definition 1.9.** Let  $\mathcal{C}, \mathcal{D}$  be multitensor categories.

1. A  $\mathcal{C}$ -module natural transformation  $\nu : F \Rightarrow G$  for  $\mathcal{C}$ -module functors  $F, G : \mathcal{M} \rightarrow \mathcal{N}$  is a natural transformation such that the following diagram commutes for all  $x \in \text{Ob}\mathcal{C}$  and  $m \in \text{Ob}\mathcal{M}$

$$\begin{array}{ccc}
F(x \triangleright m) & \xrightarrow{\nu_{x \triangleright m}} & G(x \triangleright m) \\
\downarrow s_{x,m}^F & & \downarrow s_{x,m}^G \\
x \triangleright F(m) & \xrightarrow{1_{x \triangleright \nu_m}} & x \triangleright G(m).
\end{array} \quad (18)$$

2. A  $\mathcal{D}$ -right module natural transformation  $\nu : F \Rightarrow G$  for  $\mathcal{D}$ -right module functors  $F, G : \mathcal{M} \rightarrow \mathcal{N}$  is a natural transformation such that the following diagram commutes for all  $x \in \text{Ob}\mathcal{D}$  and  $m \in \text{Ob}\mathcal{M}$

$$\begin{array}{ccc}
F(m) \triangleleft x & \xrightarrow{\nu_{m \triangleleft x}} & G(m) \triangleleft x \\
\downarrow t_{m,x}^F & & \downarrow t_{m,x}^G \\
F(m \triangleleft x) & \xrightarrow{\nu_{m \triangleleft x}} & G(m \triangleleft x).
\end{array} \quad (19)$$

3. A  $(\mathcal{C}, \mathcal{D})$ -bimodule natural transformation  $\nu : F \rightarrow G$  between  $(\mathcal{C}, \mathcal{D})$ -bimodule functors  $F, G : \mathcal{M} \rightarrow \mathcal{N}$  is a natural transformation  $\nu : F \Rightarrow G$  that is a  $\mathcal{C}$ -module and a  $\mathcal{D}$ -right module natural transformation.

For  $\mathcal{C}$ -module categories  $\mathcal{M}, \mathcal{N}$  we denote by  $\text{Func}(\mathcal{M}, \mathcal{N})$  the category of  $\mathcal{C}$ -module functors  $F : \mathcal{M} \rightarrow \mathcal{N}$  and  $\mathcal{C}$ -module natural transformations between them and write  $\text{End}_{\mathcal{C}}(\mathcal{M}) = \text{Func}_{\mathcal{C}}(\mathcal{M}, \mathcal{M})$ . Analogously, for  $(\mathcal{C}, \mathcal{D})$ -bimodule categories  $\mathcal{M}, \mathcal{N}$ , we write  $\text{Func}_{(\mathcal{C}, \mathcal{D})}(\mathcal{M}, \mathcal{N})$  for the category of  $(\mathcal{C}, \mathcal{D})$ -bimodule functors  $F : \mathcal{M} \rightarrow \mathcal{N}$  and bimodule natural transformations between them and  $\text{End}_{(\mathcal{C}, \mathcal{D})}(\mathcal{M}) = \text{Func}_{(\mathcal{C}, \mathcal{D})}(\mathcal{M}, \mathcal{M})$ .

Composites of (bi)module functors inherit a (bi)module functor structure. If  $G : \mathcal{M} \rightarrow \mathcal{N}$  and  $F : \mathcal{N} \rightarrow \mathcal{P}$  are  $(\mathcal{C}, \mathcal{D})$ -bimodule functors, then the  $(\mathcal{C}, \mathcal{D})$ -bimodule functor structure for  $FG : \mathcal{M} \rightarrow \mathcal{P}$  is given by

$$\begin{aligned}
s^{FG} &= s^F(\text{id}_{\mathcal{C}} \times G) \circ F s^G : FG \triangleright \Rightarrow \triangleright(\text{id}_{\mathcal{C}} \times FG) \\
t^{FG} &= F t^G \circ t^F(G \times \text{id}_{\mathcal{D}}) : \triangleleft(FG \times \text{id}_{\mathcal{D}}) \Rightarrow FG \triangleleft.
\end{aligned} \quad (20)$$

For all bimodule functors  $F, F' : \mathcal{N} \rightarrow \mathcal{P}$ ,  $G, G' : \mathcal{M} \rightarrow \mathcal{N}$  and bimodule natural transformations  $\nu : F \Rightarrow F'$  and  $\mu : G \Rightarrow G'$  the natural transformations  $\nu G : FG \Rightarrow F'G$  and  $F\mu : FG \Rightarrow FG'$  are bimodule natural transformations with respect to this bimodule functor structure. As composites of bimodule natural transformations are also bimodule natural transformations, it follows that  $(\mathcal{C}, \mathcal{D})$ -bimodule categories,  $(\mathcal{C}, \mathcal{D})$ -bimodule functors and  $(\mathcal{C}, \mathcal{D})$ -bimodule natural transformations form a 2-category.

The following examples show how the data of a (bi)module category can be recovered as coherence data of (bi)module functors. They are the categorical counterparts of standard constructions for modules over rings.

**Example 1.10.** *Let  $\mathcal{C}, \mathcal{D}$  be multitensor categories and  $\mathcal{M}, \mathcal{N}$   $(\mathcal{C}, \mathcal{D})$ -bimodule categories.*

1. *For any  $x \in \text{Ob}\mathcal{D}$  the functor  $F = - \triangleleft x : \mathcal{M} \rightarrow \mathcal{M}$  is a  $\mathcal{C}$ -module functor with coherence isomorphisms  $s_{c,m} = b_{c,m,x} : (c \triangleright m) \triangleleft x \rightarrow c \triangleright (m \triangleleft x)$ . Any morphism  $\alpha \in \text{Hom}_{\mathcal{D}}(x, y)$  defines a  $\mathcal{C}$ -module natural transformation  $\nu = - \triangleleft \alpha : - \triangleleft x \Rightarrow - \triangleleft y$ . This defines a functor  $\mathcal{D} \rightarrow \text{End}_{\mathcal{C}}(\mathcal{M})$ .*
2. *If  $x \in \text{Ob}\mathcal{Z}(\mathcal{D})$  with half-braidings  $\sigma_{d,x} : d \otimes x \rightarrow x \otimes d$ , the functor  $F$  from 1. becomes a  $(\mathcal{C}, \mathcal{D})$ -bimodule functor with  $t_{m,d} = d_{m,d,x}^{-1} \circ (1_m \triangleleft \sigma_{x,d}^{-1}) \circ d_{m,x,d} : (m \triangleleft x) \triangleleft d \rightarrow (m \triangleleft d) \triangleleft x$ . For  $\alpha \in \text{Hom}_{\mathcal{Z}(\mathcal{D})}(x, y)$  the morphisms  $\nu_m = 1 \triangleleft \alpha : m \triangleleft x \rightarrow m \triangleleft y$  define a  $(\mathcal{C}, \mathcal{D})$ -bimodule natural transformation  $\nu : - \triangleleft x \Rightarrow - \triangleleft y$ . This defines a functor  $\mathcal{Z}(\mathcal{D}) \rightarrow \text{End}_{(\mathcal{C}, \mathcal{D})}(\mathcal{M})$ .*
3. *Analogously, for  $x \in \text{Ob}\mathcal{C}$   $F = x \triangleright - : \mathcal{M} \rightarrow \mathcal{M}$  with  $t_{m,d} = b_{x,m,d} : (x \triangleright m) \triangleleft d \rightarrow x \triangleright (m \triangleleft d)$  is a  $\mathcal{D}$ -right module functor. Any morphism  $\alpha \in \text{Hom}_{\mathcal{C}}(x, y)$  defines a  $\mathcal{D}$ -right module natural transformation  $\nu = \alpha \triangleright - : x \triangleright - \Rightarrow y \triangleright -$ . This defines a functor  $\mathcal{C} \rightarrow \text{End}_{\mathcal{D}^{rev}}(\mathcal{M})$ .*
4. *If  $x \in \text{Ob}\mathcal{Z}(\mathcal{C})$  with half-braidings  $\sigma_{c,x} : c \otimes x \rightarrow x \otimes c$ , the functor  $F$  from 3. becomes a  $(\mathcal{C}, \mathcal{D})$ -bimodule functor with  $s_{c,m} = c_{c,x,m} \circ (\sigma_{c,x}^{-1} \triangleright 1_m) \circ c_{x,c,m}^{-1} : x \triangleright (c \triangleright m) \rightarrow c \triangleright (x \triangleright m)$ . For any morphism  $\alpha \in \text{Hom}_{\mathcal{Z}(\mathcal{C})}(x, y)$  the morphisms  $\nu_m = \alpha \triangleright 1_m : x \triangleright m \rightarrow y \triangleright m$  define a  $\mathcal{C}$ -module natural transformation  $\nu : x \triangleright - \Rightarrow y \triangleright -$ . This defines a functor  $\mathcal{Z}(\mathcal{C}) \rightarrow \text{End}_{(\mathcal{C}, \mathcal{D})}(\mathcal{M})$ .*
5. *For any  $\mathcal{C}$ -module category  $\mathcal{M}$  and  $m \in \text{Ob}\mathcal{M}$ , the functor  $F = - \triangleright m : \mathcal{C} \rightarrow \mathcal{M}$  is a  $\mathcal{C}$ -module functor with  $s_{x,y} = c_{x,y,m} : (x \otimes y) \triangleright m \rightarrow x \triangleright (y \triangleright m)$ . Any morphism  $\alpha \in \text{Hom}_{\mathcal{M}}(m, m')$  defines a  $\mathcal{C}$ -module natural transformation  $\nu = - \triangleright \alpha : - \triangleright m \Rightarrow - \triangleright m'$ .*  
*If  $\mathcal{M}$  is a  $(\mathcal{C}, \mathcal{D})$ -bimodule category, this defines a  $(\mathcal{C}, \mathcal{D})$ -bimodule equivalence  $\mathcal{M} \rightarrow \text{Func}_{\mathcal{C}}(\mathcal{C}, \mathcal{M})$  with respect to the  $(\mathcal{C}, \mathcal{D})$ -bimodule structure on  $\text{Func}_{\mathcal{C}}(\mathcal{C}, \mathcal{M})$  given by  $(c \triangleright F)(x) = F(x \otimes c)$  and  $(F \triangleleft d)(x) = F(x) \triangleleft d$  for  $c, x \in \text{Ob}\mathcal{C}$ ,  $d \in \text{Ob}\mathcal{D}$ .*
6. *For any  $\mathcal{D}$ -right module category  $\mathcal{M}$  and  $m \in \text{Ob}\mathcal{M}$ , the functor  $F = m \triangleleft - : \mathcal{D} \rightarrow \mathcal{M}$  is a  $\mathcal{D}$ -right module functor with  $t_{x,y} = d_{x,y,m} : (m \triangleleft x) \triangleleft y \rightarrow m \triangleleft (x \otimes y)$ . Any morphism  $\alpha \in \text{Hom}_{\mathcal{M}}(m, m')$  defines a  $\mathcal{C}$ -module natural transformation  $\nu = \alpha \triangleleft - : m \triangleleft - \Rightarrow m' \triangleleft -$ .*  
*If  $\mathcal{M}$  is a  $(\mathcal{C}, \mathcal{D})$ -bimodule category, this defines a  $(\mathcal{C}, \mathcal{D})$ -bimodule equivalence  $\mathcal{M} \rightarrow \text{Func}_{\mathcal{D}^{rev}}(\mathcal{D}, \mathcal{M})$  with respect to the  $(\mathcal{C}, \mathcal{D})$ -bimodule structure on  $\text{Func}_{\mathcal{D}^{rev}}(\mathcal{D}, \mathcal{M})$  given by  $(c \triangleright F)(x) = c \triangleright F(x)$  and  $(F \triangleleft d)(x) = F(d \otimes x)$  for  $c \in \text{Ob}\mathcal{C}$ ,  $d, x \in \text{Ob}\mathcal{D}$ .*
7. *Any  $(\mathcal{C}, \mathcal{D})$ -bimodule functor  $F : \mathcal{M} \rightarrow \mathcal{N}$  defines a  $(\mathcal{D}, \mathcal{C})$ -bimodule functor  $F^{\#} : \mathcal{M}^{\#} \rightarrow \mathcal{N}^{\#}$  with coherence isomorphisms  $s_{d,m}^{F^{\#}} = t_{m,d}^F$  and  $t_{m,c}^{F^{\#}} = s_{c^*,m}^F$ . Any  $(\mathcal{C}, \mathcal{D})$ -bimodule natural transformation  $\nu : F \Rightarrow G$  induces a  $(\mathcal{D}, \mathcal{C})$ -bimodule natural transformation  $\nu^{\#} : G^{\#} \Rightarrow F^{\#}$  with  $\nu_m^{\#} = \nu_m$ .*
8. *For any  $(\mathcal{C}, \mathcal{D})$ -bimodule functor  $F : \mathcal{M} \rightarrow \mathcal{N}$ , the morphisms  $s_{c,m} : F(c \triangleright m) \rightarrow c \triangleright F(m)$  define a  $\mathcal{D}$ -right module natural isomorphism  $s_c : F(c \triangleright -) \Rightarrow c \triangleright F(-)$ . Analogously, the morphisms  $t_{m,d} : F(m) \triangleleft d \rightarrow F(m \triangleleft d)$  define a  $\mathcal{C}$ -module natural transformation  $t_d : F(-) \triangleleft d \Rightarrow F(- \triangleleft d)$ . This follows from the hexagon identity (17) for a bimodule functor and the module functor structure (20) for a composite functor.*

If  $\mathcal{C}$  is a finite multitensor category as a bimodule category over itself, then all bimodule endofunctors of  $\mathcal{C}$  are naturally isomorphic to functors of the form  $F = c \otimes - : \mathcal{C} \rightarrow \mathcal{C}$  with an object  $c \in \mathcal{Z}(\mathcal{C})$ , as in Example 1.10, 4. and all bimodule natural transformations between them are of the form  $\nu = f \otimes - : c \otimes - \Rightarrow c' \otimes -$  with a morphism  $f : c \rightarrow c'$  in  $\mathcal{Z}(\mathcal{C})$ . This identifies  $\text{End}_{\mathcal{C}}(\mathcal{C})$  with the centre  $\mathcal{Z}(\mathcal{C})$ .

**Example 1.11.** *[EGNO, Prop. 7.13.8.] Let  $\mathcal{C}$  be a finite multitensor category, viewed as a  $(\mathcal{C}, \mathcal{C})$ -bimodule category. Then the monoidal category  $\text{End}_{\mathcal{C}}(\mathcal{C})$  is canonically monoidally isomorphic to the centre  $\mathcal{Z}(\mathcal{C})$ .*



### 1.3 Finite semisimple (bi)module categories over pivotal fusion categories

We focus on *finite semisimple*  $(\mathcal{C}, \mathcal{D})$ -bimodule categories over *fusion categories*  $\mathcal{C}, \mathcal{D}$  and on  $(\mathcal{C}, \mathcal{D})$ -bimodule functors and natural transformations between them. In this case all categories  $\text{Fun}_{(\mathcal{C}, \mathcal{D})}(\mathcal{M}, \mathcal{N})$  are finite  $\mathbb{C}$ -linear abelian categories [EGNO, Prop. 7.11.6] and semisimple, see [ENO05, Th. 2.16] by Etingof et al.

Moreover, the 2-category  $\text{Bimod}(\mathcal{C}, \mathcal{D})$  of finite semisimple  $(\mathcal{C}, \mathcal{D})$ -bimodule categories  $(\mathcal{C}, \mathcal{D})$ -bimodule functors and  $(\mathcal{C}, \mathcal{D})$ -bimodule natural transformations is equipped with duals. Any  $(\mathcal{C}, \mathcal{D})$ -bimodule functor between finite semisimple  $(\mathcal{C}, \mathcal{D})$ -bimodule categories has a left adjoint  $F^l : \mathcal{N} \rightarrow \mathcal{M}$  and a right adjoint  $F^r : \mathcal{N} \rightarrow \mathcal{M}$ , and these adjoints are also  $(\mathcal{C}, \mathcal{D})$ -bimodule functors. The left and right duals of  $F$  are given by its left and right adjoint and the units and counits of the adjunction.

This follows, because module functors between finite semisimple module categories are always exact, as finite semisimple module categories are exact and module functors between exact module categories are exact [EGNO, Prop. 7.6.9]. Any finite abelian  $\mathbb{C}$ -linear category is equivalent to the category of modules over some finite-dimensional semisimple  $\mathbb{C}$ -algebra [EGNO, Def. 1.8.5]. Any right exact  $\mathbb{C}$ -linear functor between such categories is  $\otimes$ -representable [EGNO, Prop. 1.8.10] and hence has a left adjoint, namely the corresponding Hom-functor. Analogously, left exactness implies the existence of a right adjoint.

It follows that category  $\text{End}_{\mathcal{C}}(\mathcal{M})$  is a finite multifusion category. It is a fusion category if and only if  $\mathcal{M}$  is *indecomposable*, that is, not the direct sum of non-trivial module categories, see [EGNO, Sec. 7.3.6] and the remark after [EGNO, Def. 7.2.12]. The category  $\mathcal{M}$  is an  $\text{End}_{\mathcal{C}}(\mathcal{M})$ -module category with the action functor that applies endofunctors and natural transformations to objects and morphisms in  $\mathcal{M}$ .

We also require that the fusion categories  $\mathcal{C}$  and  $\mathcal{D}$  are *pivotal*. This has implications for the opposite bimodule category from Example 1.6. A  $(\mathcal{D}, \mathcal{C})$ -bimodule structure on  $\mathcal{M}^{op}$  can be defined analogously to Example 1.6 for any fusion category  $\mathcal{M}$ . However, the category  $\mathcal{M}^{\#\#}$  is in general not equivalent to the bimodule category  $\mathcal{M}$ , and one needs to distinguish the  $(\mathcal{D}, \mathcal{C})$ -bimodule category structures on  $\mathcal{M}^{op}$  that are induced by left and right duals, see the results by Douglas et al. in [DSS20, Sec. 2.4]. As shown in [S15], the pivotal structures of  $\mathcal{C}$  and  $\mathcal{D}$  relate their left and right duals and eliminate this ambiguity. This justifies the name *opposite bimodule category*.

**Proposition 1.12.** [S15, DSS20]

Let  $\mathcal{C}, \mathcal{D}$  be pivotal fusion categories and  $\mathcal{M}, \mathcal{N}$  finite semisimple  $(\mathcal{C}, \mathcal{D})$ -bimodule categories.

1. There are equivalences  $\Omega : \mathcal{M}^{\#\#} \rightarrow \mathcal{M}$  of  $(\mathcal{C}, \mathcal{D})$ -bimodule categories with  $F\Omega = \Omega F^{\#\#}$  for all  $(\mathcal{C}, \mathcal{D})$ -bimodule functors  $F : \mathcal{M} \rightarrow \mathcal{N}$ .
2. There are equivalences of  $(\mathcal{C}, \mathcal{D})$ -bimodule categories  $\mathcal{M}^{\#} \rightarrow \text{Func}_{\mathcal{C}}(\mathcal{M}, \mathcal{C})$  and  $\mathcal{M}^{\#} \rightarrow \text{Func}_{\mathcal{D}^{rev}}(\mathcal{M}, \mathcal{D})$ .

*Proof.* Claim 1. is shown in [S15]. As a functor  $\Omega = \text{id}_{\mathcal{M}}$ , and its coherence isomorphisms are given by the pivots  $\omega : ** \Rightarrow \text{id}$  as  $s_{c,m} = \omega_c \triangleright 1_m : c^{**} \triangleright m \rightarrow c \triangleright m$  and  $t_{m,d} = 1_m \triangleleft \omega_d^{-1} : m \triangleleft d \rightarrow m \triangleleft d^{**}$ . The identity  $F\Omega = \Omega F^{\#\#}$  follows directly from the definition of  $F^{\#}$  in Example 1.10, 7. and formula (20) for the coherence data of a composite bimodule functor.

Claim 2. is essentially [DSS20, Prop. 2.4.9] for module categories over pivotal fusion categories. It follows by combining [DSS20, Prop. 2.4.9] with 1. The  $(\mathcal{D}, \mathcal{C})$ -bimodule structure on  $\text{Func}_{\mathcal{C}}(\mathcal{M}, \mathcal{C})$  is given by  $(d \triangleright F)(m) = F(m \triangleleft d)$  and  $(F \triangleleft c)(m) = F(m) \otimes c$  and the one on  $\text{Func}_{\mathcal{D}^{rev}}(\mathcal{M}, \mathcal{D})$  by  $(d \triangleright F)(m) = d \otimes F(m)$  and  $(F \triangleleft c)(m) = F(c \triangleright m)$  for all  $c \in \text{Ob}\mathcal{C}$ ,  $m \in \text{Ob}\mathcal{M}$  and  $d \in \text{Ob}\mathcal{D}$ . The equivalences are given by the left adjoints of the functors  $- \triangleright m : \mathcal{C} \rightarrow \mathcal{M}$  and  $m \triangleleft - : \mathcal{D} \rightarrow \mathcal{M}$  from Example 1.10, 5. and 6.  $\square$

### 1.4 Bimodule categories with bimodule traces

(Bi)module traces on (bi)module categories over fusion categories were first introduced by Schaumann in [S13] and investigated further in [S15]. We summarise (bi)module traces for finite semisimple (bi)module categories over pivotal fusion categories from [S13, S15]. To keep notation simple, we focus on left module categories and identify  $(\mathcal{C}, \mathcal{D})$ -bimodule categories with  $\mathcal{C} \boxtimes \mathcal{D}^{rev}$ -left module categories.

**Definition 1.13.** [S13, Def. 3.7]

Let  $\mathcal{C}$  be a pivotal multifusion category and  $\mathcal{M}$  a finite semisimple  $\mathcal{C}$ -module category. A **trace** on  $\mathcal{M}$  is a collection of morphisms  $\theta_m : \text{End}_{\mathcal{M}}(m) \rightarrow \mathbb{C}$  that satisfy

1. **cyclicity:**  $\theta_m(\beta \circ \alpha) = \theta_{m'}(\alpha \circ \beta)$  for all  $\alpha \in \text{Hom}_{\mathcal{M}}(m, m')$  and  $\beta \in \text{Hom}_{\mathcal{M}}(m', m)$ .
2. **non-degeneracy:** for all  $m, m' \in \text{Ob}\mathcal{M}$  the following bilinear maps are non-degenerate.

$$\text{Hom}_{\mathcal{M}}(m', m) \times \text{Hom}_{\mathcal{M}}(m, m') \rightarrow \mathbb{C}, \quad (\beta, \alpha) \mapsto \theta_m(\beta \circ \alpha)$$

A trace on  $\mathcal{M}$  is called a  **$\mathcal{C}$ -module trace** if  $\theta_{c \triangleright m}(\alpha) = \theta_m(\text{tr}^{\mathcal{C}}(\alpha))$  for all  $\alpha \in \text{End}_{\mathcal{M}}(c \triangleright m)$ , where  $\text{tr}^{\mathcal{C}}(\alpha)$  is the partial trace of  $\alpha$  with respect to  $\mathcal{C}$

$$\text{tr}^{\mathcal{C}}(\alpha) = (\text{ev}_c^L \triangleright 1_m) \circ c_{c^*, c, m}^{-1} \circ (1_{c^*} \triangleright \alpha) \circ c_{c^*, c, m} \circ (\text{coev}_c^R \triangleright 1_m) : m \rightarrow m.$$

Analogously, a  $\mathcal{D}$ -right module trace on a  $\mathcal{D}$ -right module category  $\mathcal{M}$  is defined as a  $\mathcal{D}^{rev}$ -module trace and a  $(\mathcal{C}, \mathcal{D})$ -bimodule trace on a  $(\mathcal{C}, \mathcal{D})$ -bimodule category  $\mathcal{M}$  as a  $\mathcal{C} \boxtimes \mathcal{D}^{rev}$ -module trace.

As for spherical categories, the **dimension** of an object  $m$  in a (bi)module category  $\mathcal{M}$  with a (bi)module trace is  $\dim(m) = \theta_m(1_m)$  and for any set  $I$  of representatives of the isomorphism classes of simple objects

$$\dim(\mathcal{M}) = \sum_{m \in I} \dim(m)^2. \quad (21)$$

Note that the condition that  $\theta$  is a  $\mathcal{C}$ -module trace implies for all  $c \in \text{Ob}\mathcal{C}$  and  $m \in \text{Ob}\mathcal{M}$

$$\dim(c \triangleright m) = \dim(c) \dim(m). \quad (22)$$

It is shown in [S13, Prop. 4.4] that a  $\mathcal{C}$ -module trace on an *indecomposable* finite semisimple module category  $\mathcal{M}$  is unique up to rescaling  $\theta_m \rightarrow z\theta_m$  with  $z \in \mathbb{C}^\times$ . The existence of a  $\mathcal{C}$ -module trace on a  $\mathcal{C}$ -module category  $\mathcal{M}$  is a condition on the dimensions of simple objects of  $\mathcal{C}$  and  $\mathcal{M}$ , see [S13, Sec. 5].

**Example 1.14.** *A pivotal fusion category  $\mathcal{C}$  as a  $(\mathcal{C}, \mathcal{C})$ -bimodule category over itself has a bimodule trace if and only if  $\mathcal{C}$  is spherical.*

**Example 1.15.** *Each  $(\mathcal{C}, \mathcal{D})$ -bimodule trace on a finite semisimple  $(\mathcal{C}, \mathcal{D})$ -bimodule category  $\mathcal{M}$  defines a  $(\mathcal{D}, \mathcal{C})$ -bimodule trace on the opposite bimodule category  $\mathcal{M}^\#$  from Example 1.6.*

**Example 1.16.** [S13, Ex. 3.13] *An indecomposable module category over the pivotal fusion category  $(\text{Vec}_G, \kappa)$ , given by a pair  $(G/L, \psi)$  as in Example 1.7, admits a module trace iff  $\kappa|_L \equiv 1$ . Any indecomposable semisimple module category over  $\text{Vec}_G$  with the standard spherical structure admits a module trace.*

(Bi)module traces on (bi)module categories equip (bi)module functors between them with additional structure. It is shown in [S13, Th. 4.5] that for module categories  $\mathcal{M}$  and  $\mathcal{N}$  over a pivotal fusion category  $\mathcal{C}$  with module traces, any module functor  $F : \mathcal{M} \rightarrow \mathcal{N}$  is naturally isomorphic to its double left adjoint  $F^{ll} : \mathcal{M} \rightarrow \mathcal{N}$ . This defines a pivotal structure in the sense of [S15, Def. A.12], namely a natural 2-isomorphism  $\omega : \text{id} \Rightarrow **$ , where  $*$  is the contravariant 2-functor that assigns each module category to itself, each functor to its left dual and each module natural transformation  $\nu : F \Rightarrow G$  to the induced natural transformation  $\nu^* : G^l \Rightarrow F^l$ .

**Theorem 1.17.** [S13, Th. 4.5], [S15, Th. 5.8]

1. For all pivotal fusion categories  $\mathcal{C}$  the 2-category  $\text{Mod}^\theta(\mathcal{C})$  of  $\mathcal{C}$ -module categories with  $\mathcal{C}$ -module traces,  $\mathcal{C}$ -module functors between them and  $\mathcal{C}$ -module natural transformations is pivotal.
2. For all pivotal fusion categories  $\mathcal{C}, \mathcal{D}$  the 2-category  $\text{Bimod}^\theta(\mathcal{C}, \mathcal{D})$  of  $(\mathcal{C}, \mathcal{D})$ -bimodule categories with bimodule traces,  $(\mathcal{C}, \mathcal{D})$ -bimodule functors between them and  $(\mathcal{C}, \mathcal{D})$ -bimodule transformations is pivotal.

In particular, this yields pivotal structures on the finite multifusion categories  $\text{End}_{\mathcal{C}}(\mathcal{M})$ . If the underlying fusion category  $\mathcal{C}$  is spherical, these pivotal structure become spherical. If  $\mathcal{M}$  is also indecomposable, then  $\text{End}_{\mathcal{C}}(\mathcal{M})$  is a spherical fusion category. An earlier proof of this was given by Mueger in [Mu03, Th. 5.16].

**Corollary 1.18.** [S13, Prop. 5.10] *For any spherical fusion category  $\mathcal{C}$  and any  $\mathcal{C}$ -module category  $\mathcal{M}$  with a  $\mathcal{C}$ -module trace,  $\text{End}_{\mathcal{C}}(\mathcal{M})$  is spherical. If  $\mathcal{M}$  is indecomposable,  $\text{End}_{\mathcal{C}}(\mathcal{M})$  is a spherical fusion category.*

For any module category  $\mathcal{M}$  over a fusion category  $\mathcal{C}$  with a  $\mathcal{C}$ -module trace, the multifusion category  $\text{End}_{\mathcal{C}}(\mathcal{M})$  acts on  $\mathcal{M}$ . This action functor is given by the evaluation of endofunctors and natural transformations between them on objects and morphisms of  $\mathcal{M}$ . If  $\mathcal{C}$  is pivotal, then  $\text{End}_{\mathcal{C}}(\mathcal{M})$  is pivotal and the module trace of  $\mathcal{M}$  also satisfies the module trace condition for the  $\text{End}_{\mathcal{C}}(\mathcal{M})$ -module category structure.

**Corollary 1.19.** [S13, Cor. 4.6] Let  $\mathcal{C}$  be a pivotal fusion category and  $\mathcal{M}$  be a  $\mathcal{C}$ -module category with a  $\mathcal{C}$ -module trace  $\theta$ . Then  $\theta$  is also an  $\text{End}_{\mathcal{C}}(\mathcal{M})$ -module trace.

More explicitly, the pivotal structure from Theorem 1.17 and Corollaries 1.18 and 1.19 is given as follows. If we denote by  $F^l : \mathcal{M} \rightarrow \mathcal{M}$  the left adjoint of a  $\mathcal{C}$ -module functor  $F : \mathcal{M} \rightarrow \mathcal{M}$ , by  $\eta^F : \text{id}_{\mathcal{N}} \Rightarrow FF^l$  the unit and by  $\epsilon^F : F^l F \Rightarrow \text{id}_{\mathcal{M}}$  the counit of this adjunction, then the component morphisms  $\omega^F : F^{ll} \Rightarrow F$  of the pivotal structure are characterised by the condition

$$\theta_{F^l(n)}^{\mathcal{M}}(\beta \circ \epsilon_m^F \circ F^l(\alpha)) = \theta_n^{\mathcal{N}}(\epsilon_n^{F^l} \circ F^{ll}(\beta) \circ \omega_m^{F-1} \circ \alpha) \quad (23)$$

for all  $\alpha \in \text{Hom}_{\mathcal{N}}(n, F(m))$  and  $\beta \in \text{Hom}_{\mathcal{M}}(m, F^l(n))$ . This condition encodes the chain of natural isomorphisms that defines  $\omega^F$  in equation (4.14) in [S13].

Condition (23) implies an identity that generalises Corollary 1.19 to  $\mathcal{C}$ -module functors that are not endofunctors. It is obtained from the (co)evaluations for the right duals induced by  $\omega^F : F^{ll} \Rightarrow F$

$$\eta'^F = F^l \omega^F \circ \eta^{F^l} : \text{id}_{\mathcal{M}} \Rightarrow F^l F \quad \epsilon'^F = \epsilon^{F^l} \circ \omega^{F-1} F^l : FF^l \Rightarrow \text{id}_{\mathcal{N}}. \quad (24)$$

**Corollary 1.20.** Let  $\mathcal{C}$  be a pivotal fusion category and  $\mathcal{M}, \mathcal{N}$   $\mathcal{C}$ -module categories with  $\mathcal{C}$ -module traces. Then any  $\mathcal{C}$ -module functor  $F : \mathcal{M} \rightarrow \mathcal{N}$  satisfies

$$\theta_m^{\mathcal{M}}(\epsilon_m^F \circ F^l(\alpha) \circ \eta_m'^F) = \theta_{F(m)}^{\mathcal{N}}(\alpha) \quad (25)$$

for all  $m \in \text{Ob}\mathcal{M}$ ,  $n \in \text{Ob}\mathcal{N}$  and morphisms  $\alpha : F(m) \rightarrow F(m)$ .

*Proof.* This follows by setting  $n = F(m)$  and  $\beta = \eta_m'^F = F^l(\omega_m^F) \circ \eta_m^{F^l} : m \rightarrow F^l F(m)$  in (23). By cyclicity of  $\theta^{\mathcal{M}}$ , the left-hand side of (23) is equal to the left-hand side of (25). The right-hand side of (23) can be simplified using the naturality of  $\omega^F$  and the for the defining identities for the unit and counit of an adjunction and yields the right-hand side of (25).  $\square$

Note that for an endofunctor  $F : \mathcal{M} \rightarrow \mathcal{M}$ , condition (25) is just the partial trace condition from Definition 1.13 for the  $\text{End}_{\mathcal{C}}(\mathcal{M})$ -module structure on  $\mathcal{M}$  and Corollary 1.20 reduces to Corollary 1.19.

## 2 Diagrammatic calculus

### 2.1 Diagrams for spherical fusion categories

We use the usual graphical calculus for monoidal categories, suppressing the tensor unit and coherence data. Morphisms in diagrams are composed from top to bottom and tensor products from the right to the left.

We also use the usual diagrammatic notation for the duals. If the categories are pivotal, we draw oriented lines for the objects, where a line that is directed downwards and labeled  $x^*$  is replaced by a line that is directed upwards and labeled  $x$ . Lines without arrows are assumed to be oriented downwards. The diagrams for the (co)evaluations from (1) and (3) are

$$\begin{array}{cccc} \begin{array}{c} \text{---} \\ \curvearrowright \\ \text{---} \end{array} & \begin{array}{c} x \\ \curvearrowright \\ \text{---} \end{array} & \begin{array}{c} \curvearrowleft \\ \text{---} \\ x \end{array} & \begin{array}{c} x \\ \curvearrowleft \\ \text{---} \end{array} \\ \text{coev}_x^L : e \rightarrow x \otimes x^* & \text{ev}_x^L : x^* \otimes x \rightarrow e & \text{coev}_x^R : e \rightarrow x^* \otimes x & \text{ev}_x^R : x \otimes x^* \rightarrow e, \end{array} \quad (26)$$

and the defining conditions (2) on the left duals read

$$\begin{array}{ccc} \begin{array}{c} \text{---} \\ \curvearrowright \\ \text{---} \\ \text{---} \end{array} & = & \begin{array}{c} \text{---} \\ \text{---} \end{array} \\ \begin{array}{c} \text{---} \\ \curvearrowleft \\ \text{---} \\ \text{---} \end{array} & = & \begin{array}{c} \text{---} \\ \text{---} \end{array} \end{array} \quad (27)$$

Pivotality is expressed in the diagram

$$(28)$$

for all morphisms  $\nu : x \rightarrow y$ , and a pivotal category is spherical iff

$$(29)$$

## 2.2 Diagrams for (bi)module categories, functors and natural transformations

In the following, we use diagrammatic calculus for 2-categories and apply it to the 2-categories  $\text{Cat}$  of (small) categories, functors and natural transformations and to the 2-categories  $\text{Bimod}^\theta(\mathcal{C}, \mathcal{D})$  and  $\text{Mod}^\theta(\mathcal{C})$  from Theorem 1.17. The diagrammatic calculus goes back to Joyal and Street [JS91] in the smooth setting, and was also studied by Barrett et al. [BMS12] in the PL setting. We summarise the description from [BMS12].

### 2.2.1 Diagrams for 2-categories

A **2-category diagram** for a 2-category  $\mathcal{C}$  is a direct generalisation of a diagram for a monoidal category. It is a PL stratification  $\emptyset \subset X^0 \subset X^1 \subset X^2 = [0, 1]^2$  of the unit square. Elements of  $X^0$  are called **vertices**, connected components of  $X^1 \setminus X^0$  **lines** and connected components of  $X^2 \setminus X^1$  **regions** of the diagram. Lines may end at the top and bottom of the square only and all vertices are in the interior. A diagram is called **progressive**, if its horizontal projection is regular, i. e. its restriction to each line is a PL isomorphism onto the image. It is called **generic**, if no two vertices are at the same height. In pictures, we often omit the unit square that borders the diagram for better legibility.

Regions in the diagram are labeled by objects of  $\mathcal{C}$ , lines by 1-morphisms and vertices by 2-morphisms. Diagrams are read from top to bottom, and can be composed horizontally if the top of one diagram matches the bottom of the other. This corresponds to the vertical composition of 2-morphisms. Horizontal composition is from the right to the left. This is analogous to the usual calculus for monoidal categories, up to the fact that regions of the diagrams are labeled with objects, lines with 1-morphisms and vertices with 2-morphisms.

A diagram whose right-hand side is labeled by an object  $\mathcal{A}$ , whose left-hand side by an object  $\mathcal{B}$  and with lines at its upper and lower boundary labeled with 1-morphisms  $F_1, \dots, F_n$  and  $G_1, \dots, G_m$ , from the right to the left, describes a 2-morphism  $\nu : F_n \cdots F_1 \Rightarrow G_m \cdots G_1$  between 1-morphisms  $F_n \cdots F_1 : \mathcal{A} \rightarrow \mathcal{B}$  and  $G_m \cdots G_1 : \mathcal{A} \rightarrow \mathcal{B}$ . This 2-morphism is obtained by first horizontally composing the 2-morphisms at the vertices in the diagram with the 1-morphisms on the lines to the left and right and then composing the resulting 2-morphisms in their vertical order.

**Example 2.1.** *The diagram*

$$(30)$$

for the 2-category  $\mathcal{C}at$  with functors  $K, L : \mathcal{M} \rightarrow \mathcal{P}$ ,  $F : \mathcal{P} \rightarrow \mathcal{N}$ ,  $H : \mathcal{P} \rightarrow \mathcal{Q}$  and  $G : \mathcal{Q} \rightarrow \mathcal{N}$  and natural transformations  $\sigma : K \Rightarrow L$  and  $\rho : F \Rightarrow GH$  describes the natural transformation  $(\rho L) \circ (F\sigma) : FK \Rightarrow GHL$  with component morphisms  $\rho_{L(m)} \circ F(\sigma_m) : FK(m) \rightarrow FL(m) \rightarrow GHL(m)$ .

It is shown in [JS91, Th. 1.12] in the smooth context, see also [BMS12, Th. 2.12] for the PL setting, that 2-category diagrams represent the same 2-morphisms if they are related by PL isotopies that start at the identity and define a one-parameter family of isomorphisms of diagrams. An isomorphism of diagrams is a PL homeomorphism that is the identity on the boundary of the diagram and such that the homeomorphism and its inverse preserve all skeleta of the diagram. This invariance is a consequence of the identity

$$\begin{array}{ccc}
 \begin{array}{c} F \\ \vdots \\ \nu \bullet \\ \vdots \\ G \end{array} & \begin{array}{c} H \\ \vdots \\ \bullet \\ \vdots \\ K \end{array} & \begin{array}{c} \mathcal{C} \\ \mathcal{B} \\ \mathcal{A} \end{array} \\
 & \mu & \\
 & \bullet & \\
 & \vdots & \\
 & G & K
 \end{array} = \begin{array}{ccc}
 \begin{array}{c} F \\ \vdots \\ \nu \bullet \\ \vdots \\ G \end{array} & \begin{array}{c} H \\ \vdots \\ \bullet \\ \vdots \\ K \end{array} & \begin{array}{c} \mathcal{C} \\ \mathcal{B} \\ \mathcal{A} \end{array} \\
 & \mu & \\
 & \bullet & \\
 & \vdots & \\
 & G & K
 \end{array} \tag{31}
 \end{array}$$

$$(G\mu) \circ (\nu H) = (\nu K) \circ (F\mu).$$

for all 1-morphisms  $F, G : \mathcal{B} \rightarrow \mathcal{C}$  and  $H, K : \mathcal{A} \rightarrow \mathcal{B}$  and 2-morphisms  $\nu : F \Rightarrow G$  and  $\mu : H \Rightarrow K$ . It allows one to associate 2-morphisms to non-generic diagrams by perturbing them to generic ones. In the 2-category  $\mathcal{C}at$  this identity expresses the naturality of natural transformations.

### 2.2.2 Diagrams for pivotal 2-categories

If the 2-category under consideration is a pivotal 2-category in the sense [S15, Def. A.12] or, more strictly, a planar 2-category in the sense of [BMS12, Def. 3.2.1], we use the diagrams for planar 2-categories introduced in [BMS12, Def. 3.5]. The main examples are  $\text{Mod}^\theta(\mathcal{C})$  and  $\text{Bimod}^\theta(\mathcal{C}, \mathcal{D})$  from Theorem 1.17.

The diagrams for pivotal 2-categories are essentially the diagrams for a pivotal monoidal category. The only difference is that regions of the diagram are labeled with objects, lines with 1-morphisms and vertices with 2-morphisms. As for a pivotal category, the pivotal structure implies that left duals are also right duals and that double duals of a 1-morphism  $F$  are 2-isomorphic to  $F$ . We thus denote the duals of a 1-morphism  $F$  by a dashed line labeled  $F$  with an arrow that points upwards. Lines without arrows are assumed to be oriented downwards. The (co)evaluations of the duals, which generalise (1) and (3), are then given by the diagrams

$$\begin{array}{cccc}
 \begin{array}{c} \text{---} \\ \curvearrowright \\ \mathcal{A} \rightarrow \mathcal{B} \\ \text{---} \\ F \end{array} & \begin{array}{c} \text{---} \\ \curvearrowleft \\ \mathcal{B} \rightarrow \mathcal{A} \\ \text{---} \\ F \end{array} & \begin{array}{c} \text{---} \\ \curvearrowright \\ \mathcal{B} \rightarrow \mathcal{A} \\ \text{---} \\ F \end{array} & \begin{array}{c} \text{---} \\ \curvearrowleft \\ \mathcal{A} \rightarrow \mathcal{B} \\ \text{---} \\ F \end{array} \\
 \eta^F : \text{id}_{\mathcal{B}} \Rightarrow FF^l & \epsilon^F : F^l F \Rightarrow \text{id}_{\mathcal{A}} & \eta'^F : \text{id}_{\mathcal{A}} \Rightarrow F^l F & \epsilon'^F : FF^l \Rightarrow \text{id}_{\mathcal{B}}
 \end{array} \tag{32}$$

that generalise (26). The defining conditions on the left (co)evaluations, which generalise (2), read

$$\begin{array}{ccc}
 \begin{array}{c} \text{---} \\ \curvearrowright \\ \mathcal{B} \rightarrow \mathcal{A} \\ \text{---} \\ F \end{array} & = & \begin{array}{c} \text{---} \\ \text{---} \\ \mathcal{B} \rightarrow \mathcal{A} \\ \text{---} \\ F \end{array} \\
 \begin{array}{c} \text{---} \\ \curvearrowleft \\ \mathcal{A} \rightarrow \mathcal{B} \\ \text{---} \\ F \end{array} & = & \begin{array}{c} \text{---} \\ \text{---} \\ \mathcal{A} \rightarrow \mathcal{B} \\ \text{---} \\ F \end{array}
 \end{array} \tag{33}$$

and the pivotality condition that generalises (28) is expressed in the diagrammatic identity

$$\begin{array}{ccc}
 \begin{array}{c} \text{---} \\ \curvearrowright \\ \mathcal{B} \rightarrow \mathcal{A} \\ \text{---} \\ F \end{array} & = & \begin{array}{c} \text{---} \\ \text{---} \\ \mathcal{B} \rightarrow \mathcal{A} \\ \text{---} \\ F \end{array} \\
 \begin{array}{c} \text{---} \\ \curvearrowleft \\ \mathcal{A} \rightarrow \mathcal{B} \\ \text{---} \\ F \end{array} & = & \begin{array}{c} \text{---} \\ \text{---} \\ \mathcal{A} \rightarrow \mathcal{B} \\ \text{---} \\ F \end{array}
 \end{array} \tag{34}$$

In the diagrammatic calculus the pivotal structure allows one to drop the requirement that the diagrams are *progressive*, i. e. that the horizontal projection of the diagram is regular. Instead, singular points of the projection are labeled with (co)evaluations. Although we draw them as smooth maxima and minima for diagrammatic convenience, they represent vertices in a PL diagram. While a diagram with maxima and minima is never progressive itself, it stands for the progressive diagram obtained by replacing maxima and minima with vertices labeled by (co)evaluations, see [BMS12, Sec. 3.2].

This enlarges the class of diagrams that represent the same 2-morphism. It is shown in [BMS12, Th. 3.9] that planar 2-category diagrams related by orientation preserving PL homeomorphisms that preserve the unit square represent the same 2-morphism if their labels are transformed accordingly. This means that the objects labeling the regions and the 1-morphisms labeling lines of the diagrams must coincide, while the 2-morphisms at the vertices are composed with the (co)evaluations of the 1-morphisms at the incident lines.

Composing a 2-morphism  $\nu : F_n \cdots F_1 \Rightarrow G_m \cdots G_1$  with the (co)evaluations for  $F_n$  and  $G_1$  from (32) transforms it into 2-morphisms  $\nu' : F_{n-1} \cdots F_1 \Rightarrow F_n^l G_m \cdots G_1$  and  $\nu'' : F_n \cdots F_1 G_1^l \Rightarrow G_m \cdots G_2$ .

(35)

The pivotal 2-category structure ensures that all diagrams that are related by the two moves in (35) and have the same edge labels represent the same 2-morphism.

**Definition 2.2.** *Let  $\mathcal{C}$  be a 2-category. A **cyclic transformation** of a 2-morphism  $\nu : F_n \cdots F_1 \Rightarrow G_m \cdots G_1$  is a 2-morphism obtained by applying a finite sequence of the moves in (35). Two 2-morphisms  $\nu$  and  $\nu'$  are called **cyclically equivalent** if they are related by a cyclic transformation.*

In pictures, we sometimes suppress the change in the labeling and the units and counits of the adjunctions and use the label  $\nu$  for a cyclic equivalence class of 2-morphisms.

### 2.2.3 Mixed diagrams

The diagrams for pivotal 2-categories in the previous section can be used to describe morphisms in the pivotal 2-categories  $\text{Bimod}^\theta(\mathcal{C}, \mathcal{D})$  and  $\text{Mod}^\theta(\mathcal{C})$  from Theorem 1.17. In this case, regions are labeled with (bi)module categories with (bi)module traces, lines with (bi)module functors and vertices with (bi)module natural transformations. The duals are given by adjoint functors and the pivot is the natural isomorphism between a bimodule functor and its double adjoint.

To describe the interaction of the data in  $\text{Bimod}^\theta(\mathcal{C}, \mathcal{D})$  with data from  $\mathcal{C}$  and  $\mathcal{D}$ , we generalise pivotal 2-category diagrams. We consider diagrams with additional lines and vertices labeled with data from  $\mathcal{C}$  and  $\mathcal{D}$ . These diagrams may involve crossings of lines labeled by  $\mathcal{C}$  and  $\mathcal{D}$  as well as crossings of such lines with lines labeled by  $(\mathcal{C}, \mathcal{D})$ -bimodule functors.

**Definition 2.3.** Let  $\mathcal{C}, \mathcal{D}$  be spherical fusion categories. A **mixed diagram** for  $\text{Bimod}^\theta(\mathcal{C}, \mathcal{D})$  is a diagram obtained by superimposing a diagram  $D$  for  $\text{Bimod}^\theta(\mathcal{C}, \mathcal{D})$  with diagrams  $D_{\mathcal{C}}$  for  $\mathcal{C}$  and  $D_{\mathcal{D}}$  for  $\mathcal{D}^{rev}$ . It is called **generic** if

- no vertex of any diagram is on a line or vertex of any of the others,
- each point is on at most two lines from distinct diagrams,
- each point in the interior that is on lines of two distinct diagrams is a transversal crossing.

While each diagram for  $\text{Bimod}^\theta(\mathcal{C}, \mathcal{D})$  describes a 2-morphism in  $\text{Bimod}^\theta(\mathcal{C}, \mathcal{D})$ , a mixed diagram for  $\text{Bimod}^\theta(\mathcal{C}, \mathcal{D})$  can be viewed as a 2-category diagram for  $\text{Cat}$ .

For this recall from Remark 1.3 that each  $\mathcal{C}$ -module category  $\mathcal{M}$  defines a monoidal functor  $F : \mathcal{C} \rightarrow \text{End}(\mathcal{M})$  that assigns to  $c \in \text{Ob}\mathcal{C}$  the functor  $c \triangleright - : \mathcal{M} \rightarrow \mathcal{M}$  and to a morphism  $\alpha : c \rightarrow c'$  the natural transformation  $\alpha \triangleright - : c \triangleright - \Rightarrow c' \triangleright -$ . Its monoidal structure is given by the coherence isomorphisms from Definition 1.2.

The monoidal functor  $F : \mathcal{C} \rightarrow \text{End}(\mathcal{M})$  preserves duals. The adjoint of  $c \triangleright - : \mathcal{M} \rightarrow \mathcal{M}$  is  $c^* \triangleright - : \mathcal{M} \rightarrow \mathcal{M}$  with the (co)units of the adjunction given by the (co)evaluations from (1) and (3), up to coherence data:

$$\begin{aligned} \eta^{c \triangleright -} &= c_{c, c^*, -} \circ (\text{coev}_c^L \triangleright -) & \epsilon^{c \triangleright -} &= (\text{ev}_c^L \triangleright -) \circ c_{c^*, c, -}^{-1} \\ \eta'^{c \triangleright -} &= c_{c^*, c, -} \circ (\text{coev}_c^R \triangleright -) & \epsilon'^{c \triangleright -} &= (\text{ev}_c^R \triangleright -) \circ c_{c, c^*, -}^{-1}. \end{aligned}$$

The pentagon relation (6) and triangle relation (7) allow one to suppress bracketings and action of the unit object in expressions involving multiple action functors. They lead to strictification and coherence theorems for module categories that generalise the ones for monoidal categories, see [EGNO, Rem. 7.2.4].

One can therefore interpret diagrams for  $\mathcal{C}$  as 2-category diagrams for  $\text{Cat}$ , whose regions are labeled by a  $\mathcal{C}$ -module category  $\mathcal{M}$  and whose lines by action functors  $c \triangleright -$  for  $c \in \text{Ob}\mathcal{C}$ . Vertices are labeled by natural transformations that are composites of natural transformations  $\alpha \triangleright -$  for morphisms  $\alpha$  in  $\mathcal{C}$  with the coherence isomorphisms  $c$  and  $\gamma$ . The result is a natural transformation between the endofunctors given by the objects at the top and bottom of the diagrams. It is unique up to coherence data.

Analogous statements hold for  $\mathcal{D}$ -right module categories  $\mathcal{M}$ . The only difference is that the action is a right action and one has an associated monoidal functor  $F : \mathcal{D}^{rev} \rightarrow \text{End}(\mathcal{M})$ , whose coherence data is given by the natural isomorphisms  $d_{-, i, j} : (- \triangleleft i) \triangleleft j \Rightarrow - \triangleleft (i \otimes j)$  and  $\delta : - \triangleleft e \Rightarrow \text{id}_{\mathcal{M}}$  from Definition 1.2.

In this way, one can interpret any mixed diagram for  $\text{Bimod}^\theta(\mathcal{C}, \mathcal{D})$  *without crossings* as a 2-category diagram for  $\text{Cat}$  in which the objects and morphisms from  $\mathcal{C}$  and  $\mathcal{D}$  are replaced by the associated action functors and natural transformations for the bimodule category labeling their region in the diagram.

Crossings of lines labeled by  $c \in \text{Ob}\mathcal{C}$  and  $d \in \text{Ob}\mathcal{D}$  and crossings of such lines with lines labeled by (bi)module functors  $F$  also have a direct interpretation. The former correspond to the natural isomorphisms  $b_{c, -, d}$  from Definition 1.2 and the latter to the natural isomorphisms  $s^F$  and  $t^F$  from Definition 1.8. We represent them as over- and undercrossings.

**Definition 2.4.** Let  $D'$  be a generic mixed diagram for  $\text{Bimod}^\theta(\mathcal{C}, \mathcal{D})$  that superimposes diagrams  $D$ ,  $D_{\mathcal{C}}$  and  $D_{\mathcal{D}}$ . The 2-category diagram associated to  $D'$  is the diagram obtained by

- replacing labels  $c \in \text{Ob}\mathcal{C}$ ,  $d \in \text{Ob}\mathcal{D}$  in a region labeled  $\mathcal{M}$  with  $c \triangleright - : \mathcal{M} \rightarrow \mathcal{M}$ ,  $- \triangleleft d : \mathcal{M} \rightarrow \mathcal{M}$ ,
- replacing morphism labels  $\alpha$  and  $\beta$  from  $\mathcal{C}$  and  $\mathcal{D}$  by natural transformations composed of  $\alpha \triangleright -$  and  $- \triangleleft \beta$  and the coherence isomorphisms  $c, \gamma$  and  $d, \delta$  from Definition 1.2,
- transforming crossings of a line from  $D_{\mathcal{C}}$  with a line from  $D$  or  $D_{\mathcal{D}}$  into overcrossings of the line from  $D_{\mathcal{C}}$  and crossings of a line from  $D$  with a line from  $D_{\mathcal{D}}$  into overcrossings of the line from  $D$ ,
- labeling the crossing points with natural transformations as follows:
  - crossings of a line labeled by  $c \in \text{Ob}\mathcal{C}$  with a line labeled by  $d \in \text{Ob}\mathcal{D}$  by the natural isomorphism  $b_{c, -, d} : (c \triangleright -) \triangleleft d \Rightarrow c \triangleright (- \triangleleft d)$  and its inverse from Definition 1.2

$$\begin{array}{ccc} \begin{array}{c} d \quad c \\ \diagdown \quad \diagup \\ \diagup \quad \diagdown \\ c \quad d \end{array} & & \begin{array}{c} c \quad d \\ \diagdown \quad \diagup \\ \diagup \quad \diagdown \\ c \quad d \end{array} \\ b_{c, -, d} : (c \triangleright -) \triangleleft d \Rightarrow c \triangleright (- \triangleleft d) & & b_{c, -, d}^{-1} : c \triangleright (- \triangleleft d) \Rightarrow (c \triangleright -) \triangleleft d, \end{array} \tag{36}$$

- crossings of a line labeled by  $c \in \text{Ob}\mathcal{C}$  with a line from  $\mathcal{D}$  labeled  $F$  by the natural isomorphism  $s^F : F(c \triangleright -) \Rightarrow c \triangleright F(-)$  and its inverse from Definition 1.8

$$\begin{array}{ccc}
\begin{array}{c} F \quad c \\ \diagdown \quad \diagup \\ \diagup \quad \diagdown \\ s_{c,-}^F : F(c \triangleright -) \Rightarrow c \triangleright F(-) \end{array} & & \begin{array}{c} c \quad F \\ \diagdown \quad \diagup \\ \diagup \quad \diagdown \\ s_{c,-}^{F^{-1}} : c \triangleright F(-) \Rightarrow F(c \triangleright -), \end{array} \\
\end{array} \tag{37}$$

- crossings of a line labeled by  $d \in \text{Ob}\mathcal{D}$  with a line from  $\mathcal{C}$  labeled  $F$  by the natural isomorphism  $t^F : F(-) \triangleleft d \Rightarrow F(- \triangleleft d)$  and its inverse from Definition 1.8

$$\begin{array}{ccc}
\begin{array}{c} d \quad F \\ \diagdown \quad \diagup \\ \diagup \quad \diagdown \\ t_{-,d}^F : F(-) \triangleleft d \Rightarrow F(- \triangleleft d) \end{array} & & \begin{array}{c} F \quad d \\ \diagdown \quad \diagup \\ \diagup \quad \diagdown \\ t_{-,d}^{F^{-1}} : F(- \triangleleft d) \Rightarrow F(-) \triangleleft d. \end{array} \\
\end{array} \tag{38}$$

In this way, every generic mixed diagram defines a 2-category diagram for  $\text{Cat}$  that represents a unique natural transformation between the composites of the functors at the top and bottom of the diagram.

**Definition 2.5.** *The evaluation of a generic mixed diagram for  $\text{Bimod}^\theta(\mathcal{C}, \mathcal{D})$  is the natural transformation represented by the associated 2-category diagram.*

The properties of the coherence isomorphisms associated to crossing points allow one to define the evaluation of non-generic mixed diagrams. The invertibility of the isomorphisms  $b$ ,  $s^F$  and  $t^F$  translates into diagrammatic identities that are an analogue of the Reidemeister 2 move for a braid diagram

$$\begin{array}{ccccccccc}
\begin{array}{c} d \quad c \\ \diagdown \quad \diagup \\ \diagup \quad \diagdown \\ = \\ \begin{array}{c} | \\ | \end{array} \end{array} & & \begin{array}{c} d \quad c \\ \diagdown \quad \diagup \\ \diagup \quad \diagdown \\ = \\ \begin{array}{c} | \\ | \end{array} \end{array} & & \begin{array}{c} c \quad d \\ \diagdown \quad \diagup \\ \diagup \quad \diagdown \\ = \\ \begin{array}{c} | \\ | \end{array} \end{array} & & \begin{array}{c} F \quad c \\ \diagdown \quad \diagup \\ \diagup \quad \diagdown \\ = \\ \begin{array}{c} | \\ | \end{array} \end{array} & & \begin{array}{c} c \quad F \\ \diagdown \quad \diagup \\ \diagup \quad \diagdown \\ = \\ \begin{array}{c} | \\ | \end{array} \end{array} & & \begin{array}{c} d \quad F \\ \diagdown \quad \diagup \\ \diagup \quad \diagdown \\ = \\ \begin{array}{c} | \\ | \end{array} \end{array} & & \begin{array}{c} F \quad d \\ \diagdown \quad \diagup \\ \diagup \quad \diagdown \\ = \\ \begin{array}{c} | \\ | \end{array} \end{array} \\
\end{array} \tag{39}$$

Similarly, the hexagon relation (17) for a  $(\mathcal{C}, \mathcal{D})$ -bimodule functor translates into a diagrammatic identity that is an analogue of the Reidemeister 3 move for a braid diagram

$$\begin{array}{ccc}
\begin{array}{c} F \quad d \quad c \\ \diagdown \quad \diagup \quad \diagup \\ \diagup \quad \diagdown \quad \diagdown \\ = \\ \begin{array}{c} F \quad d \quad c \\ \diagdown \quad \diagup \quad \diagup \\ \diagup \quad \diagdown \quad \diagdown \end{array} \end{array} & & \begin{array}{c} F \quad d \quad c \\ \diagdown \quad \diagup \quad \diagup \\ \diagup \quad \diagdown \quad \diagdown \end{array} \\
\end{array} \tag{40}$$

The naturality conditions from Definitions 1.2 and 1.8 and the conditions on a bimodule natural transformation from (18) and (19) allow one to slide vertices under or over crossings. The naturality of the isomorphisms  $b_{c,d,m} : (c \triangleright m) \triangleleft d \rightarrow c \triangleright (m \triangleleft d)$  in  $c$  and  $d$  is expressed as

$$\begin{array}{ccc}
\begin{array}{c} d \quad c \\ \diagdown \quad \diagup \\ \diagup \quad \diagdown \\ \alpha \\ c' \end{array} = \begin{array}{c} d \quad c \\ \diagdown \quad \diagup \\ \diagup \quad \diagdown \\ \alpha \\ c' \end{array} & & \begin{array}{c} d \quad c \\ \diagdown \quad \diagup \\ \diagup \quad \diagdown \\ \beta \\ d' \end{array} = \begin{array}{c} d \quad c \\ \diagdown \quad \diagup \\ \diagup \quad \diagdown \\ \beta \\ d' \end{array} \\
\end{array} \tag{41}$$

The naturality of  $s_{c,m}^F : F(c \triangleright m) \rightarrow c \triangleright F(m)$  and  $t_{m,d}^F : F(m) \triangleleft d \rightarrow F(m \triangleleft d)$  in  $c$  and  $d$  implies

$$\begin{array}{ccc}
\begin{array}{c} F \quad c \\ \diagdown \quad \diagup \\ \diagup \quad \diagdown \\ \alpha \\ c' \end{array} = \begin{array}{c} F \quad c \\ \diagdown \quad \diagup \\ \diagup \quad \diagdown \\ \alpha \\ c' \end{array} & & \begin{array}{c} d \quad F \\ \diagdown \quad \diagup \\ \diagup \quad \diagdown \\ \beta \\ d' \end{array} = \begin{array}{c} d \quad F \\ \diagdown \quad \diagup \\ \diagup \quad \diagdown \\ \beta \\ d' \end{array} \\
\end{array} \tag{42}$$



The defining conditions (18) and (19) on a  $\mathcal{C}$ -module and  $\mathcal{D}$ -right module natural transformation  $\nu : F \Rightarrow G$  give the diagrammatic identities

(43)

In particular, identities (41) and (42) can be applied to the (co)evaluations for the duals in  $\mathcal{C}$  and  $\mathcal{D}$ . This allows one to slide maxima and minima of lines labeled with objects in  $\mathcal{C}$  and  $\mathcal{D}$  over or under lines labeled with bimodule functors. Similarly, the (co)evaluations for 1-morphisms in  $\text{Bimod}^\theta(\mathcal{C}, \mathcal{D})$  are  $(\mathcal{C}, \mathcal{D})$ -bimodule natural transformations and hence satisfy identity (43). This allows one to slide maxima and minima of lines labeled with bimodule functors over or under lines labeled with objects from  $\mathcal{C}$  or  $\mathcal{D}$ .

Note that the diagrammatic identities involving only lines and vertices labeled by  $\mathcal{C}$  and  $\mathcal{D}$  are special cases of the ones involving data from  $\text{Bimod}^\theta(\mathcal{C}, \mathcal{D})$ . The diagrams (36) for the natural isomorphism  $b_{c, -, d} : (c \triangleright -) \triangleleft d \Rightarrow c \triangleright (- \triangleleft d)$  are just the diagrams (37) and (38) for the  $\mathcal{C}$ -module functor  $- \triangleleft d : \mathcal{M} \rightarrow \mathcal{M}$  and the  $\mathcal{D}$ -right module functor  $c \triangleright - : \mathcal{M} \rightarrow \mathcal{M}$ . The identities (41) are a special case of (42) and (43).

The diagrammatic identities (39) to (43) allow one to define the evaluation of non-generic mixed diagrams. Any point of a mixed diagram that lies on more than two lines from distinct diagrams is on three lines, one from each diagram  $D, D_{\mathcal{C}}$  and  $D_{\mathcal{D}}$ . By slightly displacing the lines one can transform such a triple point into multiple crossings of two lines. The diagrammatic identities for the crossings and their inverses and the identity (40) ensures that all diagrams obtained in this way have the same evaluation.

Similarly, if there is a point on two lines from different diagrams that is not a transversal crossing, then by slightly displacing the lines one can either create a double crossing or ensure that the lines do not meet. Identities (39) ensure that all resulting diagrams have the same evaluations. Any vertex on two lines from different diagrams can be displaced slightly from the crossing. Identities (41), (42) and (43) ensure that all ways of doing so yield diagrams with the same evaluation.

**Definition 2.6.** *The evaluation of a mixed diagram for  $\text{Bimod}^\theta(\mathcal{C}, \mathcal{D})$  is defined as the evaluation of any generic mixed diagram obtained by slightly displacing the lines and vertices of the diagram.*

## 2.3 Polygon diagrams

### 2.3.1 Action on category diagrams

We also use the diagrammatic calculus to describe evaluation functors  $\text{ev} : \text{Fun}(\mathcal{M}, \mathcal{N}) \times \mathcal{M} \rightarrow \mathcal{N}$  that sends a pair  $(F, m)$  of a functor  $F : \mathcal{M} \rightarrow \mathcal{N}$  and an object  $m \in \text{Ob}\mathcal{M}$  to the object  $F(m)$  and a pair  $(\nu, \alpha)$  of a natural transformation  $\nu : F \Rightarrow G$  and a morphism  $\alpha : m \rightarrow m'$  to the morphism  $\nu_{m'} \circ F(\alpha) = G(\alpha) \circ \nu_m : F(m) \rightarrow G(m')$ .

For this, we describe objects in  $\mathcal{M}$  by a thick vertical line and morphisms between them by vertices on this line. Composition of morphisms is from the top to the bottom, and identity morphisms are omitted from the diagrams. Thus, a line whose top end is labeled by an object  $m$  in  $\mathcal{M}$  and whose bottom end by an object  $m'$  in  $\mathcal{M}$  describes a morphism  $\alpha : m \rightarrow m'$  in  $\mathcal{M}$ .

The diagram for the evaluation  $\text{ev}(\nu, \alpha) : F(m) \rightarrow G(m')$  of a natural transformation  $\nu : F \Rightarrow G$  in  $\text{Fun}(\mathcal{M}, \mathcal{N})$  on a morphism  $\alpha : m \rightarrow m'$  in  $\mathcal{M}$  is obtained by placing the diagram for  $\alpha$  to the right of a 2-category diagram for  $\nu$ , such that no vertex of the diagram for  $\nu$  is on the same height as a vertex on the line for  $\alpha$ .

The morphism  $\text{ev}(\nu, \alpha)$  is obtained by horizontally projecting the diagram for  $\nu$  on the line for  $\alpha$ . All functors labeling dashed lines to the left of a line segment or vertex on the latter are applied to the associated objects and morphisms in  $\mathcal{M}$ . Natural transformations labeling the vertices in the diagram for  $\nu$  are composed with all functors labeling lines to their left and right and then evaluated on the object of  $\mathcal{M}$  to their right. The resulting morphisms in  $\mathcal{N}$  are then composed in order of their height.

**Example 2.7.** *The diagram*

(44)

describes the evaluation  $\text{ev}(\nu, \alpha) : FK(m) \rightarrow GHL(m'')$  of  $\nu = (\rho L) \circ (F\sigma) : FK \Rightarrow GHL$  from diagram (30) on the morphism  $\alpha = \psi \circ \phi : m \rightarrow m' \rightarrow m''$  in  $\mathcal{M}$ . It is the composite

$$\text{ev}(\nu, \alpha) : FK(m) \xrightarrow{FK(\phi)} FK(m') \xrightarrow{F(\sigma_{m'})} FL(m') \xrightarrow{\rho_L(m')} GHL(m') \xrightarrow{GHL(\psi)} GHL(m'').$$

Note that the evaluation depends only on the natural transformation represented by the diagram on the left and on the morphism represented by the line on the right, but not on the relative position of vertices in the two diagrams. This follows from naturality and corresponds to the identity

$$L(\phi) \circ \sigma_m = \sigma_{m'} \circ K(\phi) \tag{45}$$

which allows one to move vertices in the diagram for  $\text{Fun}(\mathcal{M}, \mathcal{N})$  above or below vertices on the line for  $\mathcal{M}$ . One can thus drop the requirement that the former are at different heights from the latter. Any diagram that violates this condition can be deformed into one that satisfies it by slightly displacing the vertices on the line on the right. As all ways of doing so yield the same morphism, its evaluation is defined by these deformations.

We also use diagrammatic calculus to describe the composites of morphisms of the form  $\text{ev}(\nu, \alpha)$  with general morphisms in  $\mathcal{N}$ . The resulting diagrams consist of a multicoloured thick line on the right and a diagram for  $\text{Fun}(\mathcal{M}, \mathcal{N})$  to the left whose lines may end either at the top or bottom of the diagram for  $\text{Fun}(\mathcal{M}, \mathcal{N})$  or on vertices on the thick line on the right. For instance, the following diagrams describe morphisms  $\tau : J(m) \rightarrow n$  and  $\omega : n \rightarrow J(m)$  in  $\mathcal{N}$  for a functor  $J : \mathcal{M} \rightarrow \mathcal{N}$

(46)

In this diagram, the dashed line may also stand for a composite functor and may be replaced by several dashed lines that end in a common vertex of the line on the right. For  $\mathcal{C}$ -module or  $\mathcal{D}$ -right module categories  $\mathcal{M}$  and  $\mathcal{N}$ , any dashed line may be replaced by a thin black or grey line labeled with an object of  $\mathcal{C}$  or  $\mathcal{D}$  that stands for an endofunctor  $c \triangleright -$  or  $- \triangleleft d$ .

### 2.3.2 Bordered diagrams

Using the diagrammatic calculus from the previous sections, we define a generalisation of 2-category diagrams for  $\text{Cat}$ , in which boundary segments and endpoints of lines at the boundary are also labeled with categorical data. We also allow multiple lines to end in a common point on a boundary.

**Definition 2.8.** Let  $D$  be a 2-category diagram for  $Cat$ . A **bordered diagram**  $D'$  for  $D$  is a diagram obtained by labeling boundary segments and endpoints of lines at the boundary of  $D$  as follows:

- each boundary segment with an object of the adjacent category in  $D$ ,
- an endpoint of lines labeled with functors  $F_1, \dots, F_n$ , from right to left, between a segment labeled by  $a \in \text{Ob}A$  on the right and a segment labeled by  $b \in \text{Ob}B$  on the left with a morphism  $\alpha : b \rightarrow F_n \cdots F_1(a)$  if it is on the top and with a morphism  $\alpha : F_n \cdots F_1(a) \rightarrow b$  if it is on the bottom of  $D$ .



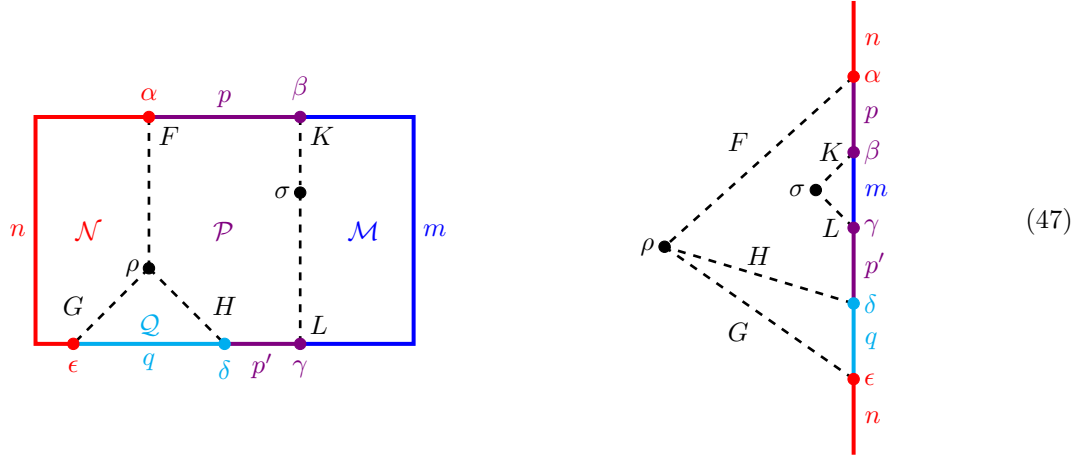
**Definition 2.9.** Let  $D$  be a 2-category diagram that represents a natural transformation  $\nu : F \Rightarrow G$  and  $D'$  a bordered diagram for  $D$  labeled with objects  $n \in \text{Ob}N$  on the left and  $m \in \text{Ob}M$  on the right.

The **evaluation** of  $D'$  is the morphism  $\text{ev}(D') = b \circ \nu_m \circ t : n \rightarrow n$ , where  $t : n \rightarrow F(m)$  and  $b : G(m) \rightarrow n$  are morphisms assigned to the top and bottom of  $D'$  as follows:

- take the image of each morphism at the top or bottom of  $D$  under the composite of all functors labeling endpoints of lines to its left,
- compose the resulting morphisms from the left to the right at the top and from the right to the left at the bottom of  $D$ .

The evaluation of a bordered diagram  $D'$  for a 2-category diagram  $D$  is represented diagrammatically by cutting its boundary square on the left-hand side and straightening its boundary to a vertical line. The naturality condition (45) allows one to move vertices of  $D$  freely with respect to boundary vertices.

**Example 2.10.** A bordered diagram  $D'$  for the diagram  $D$  in (30) and its evaluation are given by



with morphisms  $\alpha : n \rightarrow F(p)$ ,  $\beta : p \rightarrow K(m)$ ,  $\gamma : L(m) \rightarrow p'$ ,  $\delta : H(p') \rightarrow q$  and  $\epsilon : G(q) \rightarrow n$ .

Its evaluation is the morphism  $b \circ \nu_m \circ t : n \rightarrow n$ , where  $\nu = (\rho L) \circ (F\sigma) : FK \Rightarrow GHL$  is the natural transformation represented by  $D$ ,  $t = F(\beta) \circ \alpha : n \rightarrow FK(m)$  and  $b = \epsilon \circ (G\delta) \circ (GH\gamma) : GHL(m) \rightarrow n$ . By (45), this coincides with the morphism represented by the diagram on the right, which reads

$$n \xrightarrow{\alpha} F(p) \xrightarrow{F(\beta)} FK(m) \xrightarrow{F(\sigma_m)} FL(m) \xrightarrow{\gamma} F(p') \xrightarrow{\rho_{p'}} GH(p') \xrightarrow{G(\delta)} G(q) \xrightarrow{\epsilon} n.$$

### 2.3.3 Polygon diagrams

By definition, the evaluation of a bordered diagram is an endomorphism of the object labeling the left-hand side of the diagram. For bordered diagrams that involve data from the pivotal 2-category  $\text{Bimod}^\theta(\mathcal{C}, \mathcal{D})$  one can take the bimodule trace of this morphism to obtain a complex number.

**Definition 2.11.** Let  $D$  be a bordered diagram labeled with data from  $\text{Bimod}^\theta(\mathcal{C}, \mathcal{D})$ . The **cyclic evaluation** of  $D$  is the trace of its evaluation.

The cyclic evaluation of a bordered diagram has better invariance properties than the evaluation of a bordered diagram. This is most easily seen by using a diagrammatic calculus for bimodule traces, which is essentially the calculus from [S13]. If a finite semisimple category  $\mathcal{M}$  is equipped with a trace  $\theta$  as in Definition 1.13, we denote the associated morphisms  $\theta_m : \text{End}_{\mathcal{M}}(m) \rightarrow \mathbb{C}$  by horizontal lines at the upper and lower ends of the lines representing endomorphisms of  $m$ . The cyclicity condition from Definition 1.13 then takes the form

$$\begin{array}{c} \text{--- } m \\ | \\ \alpha \\ | \\ m' \\ | \\ \beta \\ | \\ m \\ \text{--- } m \end{array} = \begin{array}{c} \text{--- } m' \\ | \\ \beta \\ | \\ m \\ | \\ \alpha \\ | \\ m' \\ \text{--- } m' \end{array} \quad (48)$$

and the compatibility conditions between the trace and the  $\mathcal{C}$ -module or  $\mathcal{D}$ -right module structure read

$$\begin{array}{c} c \\ \diagdown \\ | \\ \alpha \\ | \\ m \\ \diagup \\ c \end{array} = \begin{array}{c} \text{--- } m \\ | \\ \alpha \\ | \\ m \\ \text{--- } m \end{array} \quad \begin{array}{c} d \\ \diagdown \\ | \\ \alpha \\ | \\ m \\ \diagup \\ d \end{array} = \begin{array}{c} \text{--- } m \\ | \\ \alpha \\ | \\ m \\ \text{--- } m \end{array} \quad (49)$$

If  $\mathcal{M}$  is a spherical fusion category  $\mathcal{C}$  as a module or right module category over itself, we denote the module trace by both, the diagrams for a spherical fusion category from (29) and the diagrams for a module trace as in (48) and (49), but with thin black or grey lines instead of thick coloured lines.

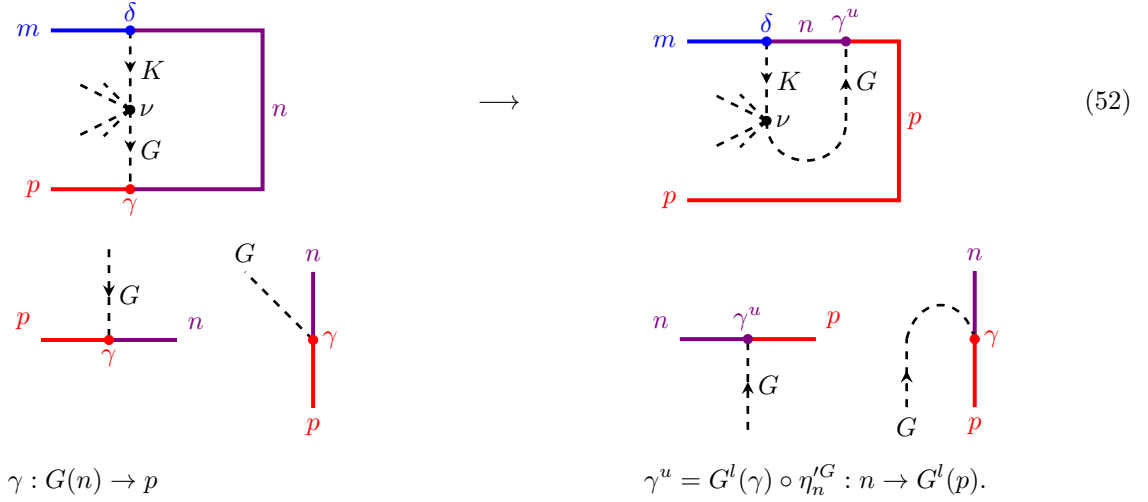
By Theorem 1.17 and Corollaries 1.18 to 1.20, (bi)module traces induce the pivotal 2-category structures on the 2-categories  $\text{Mod}^\theta(\mathcal{C})$  and  $\text{Bimod}^\theta(\mathcal{C}, \mathcal{D})$ . The defining condition (23) on the component morphisms  $\omega^F : F^l \Rightarrow F$  of the pivots and identity (25) are expressed diagrammatically as

$$\begin{array}{c} \text{--- } n \\ | \\ \mathcal{M} \\ | \\ \alpha \\ | \\ m \\ | \\ \mathcal{N} \\ | \\ \beta \\ | \\ n \\ \text{--- } n \end{array} \stackrel{(23)}{=} \begin{array}{c} \text{--- } n \\ | \\ \mathcal{N} \\ | \\ \alpha \\ | \\ m \\ | \\ \mathcal{M} \\ | \\ \beta \\ | \\ n \\ \text{--- } n \end{array} \quad \begin{array}{c} \text{--- } m \\ | \\ F \\ | \\ \mathcal{M} \\ | \\ \alpha \\ | \\ m \\ | \\ F \\ | \\ m \\ \text{--- } m \end{array} \stackrel{(25)}{=} \begin{array}{c} \text{--- } m \\ | \\ \mathcal{M} \\ | \\ \alpha \\ | \\ m \\ | \\ \mathcal{N} \\ | \\ \beta \\ | \\ m \\ \text{--- } m \end{array} \quad (50)$$

By definition, the evaluation of a bordered diagram  $D'$  for a 2-category diagram  $D$  depends on the natural transformation represented by  $D$  and on the data labeling the boundary of  $D'$ . In contrast, the *cyclic evaluation* of a bordered diagram for  $\text{Bimod}^\theta(\mathcal{C}, \mathcal{D})$  depends only on the cyclic equivalence class of the morphism represented by  $D$ , if the data at the boundary of  $D'$  is transformed accordingly.

Cyclic transformations of diagrams induce cyclic transformations of bordered diagrams. These modify the underlying natural transformation, move the object labels at the boundary and modify the morphisms at the boundary by moving them and composing them with the (co)evaluations from (32):

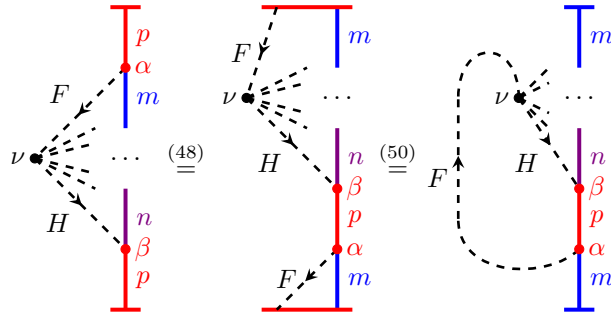
$$\begin{array}{c} \text{--- } m \\ | \\ \alpha \\ | \\ F \\ | \\ \nu \\ | \\ H \\ | \\ \beta \\ | \\ n \\ \text{--- } n \end{array} \quad \longrightarrow \quad \begin{array}{c} \text{--- } m \\ | \\ \alpha^d \\ | \\ F \\ | \\ \nu \\ | \\ H \\ | \\ \beta \\ | \\ n \\ \text{--- } n \end{array} \quad (51)$$



Identity (33) ensures that moving an endpoint from the upper (lower) to the lower (upper) side of a diagram and then up (down) again yields its original morphism label:  $(\alpha^u)^d = \alpha$  and  $(\gamma^u)^d = \gamma$ . The pivotal structure depicted in (34) ensures that this does not change the bimodule natural transformation labeling a vertex. Transforming the boundary morphisms in this way extends cyclic transformations of diagrams to cyclic transformations of bordered diagrams, as shown in Figure 1.

**Lemma 2.12.** *Let  $\mathcal{C}, \mathcal{D}$  be spherical fusion categories and  $D, D'$  bordered diagrams for  $\text{Bimod}^\theta(\mathcal{C}, \mathcal{D})$  that are related by cyclic transformations. Then the cyclic evaluations of  $D$  and  $D'$  are equal.*

*Proof.* For the cyclic transformation in (51) this follows from the cyclic invariance of the trace in (48) and its compatibility conditions with the pivotal 2-category structure of  $\text{Bimod}^\theta(\mathcal{C}, \mathcal{D})$  from (23), (25) and (50):



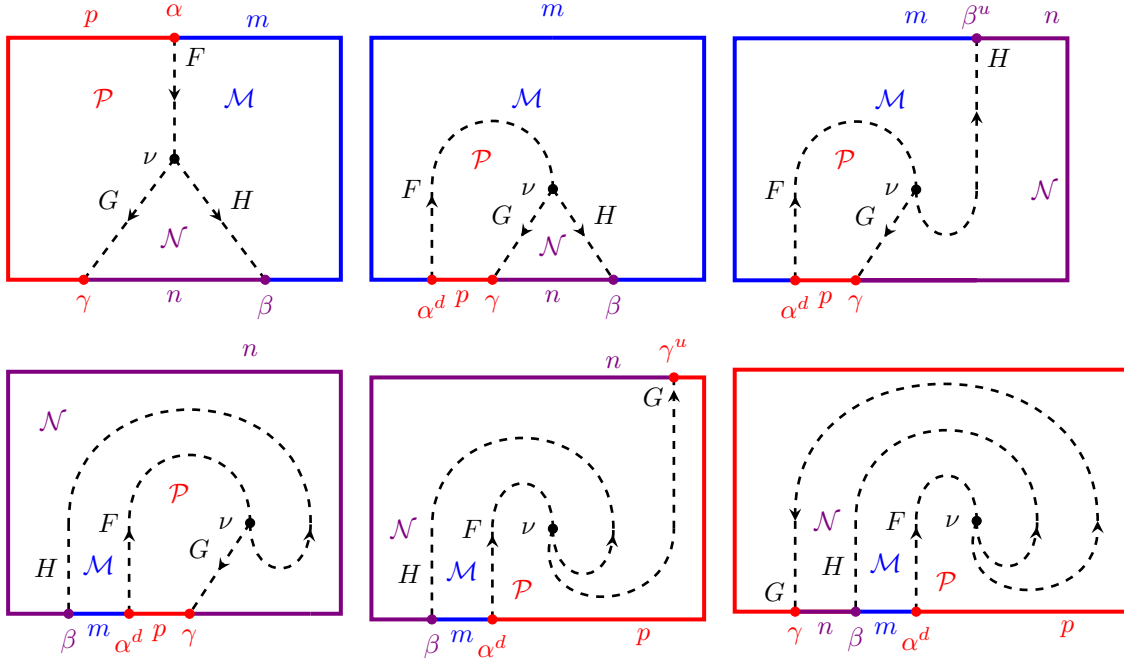
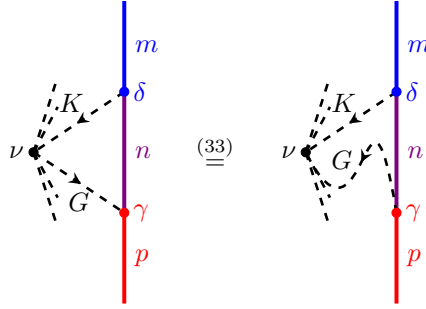


Figure 1: Some cyclic transformations of a bordered diagram.

For the cyclic transformation in (52) it is a direct consequence of identity (33):



□

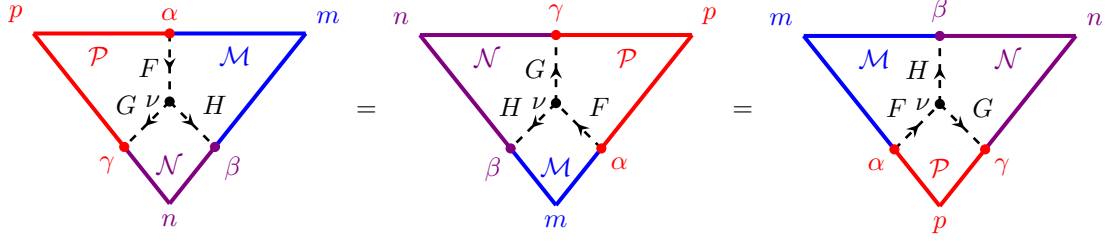
Lemma 2.12 shows that the cyclic evaluation of a bordered diagram depends only on its cyclic equivalence class. We therefore represent cyclic equivalence classes of bordered diagrams by discs with diagrams for  $\text{Bimod}^\theta(\mathcal{C}, \mathcal{D})$  in their interior and endpoints of lines at the boundary. Interior lines are oriented, and the object labels at the boundary are assigned to the segments between their endpoints. Vertices in the interior are labeled with cyclic equivalence classes of bimodule natural transformations. To the line endpoints at the boundary we assign elements of the corresponding morphism spaces at the top of a bordered diagram, if the line is incoming at the boundary, and the one for the bottom of a bordered diagram, if it is outgoing. In the following, we often represent these diagrams by polygons and hence call them polygon diagrams.

**Definition 2.13.**

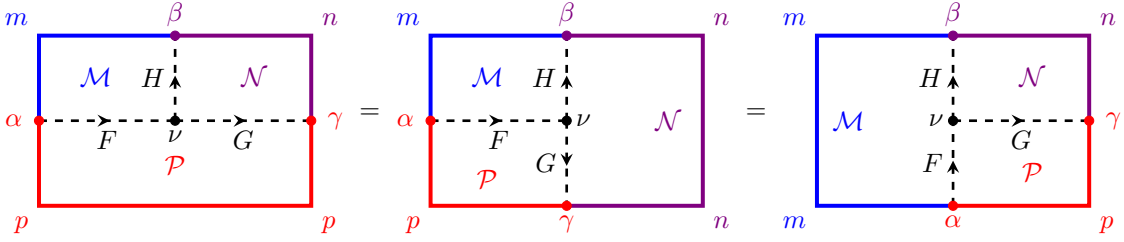
1. A **polygon diagram** for  $\text{Bimod}^\theta(\mathcal{C}, \mathcal{D})$  is a cyclic equivalence class of bordered diagrams, represented by a polygon with a diagram for  $\text{Bimod}^\theta(\mathcal{C}, \mathcal{D})$  in the interior such that all diagram lines are oriented and end in internal vertices or at the sides of the polygon.
2. The **evaluation**  $\text{ev}(D)$  of a polygon diagram  $D$  is the cyclic evaluation of the associated equivalence class of bordered diagrams.

It is clear from Lemma 2.12 that the labeling and the evaluation of a polygon diagram is invariant under rotations of the polygon. Also, one may add additional sides without line endpoints and move endpoints

of lines from a side to an adjacent side, if the labels are adjusted accordingly. For instance, some polygon diagrams for the diagram from Figure 1 are given by



and also by



Note that any diagram for a spherical fusion category  $\mathcal{C}$  that describes the trace of an endomorphism  $\phi : c \rightarrow c$  is a polygon diagram for  $\text{Bimod}^\theta(\mathcal{C}, \mathcal{C})$  with cyclic evaluation  $\text{tr}(\phi)$ . In this case, all regions of the diagram are labeled with  $\mathcal{C}$  and all lines and vertices by data from  $\mathcal{C}$ .

We also consider mirror images of polygon diagrams. If the orientation of the lines is kept fixed, there is no canonical data labeling such a mirror image. This would reverse the direction of a bimodule natural transformation labeling a vertex, which is feasible only if it is an isomorphism. However, taking a mirror image of a polygon diagram  $D$  for  $\text{Bimod}^\theta(\mathcal{C}, \mathcal{D})$  and reversing the orientation of all lines yields a polygon diagram  $D^\#$  for  $\text{Bimod}^\theta(\mathcal{D}, \mathcal{C})$ . This is obtained by replacing bimodule categories, functors and natural transformations with their opposites from Examples 1.7 and 1.10, 7. Objects and morphisms at the boundary of  $D$  are kept fixed, but a morphism  $\alpha : a \rightarrow b$  in  $\mathcal{M}$  is interpreted as a morphism  $\alpha : b \rightarrow a$  in  $\mathcal{M}^\#$ .

**Definition 2.14.** *Let  $D$  be a polygon diagram labeled by  $\text{Bimod}^\theta(\mathcal{C}, \mathcal{D})$ . The **opposite polygon diagram**  $D^\#$  is the polygon diagram by  $\text{Bimod}^\theta(\mathcal{D}, \mathcal{C})$  obtained as follows:*

- taking the mirror image of  $D$ ,
- reversing the orientation of each line in  $D$ ,
- replacing each  $(\mathcal{C}, \mathcal{D})$ -bimodule category  $\mathcal{M}$  in  $D$  by the  $(\mathcal{D}, \mathcal{C})$ -bimodule category  $\mathcal{M}^\#$ ,
- replacing each bimodule functor  $F : \mathcal{M} \rightarrow \mathcal{N}$  in  $D$  by  $F^\# : \mathcal{M}^\# \rightarrow \mathcal{N}^\#$ ,
- replacing each bimodule natural transformation  $\nu : F \Rightarrow G$  in  $D$  by  $\nu^\# : G^\# \Rightarrow F^\#$ ,
- keeping the boundary data fixed.

Geometrically,  $D^\#$  is the polygon diagram obtained by looking at  $D$  from the back, behind the plane of the drawing. The orientation reversal for lines is necessary, because a functor labeling a line goes from the category on the left of the line to the category on the right, viewed in the direction of its orientation. Looking at the diagram from the back exchanges left and right and hence reverses the orientation of the line.

**Corollary 2.15.** *For any polygon diagram  $D$  one has  $\text{ev}(D) = \text{ev}(D^\#)$ .*

*Proof.* Taking the mirror image, reversing each line and replacing line labels  $F : \mathcal{M} \rightarrow \mathcal{N}$  by  $F^\# : \mathcal{M}^\# \rightarrow \mathcal{N}^\#$  replaces a functor  $F_1 \cdots F_n : \mathcal{M} \rightarrow \mathcal{N}$  by the functor  $(F_n^\#)^l \cdots (F_1^\#)^l = (F_1^\# \cdots F_n^\#)^l : \mathcal{N}^\# \rightarrow \mathcal{M}^\#$ . A bimodule natural transformation  $\nu : F_1 \cdots F_n \Rightarrow G_1 \cdots G_m$  in  $D$  is replaced by a natural transformation from  $(F_1^\# \cdots F_n^\#)^l$  to  $(G_1^\# \cdots G_m^\#)^l$  in  $D'$ , which is a cyclic transform of  $\nu^\# : G_1^\# \cdots G_m^\# \Rightarrow F_1^\# \cdots F_n^\#$ . Each morphism  $\alpha \in \text{Hom}_{\mathcal{N}}(n, F(m))$  in  $D$  is replaced by a morphism  $\alpha \in \text{Hom}_{\mathcal{M}^\#}(m, (F^\#)^l(n)) = \text{Hom}_{\mathcal{M}}((F^\#)^l(n), m)$  which is related to  $\alpha$  via the (co)unit of the adjunction  $(F^\#)^l \dashv F^\#$ . Identities (33) and (34) and the induced bimodule trace on the opposite category (cf. Example 1.15) then ensure that the evaluations of  $D$  and  $D^\#$  are equal.  $\square$

### 3 Gluing polygon diagrams

In this section we describe how polygon diagrams for the pivotal 2-category  $\text{Bimod}^\theta(\mathcal{C}, \mathcal{D})$  can be glued by summing over simple objects and bases of the morphism spaces at their boundary. Taking the product of the evaluations of two diagrams and performing these summations yields the evaluation of the glued diagram.

#### 3.1 Projections and inclusions for simple objects

Let  $\mathcal{M}$  a finite semisimple  $\mathbb{C}$ -linear category, equipped with a trace  $\theta$  in the sense of Definition 1.13 and let  $I$  be a set of representatives of the isomorphism classes of its simple objects. Then every object  $x$  in  $\mathcal{M}$  can be expressed as a direct sum  $x \cong \bigoplus_{m \in I} m^{\oplus n_{xm}}$  with multiplicities  $n_{xm} = \dim_{\mathbb{C}} \text{Hom}_{\mathcal{M}}(m, x) \in \mathbb{N}_0$ . One can choose bases  $\{p_{xm}^\alpha\}$  of  $\text{Hom}_{\mathcal{M}}(x, m)$  and  $\{j_{xm}^\alpha\}$  of  $\text{Hom}_{\mathcal{M}}(m, x)$  with  $m \in I$  and  $\alpha \in \{1, \dots, n_{xm}\}$  such that

$$p_{xm'}^\beta \circ j_{xm}^\alpha = \frac{\delta_{\alpha\beta} \delta_{mm'}}{\dim(m)} 1_m \quad 1_x = \sum_{m \in I} \sum_{\alpha=1}^{n_{xm}} \dim(m) j_{xm}^\alpha \circ p_{xm}^\alpha \quad (53)$$

for all  $m, m' \in I$ , where  $\dim(m) = \theta_m(1_m)$ . Their normalisation is fixed by (53) such that

$$\theta_m(p_{xm}^\beta \circ j_{xm}^\alpha) = \delta_{\alpha\beta}, \quad (54)$$

and this implies with the cyclicity of the trace

$$\sum_{m \in I} \dim(m) \dim_{\mathbb{C}} \text{Hom}_{\mathcal{M}}(m, x) = \dim(x). \quad (55)$$

The identities (53) imply for all morphisms  $\phi : m \rightarrow x$  and  $\psi : x \rightarrow m$

$$\phi = \sum_{\alpha=1}^{n_{xm}} \theta_m(p_{xm}^\alpha \circ \phi) j_{xm}^\alpha \quad \psi = \sum_{\alpha=1}^{n_{ym}} \theta_m(\psi \circ j_{xm}^\alpha) p_{xm}^\alpha \quad (56)$$

and for all morphisms  $\chi : x \rightarrow y$

$$\chi = \sum_{m \in I} \sum_{\alpha=1}^{n_{xm}} \sum_{\beta=1}^{n_{ym}} \dim(m) \theta_m(p_{ym}^\beta \circ \chi \circ j_{xm}^\alpha) j_{ym}^\beta \circ p_{xm}^\alpha. \quad (57)$$

These identities are represented by the diagrams

$$\sum_{\alpha} \left( \begin{array}{c} m \\ \bullet \\ \phi \\ x \\ \bullet \\ \alpha \\ m \end{array} \right) \begin{array}{c} m \\ \bullet \\ \alpha \\ x \\ \bullet \\ \phi \\ m \end{array} \stackrel{(56)}{=} \begin{array}{c} m \\ \bullet \\ \phi \\ x \\ \bullet \\ \alpha \\ m \end{array} \quad \sum_{\alpha} \left( \begin{array}{c} m \\ \bullet \\ \alpha \\ x \\ \bullet \\ \psi \\ m \end{array} \right) \begin{array}{c} x \\ \bullet \\ \alpha \\ m \\ \bullet \\ \psi \\ m \end{array} \stackrel{(56)}{=} \begin{array}{c} x \\ \bullet \\ \psi \\ m \\ \bullet \\ \alpha \\ m \end{array} \quad \sum_m \sum_{\alpha, \beta} \dim(m) \left( \begin{array}{c} m \\ \bullet \\ \alpha \\ x \\ \bullet \\ \chi \\ y \\ \bullet \\ \beta \\ m \end{array} \right) \begin{array}{c} x \\ \bullet \\ \alpha \\ m \\ \bullet \\ \beta \\ y \end{array} \stackrel{(57)}{=} \begin{array}{c} x \\ \bullet \\ \chi \\ y \\ \bullet \\ \beta \\ m \end{array} \quad (58)$$

If  $\mathcal{M}$  and  $\mathcal{N}$  are bimodule categories with bimodule traces over spherical fusion categories  $\mathcal{C}$  and  $\mathcal{D}$  and  $F : \mathcal{M} \rightarrow \mathcal{N}$  is a  $\mathbb{C}$ -linear functor, then one can characterise  $F$  by decomposing the images of simple objects  $m \in I_{\mathcal{M}}$  into simple objects  $n \in I_{\mathcal{N}}$ . We write  $p_{Fmn}^\alpha = p_{F(m)n}^\alpha : F(m) \rightarrow n$  and  $j_{Fmn}^\alpha = j_{F(m)n}^\alpha : n \rightarrow F(m)$  for the associated projection and inclusion morphisms satisfying (53) and denote them by

$$\begin{array}{c} F \\ \bullet \\ m \\ \bullet \\ \alpha \\ n \end{array} \quad \begin{array}{c} n \\ \bullet \\ \alpha \\ m \\ \bullet \\ F \end{array} \quad (59)$$





dashed lines, and the upward arrows denote the duals in  $\mathcal{C}$  and  $\mathcal{D}$ . Identities (60), together with (5), (22) and (55), then imply for all simple objects  $n \in I_{\mathcal{M}}$

$$\sum_{i,m,\alpha} \dim(i) \dim(m) \begin{array}{c} n \\ \uparrow \alpha \\ i \\ \downarrow \alpha \\ m \\ \uparrow \alpha \\ n \end{array} = \dim(\mathcal{C}) \begin{array}{c} n \\ \uparrow \\ n \end{array} \quad (65)$$

### 3.2 Gluing identities for polygon diagrams

We consider the pivotal 2-category  $\text{Bimod}^\theta(\mathcal{C}, \mathcal{D})$  for spherical fusion categories  $\mathcal{C}, \mathcal{D}$ . We fix sets  $I_{\mathcal{C}}, I_{\mathcal{D}}$  and  $I_{\mathcal{M}}$  of representatives of the isomorphism classes of simple objects in  $\mathcal{C}, \mathcal{D}$  and in each bimodule category  $\mathcal{M}$ . For each object  $x$  in  $\mathcal{C}, \mathcal{D}$  or  $\mathcal{M}$  and each simple object  $i$  in the set of representatives, we choose projection morphisms  $p_{xi}^\alpha : x \rightarrow i$  and inclusion morphisms  $j_{xi}^\alpha : i \rightarrow x$  that satisfy (53).

Then we can glue and cut polygon diagrams by summing over the simple objects at their boundary segments and over bases of the morphism spaces at their boundary vertices.

**Theorem 3.1.** *The cyclic evaluations of the polygon diagrams for  $\text{Bimod}^\theta(\mathcal{C}, \mathcal{D})$  satisfy:*

1. **Gluing sides:** for all objects  $m \in I_{\mathcal{M}}, n \in I_{\mathcal{N}}$

$$\sum_{\alpha} \begin{array}{c} \text{Hexagon} \\ \text{Left side: } \mathcal{M} \text{ (blue), } \mathcal{N} \text{ (red)} \\ \text{Right side: } \mathcal{M} \text{ (blue), } \mathcal{N} \text{ (red)} \\ \text{Vertices: } \alpha \end{array} = \begin{array}{c} \text{Hexagon} \\ \text{Left side: } \mathcal{M} \text{ (blue)} \\ \text{Right side: } \mathcal{N} \text{ (red)} \\ \text{Vertex: } \alpha \end{array} \quad (66)$$

2. **Gluing around a vertex:** for all objects  $m \in I_{\mathcal{M}}$

$$\sum_{n,\alpha} \dim(n) \begin{array}{c} \text{Hexagon} \\ \text{Left side: } \mathcal{M} \text{ (blue), } \mathcal{N} \text{ (red)} \\ \text{Right side: } \mathcal{M} \text{ (blue), } \mathcal{N} \text{ (red)} \\ \text{Vertex: } \alpha \end{array} = \begin{array}{c} \text{Hexagon} \\ \text{Left side: } \mathcal{N} \text{ (red)} \\ \text{Right side: } \mathcal{M} \text{ (blue)} \\ \text{Vertex: } \alpha \end{array} \quad (67)$$

3. **Gluing a 2-gon:** for all objects  $m, n \in I_{\mathcal{M}}, x \in \text{Ob}\mathcal{C}$  or  $x \in \text{Ob}\mathcal{D}$  and all morphisms  $\phi : x \rightarrow x$

$$\sum_{m,n,\alpha} \dim(m) \dim(n) \begin{array}{c} \text{2-gon} \\ \text{Left side: } \mathcal{M} \text{ (blue)} \\ \text{Right side: } \mathcal{M} \text{ (blue)} \\ \text{Top vertex: } \alpha \\ \text{Bottom vertex: } \alpha \\ \text{Internal vertex: } x \\ \text{Morphism: } \phi \end{array} = \dim(\mathcal{M}) \begin{array}{c} \text{2-gon} \\ \text{Left side: } \mathcal{M} \text{ (blue)} \\ \text{Right side: } \mathcal{M} \text{ (blue)} \\ \text{Top vertex: } x \\ \text{Bottom vertex: } x \\ \text{Morphism: } \phi \end{array} \quad (68)$$

4. Inserting a diagram for  $\mathcal{C}$  or  $\mathcal{D}$ :

for all objects  $i \in I_{\mathcal{C}}$ ,  $x \in \text{Ob}\mathcal{C}$  or  $i \in I_{\mathcal{D}}$ ,  $x \in \text{Ob}\mathcal{D}$  and morphisms  $\phi : i \rightarrow x$  and  $\psi : x \rightarrow i$

$$\sum_{\alpha} \left( \text{Hexagon} \left( \begin{array}{c} i \\ \downarrow \\ \alpha \\ \downarrow \\ x \end{array} \right) \right) = \left( \begin{array}{c} i \\ \downarrow \\ \phi \\ \downarrow \\ x \\ \downarrow \\ \alpha \\ \downarrow \\ i \end{array} \right) = \text{Hexagon} \left( \begin{array}{c} i \\ \downarrow \\ \phi \\ \downarrow \\ x \end{array} \right)$$

$$\sum_{\alpha} \left( \text{Hexagon} \left( \begin{array}{c} x \\ \downarrow \\ \alpha \\ \downarrow \\ i \end{array} \right) \right) = \left( \begin{array}{c} i \\ \downarrow \\ \alpha \\ \downarrow \\ x \\ \downarrow \\ \psi \\ \downarrow \\ i \end{array} \right) = \text{Hexagon} \left( \begin{array}{c} x \\ \downarrow \\ \psi \\ \downarrow \\ i \end{array} \right) \quad (69)$$

Here, the polygon diagrams on each side of an equation stand for the product of their cyclic evaluations. It is assumed that all parts of the diagrams that are not drawn coincide on the left-hand side and right-hand side and that the object and morphism labels occur nowhere else in the diagrams. The vertex label  $\alpha$  stands for the chosen projection and inclusion morphisms. The summations are over simple objects in the sets of representatives and over bases of the morphism spaces. The functor  $F$  in (66) and (67) may be a composite functor consisting of several lines or an action functor  $c \triangleright -$  or  $- \triangleleft d$ .

*Proof.* Identity (66) follows from (56). The data at the boundaries and in the interiors of the first and second diagram in (66) that is not drawn combines into morphisms  $\mu : n \rightarrow F(m)$  and  $\nu : F(m) \rightarrow n$ , respectively. The diagram on the right-hand side of (66) is then given by the trace of  $\nu \circ \mu$ . Equation (56) implies that the cyclic evaluations on the left-hand side and right-hand side of (66) are given by

$$\sum_{\alpha} \left( \begin{array}{c} n \\ \downarrow \\ \mu \\ \downarrow \\ F \\ \downarrow \\ m \\ \downarrow \\ \alpha \\ \downarrow \\ n \end{array} \right) = \left( \begin{array}{c} n \\ \downarrow \\ \alpha \\ \downarrow \\ F \\ \downarrow \\ m \\ \downarrow \\ \nu \\ \downarrow \\ n \end{array} \right) \stackrel{(60)}{=} \left( \begin{array}{c} n \\ \downarrow \\ \mu \\ \downarrow \\ F \\ \downarrow \\ m \\ \downarrow \\ \nu \\ \downarrow \\ n \end{array} \right)$$

The proof of (69) is analogous. The only difference is that it uses the traces of  $\mathcal{C}$  or  $\mathcal{D}$ . Identity (67) is a direct consequence of the second identity in (53), depicted in (60). In this case, the contributions of the diagram in the interior and the boundary morphisms that are not drawn combine into a morphism  $\rho : F(m) \rightarrow F(m)$  in both diagrams. The cyclic evaluations of the left-hand side and right-hand side of (67) are then given by

$$\sum_{n, \alpha} \dim(n) \left( \begin{array}{c} F \\ \downarrow \\ m \\ \downarrow \\ \rho \\ \downarrow \\ F \\ \downarrow \\ m \\ \downarrow \\ \alpha \\ \downarrow \\ n \\ \downarrow \\ \alpha \\ \downarrow \\ F \\ \downarrow \\ m \end{array} \right) \stackrel{(60)}{=} \left( \begin{array}{c} F \\ \downarrow \\ m \\ \downarrow \\ \rho \\ \downarrow \\ F \\ \downarrow \\ m \end{array} \right)$$

Finally, to prove identity (68), we compute with the definition of  $\dim(n)$  and  $\dim \mathcal{M}$

$$\sum_{m, n, \alpha} \dim(m) \left( \begin{array}{c} m \\ \downarrow \\ \alpha \\ \downarrow \\ n \\ \downarrow \\ \alpha \\ \downarrow \\ m \end{array} \right) \stackrel{(48)}{=} \sum_{m, n, \alpha} \dim(m) \left( \begin{array}{c} n \\ \downarrow \\ \phi \\ \downarrow \\ \alpha \\ \downarrow \\ m \\ \downarrow \\ \alpha \\ \downarrow \\ n \end{array} \right) \stackrel{(60)}{=} \sum_n \dim(n) \left( \begin{array}{c} n \\ \downarrow \\ \phi \end{array} \right) \stackrel{(49)}{=} \dim \mathcal{M} \left( \begin{array}{c} x \\ \downarrow \\ \phi \\ \downarrow \\ x \end{array} \right) \quad \square$$

Note that the first three identities in Theorem 3.1 are precisely the elementary transformations for polygon presentations of surface groups, see for instance the books by Lee [L, Ch. 6] and by Seifert and Threlfall [ST, Ch. 6.38 and 6.40]. Identity (66) corresponds to the cutting and pasting operation, identity (67) to the folding and unfolding operation and identity (68) to the special case of the folding operation for  $S^2$ . Identity (69) describes the insertion of data from spherical categories into polygon diagrams.

## 4 State sum models with defects

### 4.1 Triangulated 3-manifolds with defects

We consider a compact oriented 3d PL manifold  $M$  with (possibly empty) boundary  $\partial M$ . Defect structures are assigned to a compact oriented embedded 2d PL submanifold  $D \subset M$  with boundary  $\partial D \subset \partial M$  that is a finite sum of circles. The submanifold  $D$  is equipped with an embedded graph  $D^1$  with vertex set  $D^0$ , whose edges may end at the boundary  $\partial D$ , but whose vertices are in the interior of  $D$ . Connected components of  $M \setminus D$  are called **regions** of  $M$ , connected components of  $D$  **defect surfaces**, connected components of  $D \setminus D^1$  **defect areas**, connected components of  $D^1 \setminus D^0$  **defect lines** and elements of  $D^0$  **defect vertices**.

We equip each defect line and defect surface with an orientation. In pictures, we indicate the orientation of a defect surface by a surface normal, and the orientation of a defect line by an arrow on the line. Regions and defect areas, lines and vertices are labeled with categorical data as follows, see Figure 2 for an illustration:

- Each region of  $M$  is assigned a spherical fusion category  $\mathcal{C}$ .
- Each oriented defect area is assigned a pair  $(\mathcal{M}, \theta)$  of a  $(\mathcal{C}, \mathcal{D})$ -bimodule category  $\mathcal{M}$  and a  $(\mathcal{C}, \mathcal{D})$ -bimodule trace  $\theta$  on  $\mathcal{M}$ , where  $\mathcal{C}$  and  $\mathcal{D}$  are the spherical fusion categories for the regions at the tip and the tail of the surface normal.

Reversing the orientation of a defect area amounts to replacing  $\mathcal{M}$  by the opposite bimodule category  $\mathcal{M}^\#$  from Example 1.6.

- Each oriented defect line is assigned a  $(\mathcal{C}, \mathcal{D})$ -bimodule functor  $F : \mathcal{M} \rightarrow \mathcal{N}$ , where  $\mathcal{M}$  and  $\mathcal{N}$  are the  $(\mathcal{C}, \mathcal{D})$ -bimodule categories to the left and to the right of the defect line, viewed in the direction of its orientation and from  $\mathcal{C}$ .

Reversing the orientation of a defect line corresponds to replacing  $F : \mathcal{M} \rightarrow \mathcal{N}$  by its left adjoint  $F^l : \mathcal{N} \rightarrow \mathcal{M}$ . Reversing the orientation of the adjacent defect areas and the orientation of the line corresponds to replacing  $\mathcal{M}, \mathcal{N}$  by  $\mathcal{M}^\#, \mathcal{N}^\#$  and  $F$  by  $F^\# : \mathcal{M}^\# \rightarrow \mathcal{N}^\#$  from Example 1.10, 7.

- A defect vertex whose incident defect lines are labeled by  $(\mathcal{C}, \mathcal{D})$ -bimodule functors is assigned a cyclic equivalence class of  $(\mathcal{C}, \mathcal{D})$ -bimodule natural transformations between them, whose sources and targets are determined by the orientation and the cyclic ordering of the incident defect lines.

Defect areas between two regions labeled both with  $\mathcal{C}$  may be labeled with  $\mathcal{C}$  as a bimodule category over itself and with its trace as a bimodule trace. Such defect areas are called **trivial defect areas**. Similarly, a defect line between two defect areas labeled with  $(\mathcal{M}, \theta)$  may be labeled with the identity functor  $F = \text{id}_{\mathcal{M}} : \mathcal{M} \rightarrow \mathcal{M}$  as a  $(\mathcal{C}, \mathcal{D})$ -bimodule functor. Such defect lines are called **trivial defect lines**. A defect vertex labeled with  $\text{id}_F$  or with a counit  $\epsilon^F, \epsilon'^F$  or unit  $\eta^F, \eta'^F$  of the adjunction  $F^l \vdash F$  is called a **trivial defect vertex**.

A compact oriented 3d PL manifold  $M$ , possibly with boundary, together with defects  $D^0 \subset D^1 \subset D$  is called a **defect 3-manifold**. A defect 3-manifold together with a labeling of the defects with categorical data is called a **3-manifold with defect data**.

To define a state sum model for a 3-manifold with defect data, we require a triangulation of  $M$ . It must be sufficiently refined to resolve all defect surfaces and must intersect the defect surfaces generically.

**Definition 4.1.** *Let  $M$  be a defect 3-manifold and  $T$  a triangulation of  $M$ .*

1. *A triangle in  $T$  is called **transversal**, if*
  - *each of its sides contains at most one point on a defect surface,*
  - *its intersection with each defect surface is empty or a line with endpoints on its sides,**and **generic** if*

- none of its vertices is on a defect surface,
  - none of its sides intersects a defect line,
  - it does not contain a defect vertex.
2. A tetrahedron in  $T$  is transversal, if all of its faces are transversal and its intersection with each defect surface is either empty or a polygon with vertices on its edges. It is generic, if all its faces are generic.
  3. The triangulation  $T$  is transversal or generic if all of its tetrahedra are transversal or generic.

It follows directly that a generic transversal tetrahedron either intersects a single defect surface in three edges incident at a common vertex, as in Figure 2 (a), intersects a defect surface in two pairs of opposite edges, as in Figure 2 (b), or does not intersect any defect surface at all.

Any transversal triangulation can be deformed into a generic one by slightly perturbing the defect surfaces and the defect graphs. By taking derived subdivisions, see Rourke and Sanderson [RS, Ch. 2], and perturbing defect surfaces and defect graphs one can transform any triangulation into one that is both transversal and generic. In particular, one can achieve that the defect manifold is a subcomplex of a first derived subdivision.

We orient the edges of a generic transversal triangulation in such a way that

- (i) edges in each triangle do not form a cycle,
- (ii) in each tetrahedron, the edges that intersect a defect surface are oriented parallel to the surface normal.

This does not restrict generality. Condition (i) can be achieved by numbering the vertices of the triangulation and orienting each edge in such a way that it points from the vertex with the smaller number to the vertex with the bigger number. This is possible because any PL triangulation is determined by an underlying combinatorial simplicial complex, see for instance [RS, Th. 2.11].

Given a generic transversal triangulation that satisfies (i), reverse the orientation of each edge that intersects a defect surface and is oriented against its normal. Each triangle that intersects a defect surface intersects it in exactly two edges. After this orientation reversal these two edges are either both incoming or outgoing at a common vertex and hence cannot be part of a cycle. The resulting triangulation satisfies (i) and (ii).

A defect 3-manifold together with an oriented triangulation is called a **triangulated defect 3-manifold**. A 3-manifold with defect data together with an oriented triangulation is called a **triangulated 3-manifold with defect data**. They are called **transversal** or **generic** if the triangulation is transversal or generic.

## 4.2 Labeling of the triangulation

To define the state sum of a generic transversal triangulated 3-manifold with defect data, we assign objects and morphisms of the associated categories to the edges and triangles of the triangulation. For this, we fix sets  $I$  of representatives of the isomorphism classes of simple objects and associated projection and inclusion morphisms  $p_{xi}^\alpha : x \rightarrow i$  and  $j_{xi}^\alpha : i \rightarrow x$  satisfying (53) for all spherical fusion categories at the regions of  $M$  and for all bimodule categories at the defect areas.

**Definition 4.2.** *Let  $M$  be generic transversal triangulated 3-manifold with defect data. A **labeling** of  $M$  is an assignment of the following data to the edges of the triangulation:*

- (i) to each oriented edge  $e$  contained in a region labeled by  $\mathcal{C}$ , a simple object  $l(e) \in I_{\mathcal{C}}$ ,
- (ii) to each oriented edge  $e$  that intersects a defect area labeled  $\mathcal{M}$ , a simple object  $l(e) \in I_{\mathcal{M}}$ .

A pair  $(M, l)$  of a generic transversal triangulated 3-manifold  $M$  with defect data and a labeling  $l$  is called a **labeled defect 3-manifold**.

Note that the edge orientation is arbitrary in (i), but fixed by the orientations of the defect surfaces in (ii). In (i) we assign to the edge with the opposite orientation the unique object in  $I_{\mathcal{C}}$  that represents the isomorphism class of the dual object  $l(e)^*$ . In (ii) orientation may only be reversed simultaneously for all edges of a tetrahedron that intersect a defect surface, and we assign the same object to the edge with the opposite orientation. This corresponds to passing from the bimodule category  $\mathcal{M}$  to its opposite  $\mathcal{M}^\#$ .

A labeling of a triangulated manifold with defect data defines a labeling of each triangle in the triangulation. To each labeled triangle, we associate two morphism spaces, one for each orientation. For a triangle labeled by objects in  $(\mathcal{C}, \mathcal{D})$ -bimodule categories  $\mathcal{M}, \mathcal{N}$  that intersects a defect line labeled by a bimodule functor  $F : \mathcal{M} \rightarrow \mathcal{N}$  or  $G : \mathcal{N} \rightarrow \mathcal{M}$ , the associated morphisms spaces are

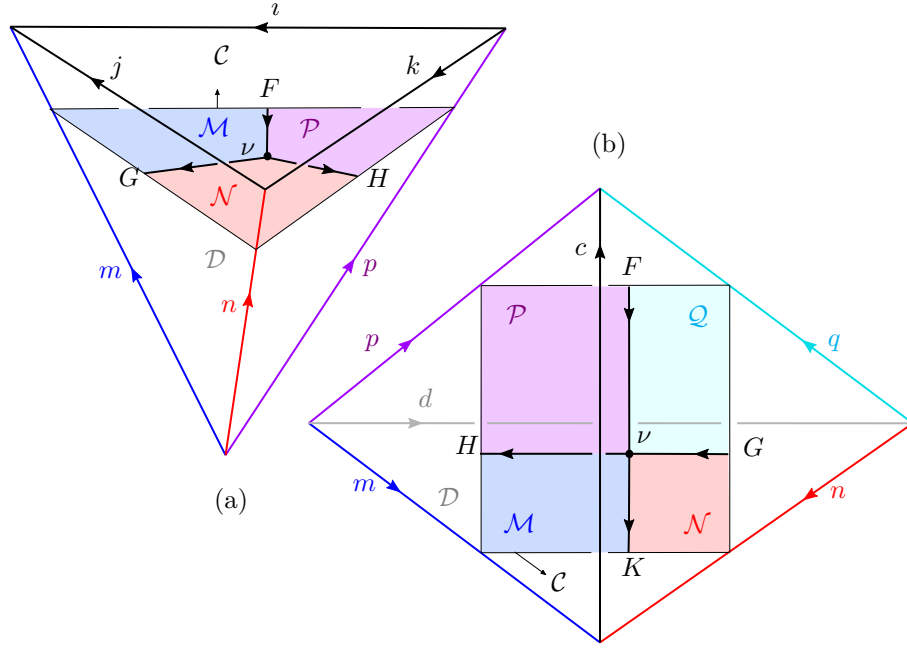


Figure 2: Generic transversal tetrahedra that intersect a defect surface.

(a) labeling with  $F : \mathcal{P} \rightarrow \mathcal{M}$ ,  $G : \mathcal{N} \rightarrow \mathcal{M}$ ,  $H : \mathcal{P} \rightarrow \mathcal{N}$  and  $\nu : F \Rightarrow GH$ ,

(b) labeling with  $F : \mathcal{Q} \rightarrow \mathcal{P}$ ,  $G : \mathcal{N} \rightarrow \mathcal{Q}$ ,  $H : \mathcal{M} \rightarrow \mathcal{P}$ ,  $K : \mathcal{N} \rightarrow \mathcal{M}$  and  $\nu : FG \Rightarrow HK$ .

$  \begin{array}{c}  m \in I_{\mathcal{M}} \quad n \in I_{\mathcal{N}} \\  \swarrow \quad \searrow \\  \downarrow F \\  c \in I_{\mathcal{C}}  \end{array}  $	$  \begin{array}{c}  n \in I_{\mathcal{N}} \quad m \in I_{\mathcal{M}} \\  \swarrow \quad \searrow \\  \uparrow F \\  c \in I_{\mathcal{C}}  \end{array}  $	$  \begin{array}{l}  + : \text{Hom}_{\mathcal{N}}(F(c \triangleright m), n) \\  - : \text{Hom}_{\mathcal{N}}(n, F(c \triangleright m))  \end{array}  \tag{70}  $
$  \begin{array}{c}  m \in I_{\mathcal{M}} \quad n \in I_{\mathcal{N}} \\  \swarrow \quad \searrow \\  \uparrow G \\  c \in I_{\mathcal{C}}  \end{array}  $	$  \begin{array}{c}  n \in I_{\mathcal{N}} \quad m \in I_{\mathcal{M}} \\  \swarrow \quad \searrow \\  \downarrow G \\  c \in I_{\mathcal{C}}  \end{array}  $	$  \begin{array}{l}  + : \text{Hom}_{\mathcal{M}}(c \triangleright m, G(n)) \\  - : \text{Hom}_{\mathcal{M}}(G(n), c \triangleright m)  \end{array}  $
$  \begin{array}{c}  d \in I_{\mathcal{D}} \\  \swarrow \quad \searrow \\  \downarrow F \\  m \in I_{\mathcal{M}} \quad n \in I_{\mathcal{N}}  \end{array}  $	$  \begin{array}{c}  d \in I_{\mathcal{D}} \\  \swarrow \quad \searrow \\  \uparrow F \\  n \in I_{\mathcal{N}} \quad m \in I_{\mathcal{M}}  \end{array}  $	$  \begin{array}{l}  + : \text{Hom}_{\mathcal{N}}(F(m \triangleleft d), n) \\  - : \text{Hom}_{\mathcal{N}}(n, F(m \triangleleft d))  \end{array}  $
$  \begin{array}{c}  d \in I_{\mathcal{D}} \\  \swarrow \quad \searrow \\  \uparrow G \\  m \in I_{\mathcal{M}} \quad n \in I_{\mathcal{N}}  \end{array}  $	$  \begin{array}{c}  d \in I_{\mathcal{D}} \\  \swarrow \quad \searrow \\  \downarrow G \\  n \in I_{\mathcal{N}} \quad m \in I_{\mathcal{M}}  \end{array}  $	$  \begin{array}{l}  + : \text{Hom}_{\mathcal{M}}(m \triangleleft d, G(n)) \\  - : \text{Hom}_{\mathcal{M}}(G(n), m \triangleleft d)  \end{array}  $

Here, the triangles are equipped with the orientation induced by their edge orientation and the embedding in the plane, via the right-hand rule. The first triangle in each line has positive (+) and the second negative (-) orientation. The arrows indicate the orientation of the defect line relative to the orientation of the triangle. They agree, if the arrow points downwards, and are opposite, if it points upwards. As the orientation of the defect lines is fixed, reversing the orientation of the triangle reverses the orientation of this arrow.

The morphism spaces are obtained from the triangles as follows: The objects in  $\mathcal{C}$  and  $\mathcal{D}$  act on the object of  $\mathcal{M}$  or  $\mathcal{N}$  with whom they share a vertex with one incoming and one outgoing edge. Arrows labeled with  $\mathcal{C}$  have this vertex as their starting vertex, arrows labeled by  $\mathcal{D}$  as their target vertex. The morphisms go from the object on the left to the one on the right. The functor is applied to the object on the left, if its arrow points downwards, and to the one on the right, if it points upwards.

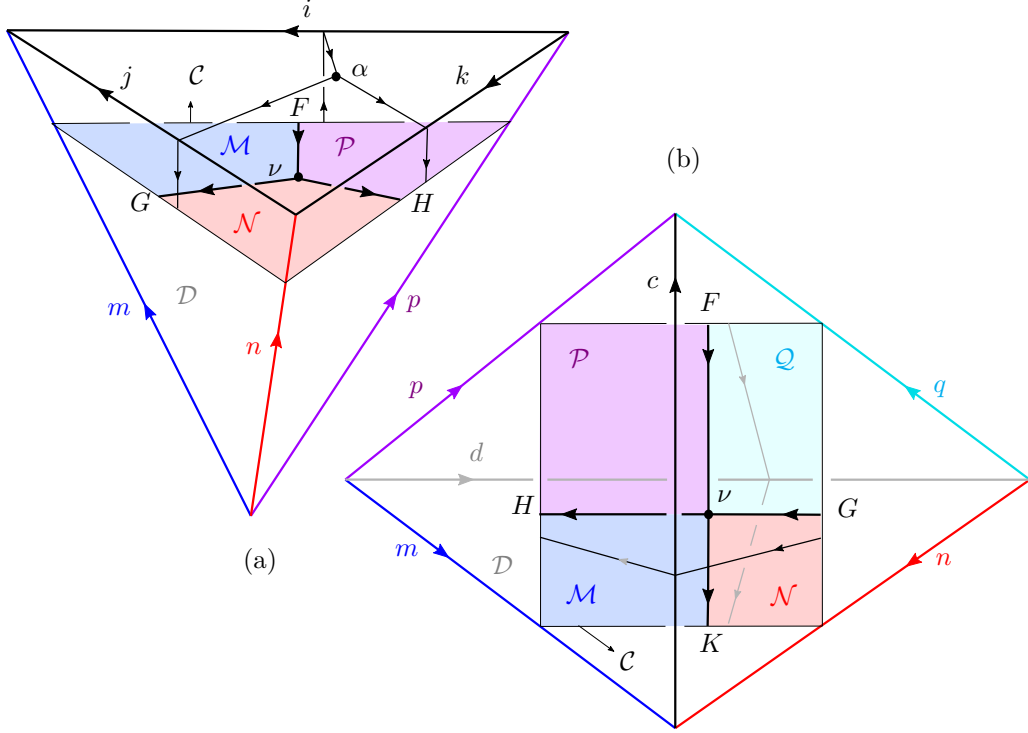


Figure 3: Projecting the data from spherical categories on the polygon.

For  $\mathcal{M} = \mathcal{N}$  and  $F = G = \text{id}_{\mathcal{M}}$ , the diagrams in the first and the second row and in the third and the fourth row in (70) coincide. Setting  $\mathcal{M} = \mathcal{N} = \mathcal{C}$ ,  $\triangleright = \otimes = \triangleleft$  and  $F = G = \text{id}_{\mathcal{C}}$  yields the usual assignment of morphisms to triangles for the Turaev-Viro-Barrett-Westbury invariants of a spherical fusion category.

### 4.3 Generalised 6j symbols

We now associate a generalised 6j symbol to each labeled generic transversal tetrahedron  $t$  with a defect surface. Note that such a defect tetrahedron is more than a combinatorial tetrahedron with categorical data assigned to each oriented edge. It consists of a combinatorial tetrahedron  $t$ , an oriented defect polygon  $P$ , an assignment of certain edges of  $t$  to the vertices of  $P$  and an assignment of the vertices of  $t$  to the two regions labeled by  $\mathcal{C}$  and  $\mathcal{D}$ . In particular, a labeled generic transversal tetrahedron inherits an orientation, because the defect surface is oriented and assigning  $\mathcal{C}$  and  $\mathcal{D}$  to the two sides of the surface specifies a surface normal.

The orientation of  $t$  induces an orientation of all of its triangles. To each oriented triangle we assign a morphism in the associated morphism space from (70). To a tetrahedron with these assignments, we associate a polygon diagram  $D$  as follows:

1. The defect surface in  $t$  is a polygon  $P$ . The defect data in  $P$ , viewed from the region labeled  $\mathcal{C}$  towards the region labeled  $\mathcal{D}$ , defines a cyclic equivalence class of diagrams for  $\text{Bimod}^{\theta}(\mathcal{C}, \mathcal{D})$ .
2. Pushing the endpoints of defect lines on each side of  $P$  to the middle without creating crossings does not change the cyclic equivalence class of the diagram. We thus assume that each side of  $P$  is the endpoint of exactly one defect line as in Figure 2, possibly labeled with a composite of functors.
3. Draw  $t$  such that edges and triangles labeled by data from  $\mathcal{C}$  and  $\mathcal{D}$  lie on the corresponding sides of the polygon  $P$  and that edges intersecting  $P$  are oriented by the surface normal.
4. For each edge  $e$  of  $t$  that does not intersect  $P$ , draw the dual edge  $\bar{e}$ , starting and ending on the boundary  $\partial P$  and with its endpoints are displaced slightly from the endpoints of defect lines. They are displaced towards the starting and target end of  $e$ , if  $e$  is contained in the region for  $\mathcal{C}$  and  $\mathcal{D}$ , respectively. Orient  $\bar{e}$  by duality, as shown in Figure 3, and project it on  $P$ .

5. Label the vertices of  $P$  with the simple objects of the associated edges of  $t$  and the projected edges with the simple objects of their duals in  $t$ . Label the endpoints of defect lines and the projected vertices in  $P$  with the morphisms assigned to the corresponding triangles in  $t$ . The result is a polygon diagram  $D$ . The diagrams for the tetrahedra in Figures 2 and 3 are shown in (71).

Note that the word *project* in 3. is used informally here. For the tetrahedron in Figure 3 (a) it means drawing a trivalent vertex on  $P$  whose incident edges are connected with the endpoints on  $\partial P$ . For the tetrahedron in Figure 3 (b) it amounts to drawing two edges that connect endpoints on opposite sides of  $P$ . The properties of diagrams for spherical fusion categories and identities (39) to (43) ensure that all ways of doing so yield polygon diagrams with the same evaluation.

Note also that tetrahedra that do not intersect defect surfaces can be viewed as special cases of Figure 2 (a) and (b). Each such tetrahedron has one vertex with only outgoing edges, which can be taken as the lower vertex in Figure 2 (a) or as the left vertex in Figure 2 (b). Up to orientation reversal the tetrahedron then coincides with the one in Figure 2 (a) or (b), if the defect surfaces are labeled with the spherical fusion category  $\mathcal{C}$  as a  $(\mathcal{C}, \mathcal{C})$ -bimodule category, with identity functors and with identity natural transformations.

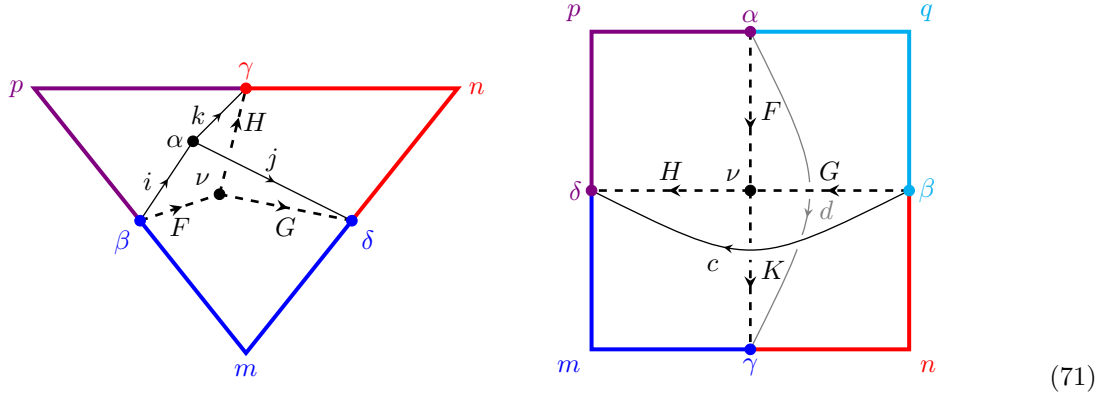
Interpreting a combinatorial tetrahedron as a tetrahedron with trivial defects amounts to a choice of orientation: one needs to specify an orientation for the trivial defect surface and to specify its surface normal. We therefore treat *oriented* tetrahedra labeled by a spherical fusion category  $\mathcal{C}$  as generic transversal tetrahedra with trivial defect data. In the following, we assume that all tetrahedra are equipped with an orientation.

**Definition 4.3.** Let  $(t, l)$  be a labeled generic transversal tetrahedron with an assignment  $b$  of morphisms in the spaces (70) to its faces. The **generalised 6j symbol**  $6j(t, l, b)$  is the cyclic evaluation of the associated polygon diagram  $D$ . This defines a linear map

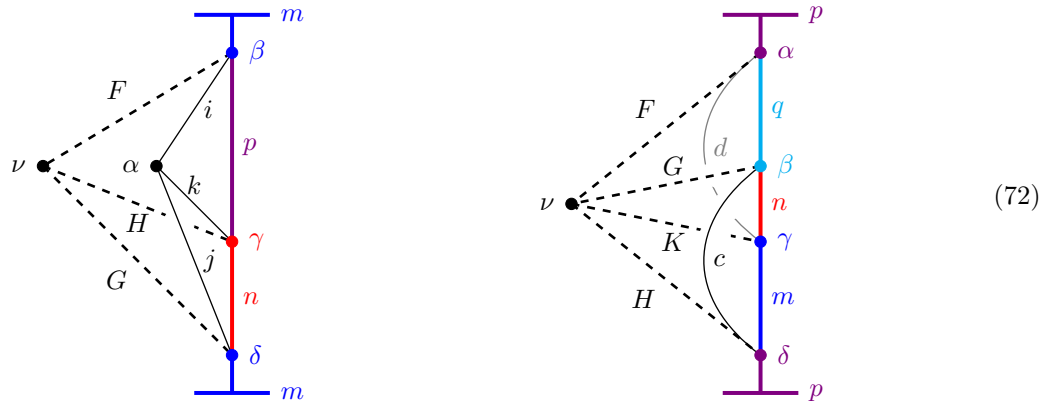
$$6j(t, l) : \bigotimes_{f \in \Delta} \text{Hom}(f, l) \rightarrow \mathbb{C}, \quad b \mapsto 6j(t, l, b)$$

where  $\Delta$  denotes the set of triangles of  $t$  and  $\text{Hom}(f, l)$  the associated morphism space from (70).

**Example 4.4.** The generalised 6j symbols for the tetrahedra in Figure 2 are the cyclic evaluations of



and given by the diagrams





Definition 4.3 also defines the usual 6j symbols of tetrahedra labeled by a spherical fusion category  $\mathcal{C}$  that occur in the Turaev-Viro-Barrett-Westbury state sum. However, they are not defined as 6j symbols of combinatorial tetrahedra, as in [BW96], but as 6j symbols of *oriented* combinatorial tetrahedra.

The 6j symbols from Definition 4.3 encode the natural transformations on the defect polygon and the coherence isomorphisms for the defect data. If the former are trivial, we obtain the following cases:

- If  $\mathcal{P} = \mathcal{N} = \mathcal{M}$ ,  $F = G = H = \text{id}_{\mathcal{M}}$  and  $\nu = \text{id}_{\text{id}_{\mathcal{M}}}$  for the tetrahedron in Figure 2 (a) and the associated 6j symbol in (72), we obtain a number that characterises the isomorphism  $c_{j,k,p} : (j \otimes k) \triangleright p \rightarrow j \triangleright (k \triangleright p)$  from Definition 1.2. It follows from (53) that it is given by

$$c_{j,k,p} = \sum_{\substack{i,m,n \\ \alpha,\beta,\gamma,\delta}} \frac{\dim(i)}{\dim(m)} \frac{\dim(m)}{\dim(n)} \quad (73)$$

where the sum runs over simple objects  $i \in I_{\mathcal{C}}$ ,  $m, p \in I_{\mathcal{M}}$  and bases of the associated morphism spaces. There is an analogous generalised 6j symbol for  $\mathcal{D}$ -right module categories, which arises from a tetrahedron analogous to Figure 2 (a), but with a vertex in the region labeled by  $\mathcal{D}$  and with the orientations of the coloured edges reversed.

- In particular, if  $\mathcal{M}$  is a spherical fusion category  $\mathcal{C}$  as a  $\mathcal{C}$ -left module category over itself, we obtain the usual 6j symbol for the spherical fusion category  $\mathcal{C}$  that encodes the associator on simple objects:

$$a_{j,k,p} = \sum_{\substack{i,m,n \\ \alpha,\beta,\gamma,\delta}} \frac{\dim(i)}{\dim(m)} \frac{\dim(m)}{\dim(n)} \quad (74)$$

- Setting  $\mathcal{Q} = \mathcal{P} = \mathcal{N} = \mathcal{M}$ ,  $F = G = H = K = \text{id}_{\mathcal{M}}$  and  $\nu = \text{id}_{\text{id}_{\mathcal{M}}}$  in Figure 2 (b) and (72) yields the 6j symbol that characterises the isomorphism  $b_{c,n,d} : (c \triangleright n) \triangleleft d \rightarrow c \triangleright (n \triangleleft d)$  from Definition 1.2:

$$b_{c,n,d} = \sum_{\substack{m,p,q \\ \alpha,\beta,\gamma,\delta}} \frac{\dim(m)}{\dim(p)} \frac{\dim(p)}{\dim(q)} \quad (75)$$

- In particular, for  $\mathcal{M} = \mathcal{C} = \mathcal{D}$  identity (75) yields the usual 6j symbol for a spherical fusion category  $\mathcal{C}$  that encodes its associator, but in a diagrammatic representation different from (74)

$$a_{c,n,d} = \sum_{\alpha,\beta,\gamma,\delta}^{m,p,q} \begin{matrix} \dim(m) \\ \dim(p) \\ \dim(q) \end{matrix} \quad \begin{array}{c} \text{--- } p \\ \bullet \alpha \\ \text{--- } q \\ \bullet \beta \\ \text{--- } n \\ \bullet \gamma \\ \text{--- } m \\ \bullet \delta \\ \text{--- } p \end{array} \quad \begin{array}{c} d \quad c \quad n \\ \diagdown \quad \diagup \\ \bullet \beta \\ \text{--- } q \\ \bullet \alpha \\ \text{--- } p \\ \bullet \delta \\ \text{--- } m \\ \bullet \gamma \\ \diagup \quad \diagdown \\ c \quad d \quad n \end{array} \quad (76)$$

- If we set  $\mathcal{Q} = \mathcal{P}$ ,  $\mathcal{N} = \mathcal{M}$ ,  $G = H : \mathcal{M} \rightarrow \mathcal{P}$ ,  $F = \text{id}_{\mathcal{P}}$ ,  $K = \text{id}_{\mathcal{M}}$ ,  $\nu = \text{id}_G$  and  $c = e$  in Figures 2 (b) and (72), we obtain the 6j symbol for the isomorphism  $t_{n,d}^G : G(n) \triangleleft d \rightarrow G(n \triangleleft d)$  from Definition 1.8:

$$t_{n,d}^G = \sum_{\alpha,\beta,\gamma,\delta}^{m,p,q} \begin{matrix} \dim(m) \\ \dim(p) \\ \dim(q) \end{matrix} \quad \begin{array}{c} \text{--- } p \\ \bullet \alpha \\ \text{--- } q \\ \bullet \beta \\ \text{--- } n \\ \bullet \gamma \\ \text{--- } m \\ \bullet \delta \\ \text{--- } p \end{array} \quad \begin{array}{c} d \quad G \quad n \\ \diagdown \quad \text{---} \\ \bullet \beta \\ \text{--- } q \\ \bullet \alpha \\ \text{--- } p \\ \bullet \delta \\ \text{--- } m \\ \bullet \gamma \\ \diagup \quad \text{---} \\ G \quad d \quad n \end{array} \quad (77)$$

- Setting instead  $\mathcal{P} = \mathcal{M}$ ,  $\mathcal{Q} = \mathcal{N}$ ,  $F = K : \mathcal{N} \rightarrow \mathcal{M}$ ,  $G = \text{id}_{\mathcal{N}}$ ,  $H = \text{id}_{\mathcal{M}}$ ,  $\nu = \text{id}_F$  and  $d = e$  in Figures 2 (b) and (72) yields the 6j symbol for the isomorphism  $s_{c,n}^F : F(c \triangleright n) \rightarrow c \triangleright F(n)$  from Definition 1.8:

$$s_{c,n}^F = \sum_{\alpha,\beta,\gamma,\delta}^{m,p,q} \begin{matrix} \dim(m) \\ \dim(p) \\ \dim(q) \end{matrix} \quad \begin{array}{c} \text{--- } p \\ \bullet \alpha \\ \text{--- } q \\ \bullet \beta \\ \text{--- } n \\ \bullet \gamma \\ \text{--- } m \\ \bullet \delta \\ \text{--- } p \end{array} \quad \begin{array}{c} F \quad c \quad n \\ \text{---} \quad \diagup \\ \bullet \beta \\ \text{--- } q \\ \bullet \alpha \\ \text{--- } p \\ \bullet \delta \\ \text{--- } m \\ \bullet \gamma \\ \diagdown \quad \text{---} \\ c \quad F \quad n \end{array} \quad (78)$$

In all cases the diagrammatic expressions for the inverses of the coherence isomorphisms are obtained by reflecting the diagrams on a horizontal axis. This corresponds to evaluating the associated polygon diagrams counterclockwise and to an orientation reversal of the associated defect surface. This is possible, because all of the bimodule natural transformations in these tetrahedra are bimodule natural isomorphisms and hence their directions can be reversed, see the discussion before Definition 2.14.

We now investigate how the 6j symbols depend on the orientations of edges labeled by objects in spherical fusion categories. Recall that reversing the orientation of such an edge does not affect the orientation of the the orientations of the adjacent triangles and tetrahedra. Although it induces an odd permutation of the vertex numbers, which may be viewed as an orientation reversal for the associated *combinatorial* tetrahedron, the orientations in our formalism are fixed as part of the data.

Reversing the orientation of such an edge and replacing its label by its dual induces natural isomorphisms between the morphism spaces for the adjacent triangles.

For a  $\mathcal{C}$ -module functor  $F : \mathcal{M} \rightarrow \mathcal{N}$  and the first morphism space from (70), we obtain the following isomorphism that is natural in  $c \in \text{Ob}\mathcal{C}$ ,  $m \in \text{Ob}\mathcal{M}$  and  $n \in \text{Ob}\mathcal{N}$

(79)

For a  $\mathcal{C}$ -module functor  $G : \mathcal{N} \rightarrow \mathcal{M}$  and the third morphism space from (70) we have the isomorphism

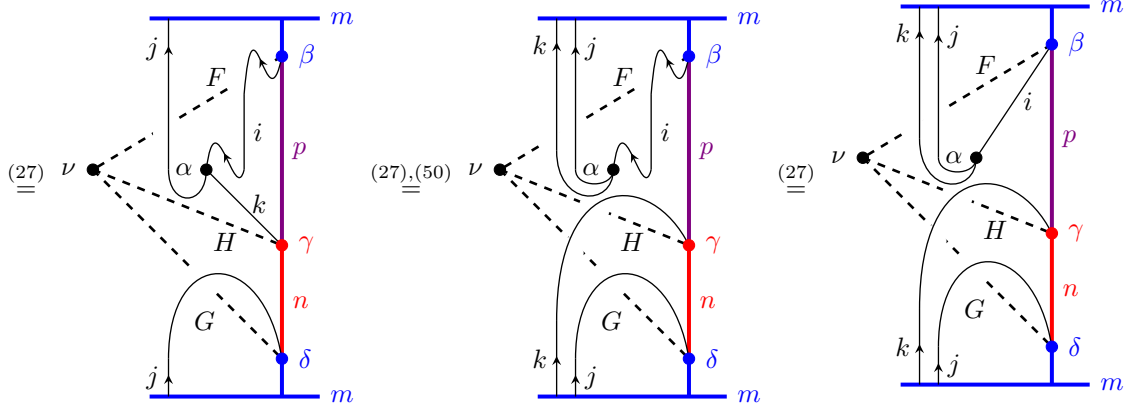
(80)

The isomorphisms for the other morphism spaces from (70) are analogous, just that the black line labeled  $c$  may be replaced by a grey line labeled  $d$  that crosses under the dashed lines for the functors.

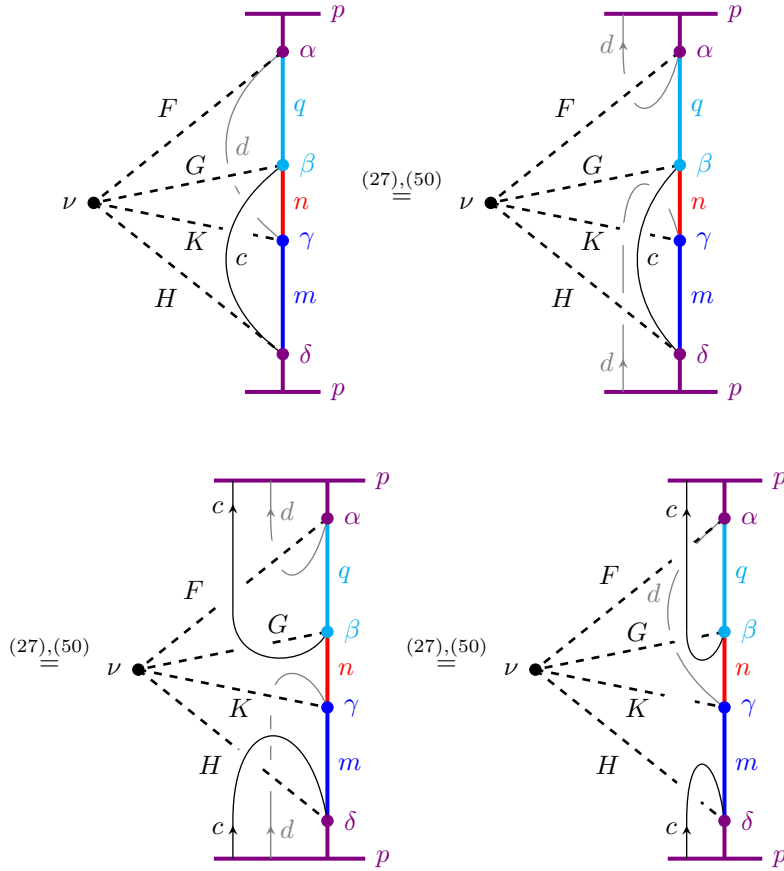
With these transformations of the morphism spaces one finds that reversing the orientation of an edge labeled by a spherical fusion category does not affect the generalised  $6j$  symbols of defect tetrahedra.

**Lemma 4.5.** *The  $6j$  symbol of a labeled generic transversal tetrahedron is invariant under reversing an edge labeled with an object  $c \in I_{\mathcal{C}}$  or  $d \in I_{\mathcal{D}}$ , replacing its label with the dual and transforming the morphisms at its triangles according to (79) and (80).*

*Proof.* This follows by a direct diagrammatic computation from (79) and (80), together with identity (27) and the second identity in (50) for the trace, applied to the black and grey lines of the diagram. It also uses identities (39) to (43) that encode the Reidemeister moves and the naturality conditions for the over- and undercrossings. For the first diagram in (72) this yields



and for the second diagram in (72)



□

The generalised 6j symbols are also invariant under a simultaneous orientation reversal of the defect surface and all defect lines on the surface, if the defect data is transformed accordingly.

**Lemma 4.6.** *The 6j symbol of a labeled generic transversal tetrahedron is invariant under*

- reversing the orientation of all defect areas and all defect lines,
- replacing each  $(\mathcal{C}, \mathcal{D})$ -bimodule category  $\mathcal{M}$  by the  $(\mathcal{D}, \mathcal{C})$ -bimodule category  $\mathcal{M}^\#$ ,
- replacing each bimodule functor  $F : \mathcal{M} \rightarrow \mathcal{N}$  by  $F^\# : \mathcal{M}^\# \rightarrow \mathcal{N}^\#$ ,
- replacing each bimodule natural transformation  $\nu : F \Rightarrow G$  by  $\nu^\# : G^\# \Rightarrow F^\#$ .

*Proof.* By Lemma 4.5, one may additionally reverse the orientation of all edges labeled with objects in spherical fusion categories and replace those objects by their duals without changing the associated 6j symbol.

Let  $t$  be a generic transversal tetrahedron and  $t'$  the tetrahedron obtained from  $t$  by reversing the orientations of all defect areas, defect lines and edges of  $t$  and transforming their labels accordingly. For each triangle of  $t$  the corresponding triangle of  $t'$  has the same morphism space assigned to it by (70), but interpreted as a morphism space in the opposite category. For instance,  $\text{Hom}_{\mathcal{M}}(F(c \triangleright m), n)$  is viewed as  $\text{Hom}_{\mathcal{M}^\#}(n, F(m \triangleleft c^*))$  and  $\text{Hom}_{\mathcal{M}}(m \triangleleft d, G(n))$  is viewed as  $\text{Hom}_{\mathcal{M}^\#}(G(n), d^* \triangleright m)$ .

Projecting the data from the spherical fusion categories on the defect plane of  $t'$  then yields a mirror image of the polygon diagram for  $t$ , in which the orientation of all interior lines is reversed, each bimodule category  $\mathcal{M}$  is replaced by its opposite  $\mathcal{M}^\#$ , each bimodule functor  $F$  by  $F^\#$ , each bimodule natural transformation  $\nu$  by  $\nu^\#$  and each object in a spherical fusion category by its dual. As the left action of  $c \in \text{Ob}\mathcal{C}$  or the right action of  $d \in \text{Ob}\mathcal{D}$  on  $\mathcal{M}$  corresponds to the right action of  $c^*$  and the left action of  $d^*$  on  $\mathcal{M}^\#$ , the evaluations of the polygon diagrams for  $t'$  and  $t$  are equal by Corollary 2.15.  $\square$

## 4.4 State sum model with defects

In this section we show how the generalised 6j symbols for generic transversal defect tetrahedra combine to state sums for a generic transversal triangulated 3-manifolds with defect data.

Let  $M$  be a generic transversal triangulated 3-manifold with defect data with regions  $r \in R$  and oriented defect areas  $a \in A$ . We denote by  $\mathcal{C}_r$  the spherical fusion category assigned to the region  $r$  and by  $\mathcal{M}_a$  the bimodule category assigned to the defect area  $a$ . A vertex, edge or triangle of the triangulation is called **boundary** if its is contained in  $\partial M$  and **internal** otherwise. We use the following notation:

- Tet for the set of tetrahedra of the triangulation,
- $\Delta$  for its set of triangles,  $\Delta_{\partial M}$  for its set of boundary triangles and  $\Delta_i$  for its set of internal triangles,
- $E$  for its set of edges,  $E_{\partial M}$  for its set of boundary edges and  $E_i$  for its set of internal edges,  $E_r$  for its set of edges in the region  $r$  and  $E_a$  for its set of edges that intersect a defect area  $a$ ,
- $V$  for its set of vertices,  $V_{\partial M}$  for its set of boundary vertices,  $V_i$  for its set of internal vertices and  $V_r$  for its set of vertices in the region  $r$ .

We fix for each spherical fusion category  $\mathcal{C}$  and each bimodule category  $\mathcal{M}$  sets  $I_{\mathcal{C}}$  and  $I_{\mathcal{M}}$  of representatives of the isomorphism classes of simple objects and associated projection and inclusion morphisms as in Section 3. For each labeling  $l$  of  $M$  as in Definition 4.2 we denote by  $l(e) \in I_{\mathcal{C}_r}$  or  $l(e') \in I_{\mathcal{M}_a}$  the simple object assigned to  $e \in E_r$  or  $e' \in E_a$ . For an oriented triangle  $f$  labeled with simple objects in the sets of representatives and associated projection or inclusion morphisms, we write  $\text{Hom}(f)$  for the associated morphism space from (70).

Each tetrahedron  $t \in \text{Tet}$  is equipped with the orientation induced by  $M$ . For the tetrahedra that intersect defect surfaces, this is already encoded in their labeling with defect data. For tetrahedra that do not intersect defect surfaces, we always assume this orientation choice without emphasising it notationally.

**Definition 4.7.** *Let  $M$  be a generic transversal triangulated 3-manifold with defect data,  $l_{\partial M}$  a labeling of its boundary edges with simple objects in the chosen sets of representatives and  $b$  an assignment of morphisms from the morphism spaces (70) to its boundary triangles. The state sum of  $(M, l_{\partial M}, b)$  is*

$$\mathcal{Z}(M, l_{\partial M}, b) = \frac{1}{\prod_{r \in R} \prod_{v \in V_r} \dim \mathcal{C}_r^{\epsilon(v)}} \sum_l \sum_{\text{Hom}(\Delta_i)} \prod_{t \in \text{Tet}} 6j(t) \prod_{e \in E} \dim l(e)^{\epsilon(e)}, \quad (81)$$

where

- $\epsilon(v) = 1$  for  $v \in V_i$ ,  $\epsilon(e) = 1$  for  $e \in E_i$  and  $\epsilon(v) = 1/2$  for  $v \in V_{\partial M}$ ,  $\epsilon(e) = 1/2$  for  $e \in E_{\partial M}$ ,
- $\Sigma_l$  is the sum over all labelings of  $M$  of internal edges with simple objects in the sets  $I_{\mathcal{C}_r}$  and  $I_{\mathcal{M}_a}$ ,
- $\Sigma_{\text{Hom}(\Delta_i)}$  is the sum over all projection and inclusion morphisms for internal triangles,
- $\prod_{t \in \text{Tet}} 6j(t)$  stands for the product over the generalised 6j symbols of all tetrahedra.

We denote by  $\mathcal{Z}(M, I_{\partial M})$  the associated linear map

$$\mathcal{Z}(M, I_{\partial M}) : \bigotimes_{f \in \Delta_{\partial M}} \text{Hom}(f) \rightarrow \mathbb{C}, \quad b \mapsto \mathcal{Z}(M, l_{\partial M}, b) \quad (82)$$

and by  $\mathcal{Z}'(M, l_{\partial M}, b)$  the rescaled state sum without the dimension factors of boundary edges and vertices

$$\mathcal{Z}(M, l_{\partial M}, b) = \left( \frac{\prod_{e \in E_{\partial M}} \dim l(e)}{\prod_{r \in R} \prod_{v \in V_r \cap V_{\partial M}} \dim \mathcal{C}_r} \right)^{1/2} \mathcal{Z}'(M, l_{\partial M}, b). \quad (83)$$

It is clear that the linear map  $\mathcal{Z}(M, l_{\partial M})$  does not depend on the choice of projection and inclusion morphisms for the interior triangles. If the simple objects assigned to the edges of the triangulation are fixed, then the projection and inclusion morphisms assigned to the interior triangles are fixed by (53) up to simultaneous rescaling  $p_{xm}^\alpha \rightarrow \lambda p_{xm}^\alpha$  and  $j_{xm}^\alpha \rightarrow \lambda^{-1} j_{xm}^\alpha$  for  $\lambda = \lambda(x, m, \alpha) \in \mathbb{C}^\times$ . As each interior triangle arises in exactly two tetrahedra with opposite orientations, the state sum is invariant under such rescalings.

To determine the dependence of the state sum on the choice of representatives of simple objects, let  $M$  be a triangulated 3-manifold with defect data. Fix two sets of representatives  $I, I'$  for each category labeling a region or defect area and an isomorphism  $\phi_{xx'} : x \rightarrow x'$  for each pair of isomorphic objects  $x \in I, x' \in I'$ . Note that this isomorphism is unique up to rescaling with  $\mathbb{C}^\times$  and that it induces an isomorphism  $\phi_f : \text{Hom}(f) \rightarrow \text{Hom}(f)'$  between the morphism spaces for a triangle  $f$  labeled by isomorphic objects in  $I$  and  $I'$ . More explicitly, these isomorphisms are given by

$$\begin{aligned} \phi_f : \text{Hom}(m, F(j \triangleright n)) &\rightarrow \text{Hom}(m', F(j' \triangleright n')), & \alpha &\mapsto F(\phi_{jj'} \triangleright \phi_{nn'}) \circ \alpha \circ \phi_{mm'}^{-1} \\ \phi_f : \text{Hom}(F(j \triangleright n), n) &\rightarrow \text{Hom}(F(j' \triangleright n'), n'), & \beta &\mapsto \phi_{mm'} \circ \beta \circ F(\phi_{jj'}^{-1} \triangleright \phi_{nn'}^{-1}). \end{aligned}$$

Definition 4.3 and the cyclic invariance of the trace imply that the 6j symbols are invariant under these isomorphisms, if they are applied to all morphism spaces simultaneously. This yields

**Corollary 4.8.** *Let  $M$  be a generic transversal triangulated 3-manifold with defect data. Let  $l_{\partial M}$  and  $l'_{\partial M}$  be labelings of the boundary triangles with simple objects in two sets of representatives  $I, I'$ . Then*

$$\mathcal{Z}(M, l_{\partial M}) = \mathcal{Z}(M, l'_{\partial M}) \circ (\otimes_{f \in \Delta_{\partial M}} \phi_f) : \bigotimes_{f \in \Delta_{\partial M}} \text{Hom}(f) \rightarrow \mathbb{C}.$$

In particular, it follows that the state sum for a *closed* generic transversal triangulated 3-manifold with defect data does not depend on the choice of representatives of simple objects.

It is also apparent from Definition 4.7 that the state sum (81) is a direct generalisation of the usual Turaev-Viro-Barrett-Westbury state sum from [BW96, TV92] and coincides with it if all defect areas, defect lines and defect vertices are trivial. This amounts to replacing all bimodule categories in (81) by a single spherical fusion category  $\mathcal{C}$ , viewed as a  $(\mathcal{C}, \mathcal{C})$ -bimodule category, and all bimodule functors and natural transformations by identity functors and natural transformations.

**Corollary 4.9.** *For any triangulated 3-manifold without defects and any generic transversal triangulated 3-manifold with trivial defect data, labeled by a spherical fusion category  $\mathcal{C}$ , the state sum from Definition 4.7 reduces to the Turaev-Viro-Barrett-Westbury state sum*

$$\mathcal{Z}(M, l_{\partial M}, b) = \frac{1}{\dim \mathcal{C}^{|V_i| + |V_{\partial M}|/2}} \sum_l \sum_{\text{Hom}(\Delta_i)} \prod_{t \in \text{Tet}} 6j(t) \prod_{e \in E} \dim l(e)^{\epsilon(e)}. \quad (84)$$

Another direct consequence of Definition 4.7 is that the state sum can be computed by gluing triangulated 3-manifolds along a boundary components. As in the case without defects, this allows one to compute state sums by cutting 3-manifolds into simpler pieces. The only additional restriction is that the defect surfaces must meet the cut transversally and all pieces must be generic and transversal.

**Corollary 4.10.** *Let  $M_1$  and  $M_2$  be generic transversal triangulated 3-manifolds with defect data and  $M$  obtained by gluing  $M_1$  and  $M_2$  along a boundary component  $\Sigma \subset \partial M_i$ . Then*

$$\mathcal{Z}(M, l_{\partial M}, b) = \sum_{l_\Sigma} \mathcal{Z}(M_1, l_{\partial M_1}, b_1) \cdot \mathcal{Z}(M_2, l_{\partial M_2}, b_2), \quad (85)$$

where the labelings  $l_{\partial M}$  and  $b$  of  $\partial M$  are induced by the labelings  $l_{\partial M_i}$  and  $b_i$  of  $\partial M_i$  and the sum is over the labelings of edges in  $\Sigma$  with simple objects and over dual bases of the morphism spaces for triangles in  $\Sigma$ .

## 5 Topological invariance

### 5.1 Moves between triangulated PL manifolds

To establish triangulation independence for state sum models with defects, we require some background from PL topology. We consider different moves on triangulations that relate PL homeomorphic 3-manifolds with

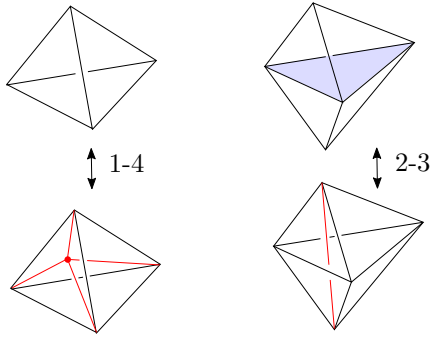


Figure 4: Bistellar moves for a tetrahedron.

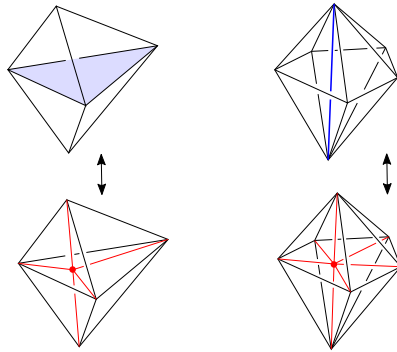


Figure 5: Stellar subdivisions for a triangle and an edge of a triangulation.

and without boundary. The main references are the articles [P91, P90] by Pachner, see also the articles [Li99] by Lickorish and [C95] by Casali.

**Theorem 5.1.** [P91, Th. 5.5],[Li99, Th. 5.9]

*Two closed triangulated  $n$ -dimensional PL manifolds are PL homeomorphic iff they are related by a finite sequence of bistellar moves.*

**Theorem 5.2.** [C95]

*Two triangulated  $n$ -dimensional PL manifolds with boundary, whose boundary triangulations coincide, are PL homeomorphic iff they are related by bistellar moves.*

The **bistellar moves** for a 3-manifold are the 2-3 move and the 1-4 move depicted in Figure 4. The 1-4 move subdivides a tetrahedron into four by inserting a new vertex in its interior or reverses this step. The 2-3 move replaces two tetrahedra that share a triangle by three tetrahedra that share an edge or reverses this step.

We also consider **stellar subdivisions**, see for instance [RS]. The stellar subdivision for a tetrahedron is the 1-4 move from Figure 4. The stellar subdivisions for a triangle and an edge are shown in Figure 5. A stellar subdivision of a triangle  $\Delta$  inserts a vertex in the interior of  $\Delta$  and connects it to the vertices of  $\Delta$  and to the opposite vertices of all tetrahedra containing  $\Delta$ . A stellar subdivision of an edge  $e$  inserts a vertex in the interior of  $e$  and connects it to the opposite vertices of all triangles containing  $e$ .

It is shown in [BW96] that stellar subdivisions are composites of 1-4 and 2-3 moves. The stellar subdivision for a triangle  $\Delta$  is obtained by first applying a 1-4 move to one of the two tetrahedra containing  $\Delta$  and then a 2-3 move to the other tetrahedron and the adjacent tetrahedron created by the 1-4 move, see the proof of Theorem 4.6 in [BW96]. The stellar subdivision for an edge  $e$  shared by  $n$  tetrahedra is obtained by first applying a 1-4 move to one of the tetrahedra containing  $e$ . Then one applies a sequence of  $(n - 2)$  2-3 moves clockwise to the remaining tetrahedra containing  $e$ . These 2-3 moves connect the new vertex to the vertices of these tetrahedra. Finally one applies a 2-3 move that removes  $e$ , see the proof of Theorem 4.6 in [BW96].

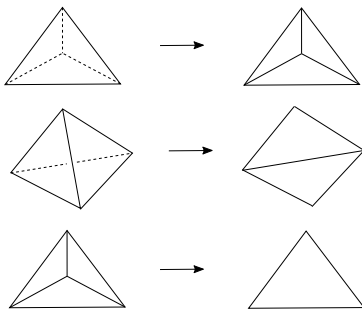


Figure 6: Elementary shellings: removing a tetrahedron with one, two or three faces in the boundary.

For 3-manifolds with boundaries one also needs to consider elementary shellings and their inverses. An **elementary shelling** of a PL 3-manifold  $M$  removes a 3-simplex  $t$  that is the join  $t = A \star B = \text{conv}(A \cup B)$  of two simplexes  $A$  and  $B$  with  $A \cap M = \partial A$  and  $B \star \partial A \subset \partial M$  and replaces  $M$  by the closure of  $M \setminus A \star B$ , see [Li99, Def. 5.2]. This amounts to removing the tetrahedron  $t$ , which has one, two or three faces in the boundary  $\partial M$ , such that its remaining faces become boundary faces, as shown in Figure 6. Correspondingly, an **inverse shelling** amounts to adding a tetrahedron to  $M$  that shares one, two or three triangles with  $\partial M$ .

Elementary shellings and their inverses on a 3-manifold  $M$  induce bistellar moves on the boundary  $\partial M$ . These are the 1-3 move, which subdivides a boundary triangle into three by adding a vertex in its interior or reverses this step, and the 2-2 move, which replaces a common edge shared by two boundary triangles with the edge connecting their remaining two vertices, as in Figure 6. It is shown in [P90, P91] that triangulations of a PL manifold with boundary are related by bistellar moves, elementary shellings and their inverses.

**Theorem 5.3.** [P91, Th. 4.14], [P90, Th. 2]

Two triangulated  $n$ -dimensional PL manifolds  $M, M'$  with boundary are PL homeomorphic iff  $M$  can be transformed into  $M'$  by a finite number of elementary shellings and bistellar moves.

**Theorem 5.4.** [P91, Th. 6.3], [Li99, Th. 5.10]

Two connected triangulated  $n$ -dimensional PL manifolds with non-empty boundary are PL homeomorphic iff they are related by a finite sequence of elementary shellings and inverse shellings.

If a triangulated  $n$ -manifold  $M$  is transformed into  $M'$  by a finite number of elementary shellings, one says that  $M$  **shells** to  $M'$ . A triangulated  $n$ -manifold  $M$  is called **shellable** if it shells to an  $n$ -simplex. It is well-known that every triangulation and, more generally, CW-decomposition of a 2-disc is shellable. This does not hold for triangulations or CW-decompositions of the 3-ball, see Ziegler [Zi98] and the references therein.

The triangulation independence of the Turaev-Viro-Barrett-Westbury state sum from [TV92, BW96] follows from its invariance under bistellar moves. It is shown in [BW96] and [T] that the invariance of the state sum under the 2-3 move in Figure 4 encodes the pentagon relation for the associator of a spherical fusion category. Its invariance under the 1-4 move in Figure 4 corresponds to an equivalent relation obtained by inverting one of the associators in the pentagon relation. It follows from the invariance under the 2-3 move and under a *bubble move*. The latter corresponds to the invertibility of the associator and states that gluing two tetrahedra with opposite orientations along four faces yields the trivial state sum.

The pentagon relation for the associator is encoded in the Biedenharn-Elliott relations for the 6j symbols and the invertibility of the associator in their orthogonality relations [BW96, Prop. 5.2]. They are obtained by expressing the associator on simple objects of  $\mathcal{C}$  as in (74) and using its naturality. In our notation they read

$$\sum_{\beta} \alpha \begin{array}{c} \text{---} m \\ | \\ \bullet \beta \\ / \quad \backslash \\ k \quad j \quad n \\ \backslash \quad / \quad | \\ \gamma \quad p \\ | \\ \bullet \delta \\ \text{---} m \end{array} \phi \begin{array}{c} \text{---} m \\ | \\ \bullet \rho \\ / \quad \backslash \\ a \quad b \quad q \\ \backslash \quad / \quad | \\ \sigma \quad n \\ | \\ \bullet \beta \\ \text{---} m \end{array} = \sum_{c, \lambda, \mu, \nu} \dim(c) \lambda \begin{array}{c} \text{---} m \\ | \\ \bullet \rho \\ / \quad \backslash \\ a \quad c \quad q \\ \backslash \quad / \quad | \\ i \quad \mu \quad n \\ | \\ \bullet \delta \\ \text{---} m \end{array} \alpha \begin{array}{c} \text{---} a \\ | \\ \bullet \phi \\ / \quad \backslash \\ k \quad j \quad b \\ \backslash \quad / \quad | \\ \nu \quad c \\ | \\ \bullet \lambda \\ \text{---} a \end{array} \nu \begin{array}{c} \text{---} p \\ | \\ \bullet \mu \\ / \quad \backslash \\ c \quad b \quad q \\ \backslash \quad / \quad | \\ j \quad n \\ | \\ \bullet \gamma \\ \text{---} p \end{array} \quad (86)$$



$$\sum_{p,\gamma,\delta} \dim(p) \dim(k) \begin{array}{c} \text{--- } m \\ | \\ \alpha \text{---} \beta \\ \quad \diagup \quad | \\ \quad k \quad j \quad n \\ \quad \diagdown \quad | \\ \quad i \quad p \\ \quad \quad \delta \\ \text{--- } m \end{array} \begin{array}{c} \text{--- } m \\ | \\ \sigma \text{---} \delta \\ \quad \diagup \quad | \\ \quad i \quad j \quad p \\ \quad \diagdown \quad | \\ \quad l \quad n \\ \quad \quad \rho \\ \text{--- } m \end{array} = \delta_{\alpha\sigma} \delta_{\beta\rho} \delta_{kl} \quad (87)$$

These relations yield a direct proof of the triangulation independence of the state sum for closed 3-manifolds [BW96, Th. 5.1]. For 3-manifolds with boundary one has

**Theorem 5.5.** [TV92, Th. 1.4], [T, Th. 1.7]

Let  $M, M'$  be compact triangulated 3-manifolds with boundary whose boundary triangulations and boundary labelings  $l_{\partial M}$  and  $b$  coincide. Then their state sums (84) are equal.

## 5.2 Neighbourhoods of defect surfaces

In the presence of defects, applying a bistellar move to a generic transversal triangulation may yield a triangulation that is no longer transversal or generic. For this reason, it is not straightforward to establish invariance of the state sums via bistellar moves. Instead, we refine the triangulations and decompose the underlying defect 3-manifold into certain neighbourhoods of defect surfaces and components contained in the regions between them. Their state sums are computed separately and then glued with Corollary 4.10. This also gives a geometrical interpretation to the state sums and facilitates the computation of examples.

The neighbourhoods of the defect surfaces we consider are similar to regular neighbourhoods, see [RS, Ch. 3], but our defect surfaces are not realised as subcomplexes of the triangulation.

**Definition 5.6.** A **fine neighbourhood** of a defect surface  $D$  is a connected generic transversal triangulated 3-manifold  $M$  with defect surface  $D \subset M$  such that  $D \cap \partial M = \partial D$ , every vertex of  $M$  is contained in  $\partial M$  and every triangle or edge in  $M$  that does not intersect  $D$  is contained in  $\partial M$ .

By applying a finite number of bistellar moves between generic transversal triangulations, any generic transversal triangulation of a defect 3-manifold  $M$  can be subdivided in such a way that the tetrahedra intersecting a given defect surface form a fine neighbourhood of the defect surface. A bistellar move between two generic transversal triangulations is called **generic transversal bistellar move** in the following.

**Lemma 5.7.** Let  $(M, D)$  be a defect 3-manifold and  $T$  a generic transversal triangulation of  $M$ . Then there is a finite sequence of generic transversal bistellar moves that transforms  $T$  into a generic transversal triangulation  $S$  such that:

- (i)  $S$  coincides with  $T$  on  $\partial M$ ,
- (ii) the tetrahedra in  $S$  contained in any region  $r \subset M$  form a 3-manifold  $R$  homeomorphic to  $\bar{r}$ ,
- (iii) the tetrahedra in  $S$  that intersect any defect surface  $\Sigma \subset D$  form a fine neighbourhood of  $\Sigma$ .

*Proof.* Let  $D = \amalg_{j=1}^n \Sigma_j$  be the defect manifold, whose connected components are the defect surfaces  $\Sigma_j$ , and  $M \setminus D = \amalg_{k=1}^m r_k$  with the regions  $r_k$  as connected components.

For each oriented edge in  $T$  that intersects  $D$  and hence is oriented by  $D$ , denote by  $r_f$  the region that contains its target vertex and by  $r_i$  the region that contains its starting vertex. Analogously, for each triangle and tetrahedron in  $T$  that intersects  $D$ , denote by  $r_f$  and  $r_i$  the regions that contain the target vertices and starting vertices of its edges that intersect  $D$ .

The triangulation  $S$  is constructed by a finite sequence of stellar subdivisions from Section 5.1, which are finite sequences of bistellar moves. We show that this can be achieved with generic transversal bistellar moves.

1. In the first step, for each tetrahedron  $t$  in  $T$  that intersects  $D$ , choose a point  $t_f \in r_f \cap \mathring{t}$  and perform a 1-4 move with  $t_f$  as the new vertex. This subdivides  $t$  into four transversal tetrahedra. By adjusting the position of  $t_f$  one can achieve that none of the new triangles contains a defect vertex and none of the new edges intersect defect lines. Hence, all four tetrahedra are generic. This yields a generic transversal triangulation  $T'$  related to  $T$  by generic transversal bistellar moves.

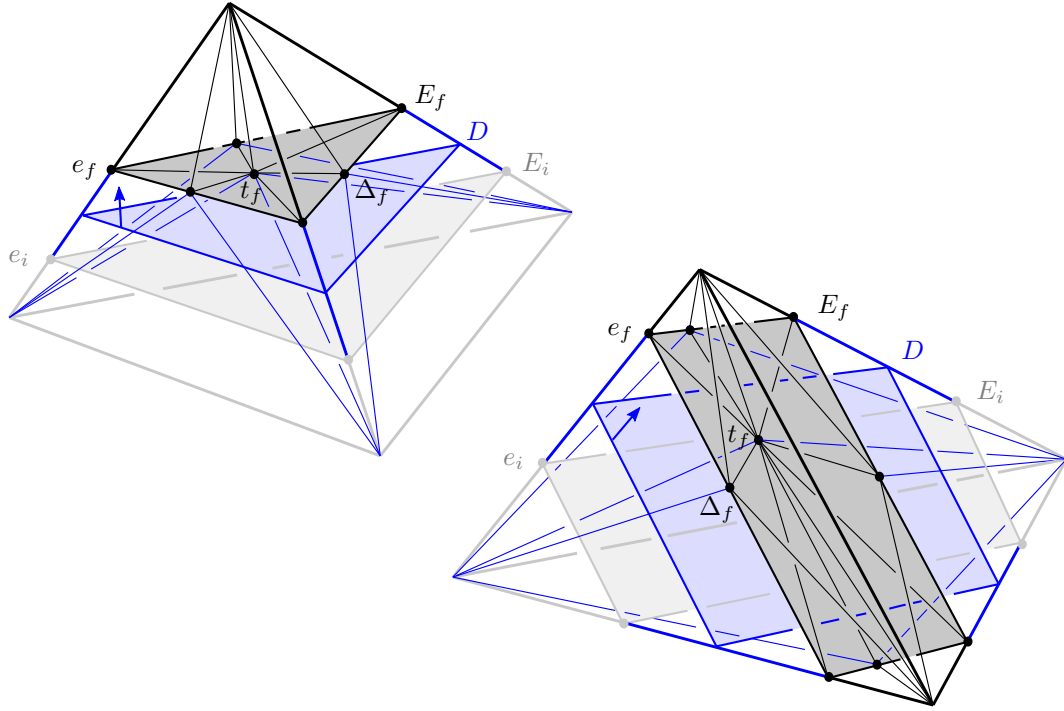


Figure 7: Subdivisions of tetrahedra intersecting the defect manifold  $D$  with new vertices  $t_f$ ,  $\Delta_f$  and  $e_f$  that span the surface  $E_f$ . Edges in the subdivision that intersect  $D$  are drawn in blue, edges that lie in the region  $r_f$  in black and edges in the region  $r_i$  in gray.

2. In the second step, for each triangle  $\Delta$  in  $T'$  that intersects  $D$  and is not contained in  $\partial M$ , choose a point  $\Delta_f \in r_f \cap \mathring{\Delta}$  and perform the stellar subdivision on  $\Delta$  with  $\Delta_f$  as the new vertex. The two bistellar moves that combine to this stellar subdivision involve only transversal tetrahedra. By adjusting the position of  $\Delta_f$  one can achieve that none of the triangles arising in these moves contains a defect vertex and none of the edges intersect a defect line. With this, all of the tetrahedra become generic and we obtain a generic transversal triangulation  $T''$  related to  $T'$  by generic transversal bistellar moves.

3. In the third step, for each edge  $e$  in  $T''$  that intersects  $D$  and is not contained in  $\partial M$ , choose a point  $e_f \in r_f \cap \mathring{e}$  and perform a stellar subdivision on  $e$  with  $e_f$  as the new vertex. All tetrahedra arising in the bistellar moves that combine to this stellar subdivision are transversal. By adjusting the position of  $e_f$ , one can achieve that none of their triangles contains a defect vertex and none of their edge intersects a defect line. Hence, all tetrahedra in this sequence of bistellar moves are generic.

This yields a generic transversal triangulation  $T'''$  related to  $T$  by generic transversal bistellar moves. The associated subdivisions of defect tetrahedra are shown in Figure 7. We equip each new edge in  $T'''$  that intersects  $D$  with the induced orientation and choose an arbitrary orientation for the other new edges.

4. We then apply steps 1 to 3 to the triangulation  $T'''$ , but now with additional vertices  $t_i \in r_i \cap \mathring{t}$ ,  $\Delta_i \in r_i \cap \mathring{\Delta}$ ,  $e_i \in r_i \cap \mathring{e}$  in the region  $r_i$  instead of  $r_f$ . The positions of these new vertices can again be chosen in such a way that this defines a finite sequence of bistellar moves between generic transversal tetrahedra.

The result is a generic transversal triangulation  $S$  that coincides with  $T$  on  $\partial M$  by construction. We denote by  $S_j$  the triangulated 3-manifold formed by all tetrahedra in  $S$  that intersect a defect surface  $\Sigma_j$ . By construction, every vertex of  $S_j$  and every edge or triangle of  $S_j$  that does not intersect  $\Sigma_j$  is contained in  $\partial S_j$ , and hence  $S_j$  is a fine neighbourhood of  $\Sigma_j$ . For each tetrahedron  $t$  in the triangulation  $T$  that intersects  $\Sigma_j$ , the union of the tetrahedra in its subdivision that are contained in a region  $r_k$  is PL homeomorphic to the closure of  $(t \setminus D) \cap r_k$ . These PL homeomorphisms and the identity maps for tetrahedra in  $T$  that do not intersect  $D$  glue to a PL homeomorphism from the union of all tetrahedra in  $S$  in  $r_k$  to  $\bar{r}_k$ .  $\square$

A fine neighbourhood of a defect surface  $D$  is shown in Example 6.2 and Figure 9. Generic transversal triangulations that do not form fine neighbourhoods of their defect surfaces are given in Examples 6.1, 6.3 and 6.4, see also Figures 11 and 12. In particular, any fine neighbourhood of  $D$  must have topology  $[0, 1] \times D$ .

**Lemma 5.8.** *Let  $M$  be a triangulated 3-manifold that shells to a fine neighbourhood of a defect surface  $D$  by elementary shellings with tetrahedra that do not intersect  $D$ . Then  $M$  is PL homeomorphic to  $[0, 1] \times D$ .*

*Proof.* If  $M$  is a fine neighbourhood of  $D$ , this follows by applying the same subdivision procedure as in the proof of Lemma 5.7, but to every edge and triangle that intersects the defect surface  $D$ , including the ones in  $\partial M$ . Denote by  $E_f$  the 2d PL surface spanned by the vertices  $t_f$ ,  $\Delta_f$  and  $e_f$ , by  $E_i$  the 2d PL surface spanned by the new vertices  $t_i$ ,  $\Delta_i$  and  $e_i$ , as shown in Figure 7. For each tetrahedron  $t$  in the original triangulation with  $t \cap D \neq \emptyset$  the tetrahedra in its subdivision that intersect  $D$  form the region between the surfaces  $E_t \cap t$  and  $E_i \cap t$  in Figure 7. This region is PL homeomorphic to  $[0, 1] \times (t \cap D)$ . The PL homeomorphisms for the tetrahedra  $t$  with  $t \cap D \neq \emptyset$  glue to a PL homeomorphism that sends the union of all tetrahedra in the subdivision that intersect  $D$  to  $[0, 1] \times D$ . As  $M$  is related to it by elementary shellings, it is PL homeomorphic to  $[0, 1] \times D$  by Theorem 5.4. For a 3-manifold  $M$  that shells to a fine neighbourhood of  $D$  with elementary shellings by tetrahedra that do not intersect  $D$  the claim follows with Theorem 5.4.  $\square$

In the following, we will often project graphs on the boundary of a manifold  $M$  with a defect surface  $D \subset M$  to the defect surface  $D$ . This is achieved via orientation preserving PL homeomorphisms  $\phi : M \rightarrow [0, 1] \times D$ . We denote by  $p_D : [0, 1] \times D \rightarrow D$ ,  $(t, d) \mapsto d$  and  $p_t : [0, 1] \times D \rightarrow [0, 1]$ ,  $(t, d) \mapsto t$  the projection maps for the product, which are PL maps by construction.

**Definition 5.9.** *Let  $M$  be a triangulated 3-manifold with a defect surface  $D \subset M$  and  $\phi : M \rightarrow [0, 1] \times D$  an orientation preserving PL homeomorphism with  $p_D \circ \phi|_D = \text{id}_D$ . The **projections** induced by  $\phi$  are the PL homeomorphisms  $P_i(\phi) : \phi^{-1}(\{i\} \times D) \rightarrow D$ ,  $m \mapsto p_D \circ \phi(m)$  for  $i = 0, 1$ .*

The diagrams obtained by projecting graphs on  $\partial M$  to a defect surface  $D \subset M$  depend on the choice of the underlying PL homeomorphism. That their *evaluations* are independent of this choice follows from the fact that different choices of PL homeomorphisms yield PL isotopic projection maps.

**Lemma 5.10.** *Let  $\phi_1, \phi_2 : M \rightarrow [0, 1] \times D$  be orientation preserving PL homeomorphisms with  $p_D \circ \phi_1|_D = p_D \circ \phi_2|_D = \text{id}_D$ . Then the projection maps  $P_i(\phi_1)$  and  $P_i(\phi_2)$  are PL isotopic for  $i = 0, 1$ .*

*Proof.* By a well-known result of Epstein [E66, Th. 6.4], an orientation preserving PL homeomorphism from a 2-manifold with compact boundary components to itself is PL isotopic to the identity iff it is homotopic to the identity. It is therefore sufficient to show that  $P_i(\phi_2)$  and  $P_i(\phi_1)$  are homotopic. For this, we construct homeomorphisms  $\phi'_i : M \rightarrow [0, 1] \times D$  that coincide with  $\phi_i$  on  $\partial M_i := \phi_i^{-1}(\{i\} \times D) = \phi_2^{-1}(\{i\} \times D)$  and homotopies from  $\phi'_2|_{\partial M_i}$  to  $\phi'_1|_{\partial M_i}$ . For  $i = 0$  and  $j = 1, 2$ , we consider the continuous maps

$$F_j : [0, 1] \times D \rightarrow [0, 1], (t, d) \mapsto \begin{cases} \frac{t}{2p_t(\phi_j(d))} & t \in [0, p_t(\phi_j(d))] \\ \frac{1-t}{2(1-p_t(\phi_j(d)))} + \frac{t-p_t(\phi_j(d))}{1-p_t(\phi_j(d))} & t \in [p_t(\phi_j(d)), 1] \end{cases}$$

and the homeomorphisms  $\phi'_j : M \rightarrow [0, 1] \times D$ ,  $m \mapsto (F_j(\phi_j(m)), p_D(\phi_j(m)))$  that satisfy  $\phi'_j(m) = \phi_j(m)$  for all  $m \in \partial M_0 \cup \partial M_1$ ,  $p_D \circ \phi'_j(d) = d$  and  $p_t \circ \phi'_j(d) = \frac{1}{2}$  for all  $d \in D$ . Then the continuous map

$$h : [0, 1] \times \partial M_0 \rightarrow D, (t, m) \mapsto p_D \circ \phi'_2 \circ \phi_1'^{-1}(\frac{t}{2}, p_D(\phi_1'(m)))$$

satisfies  $h(0, m) = P_0(\phi_2)(m)$  and  $h(1, m) = P_0(\phi_1)(m)$  for all  $m \in \partial M_0$  and is a homotopy from  $P_0(\phi_1)$  to  $P_0(\phi_2)$ . The proof that  $P_1(\phi_1)$  and  $P_1(\phi_2)$  are homotopic is analogous.  $\square$

### 5.3 State sums with defect discs

To prove the triangulation independence of the state sum, we first show that the state sums of 3-balls  $M$  that shell to fine neighbourhoods of defect discs  $D$  are given as cyclic evaluations of certain polygon diagrams.

These polygon diagrams are obtained by projecting the dual graphs of the boundary triangulations on  $\partial M$  to the defect disc. As  $M$  is PL homeomorphic to  $[0, 1] \times D$  via an orientation preserving PL homeomorphism  $\phi : M \rightarrow [0, 1] \times D$  by Lemma 5.8, this projection is given by Definition 5.9. Lemma 5.10 ensures that different choices of  $\phi$  yield graphs on  $D$  that are related by isotopies.

**Proposition 5.11.** *Let  $M$  be a 3-manifold with defect data that shells to a fine neighbourhood of a defect disc  $D$  by shellings with tetrahedra that do not intersect  $D$ . Then for all labelings  $l_{\partial M}$ ,  $b$  as in Definition 4.7*

$$\mathcal{Z}'(M, l_{\partial M}, b) = \text{ev}(P),$$

where  $\text{ev}(P)$  is the cyclic evaluation of the polygon diagram  $P$  obtained by

- projecting the dual graph of the boundary triangulation on  $\partial M$  to  $D$ ,
- labeling the edges and vertices of the resulting diagram with the data assigned by  $l_{\partial M}$  and  $b$ .

*Proof.* 1. We first suppose that  $M$  is a fine neighbourhood of the defect disc  $D$  and prove the claim by induction over the number of tetrahedra in the triangulation. For a single tetrahedron, this holds by definition of the generalised 6j symbol, see Figure 3, and of the rescaled state sum.

Any fine neighbourhood  $M$  of  $D$  with  $n + 1$  tetrahedra is obtained by gluing a single tetrahedron  $t$  to a fine neighbourhood  $M'$  of  $D$  with  $n$  tetrahedra. This follows, because the triangulation of  $M$  defines a cell complex structure on  $D$  and every cell decomposition of a disc is shellable, see for instance Sanderson [Sa57, Lemma 1]. Shellings of the defect disc correspond to 3d shellings of its fine neighbourhood  $M$ .

The tetrahedron  $t$  can be glued to  $M'$  either along one or two faces. Gluing along three faces is not possible, as  $t$  intersects  $D$  either in three edges incident at a common vertex as in Figure 2 (a) or in all except two opposite edges as in Figure 2 (b). The first case would yield a contradiction to the assumption that the defect surfaces in  $M$  and  $M'$  are both discs. In the second case there would be an internal edge in  $M$  common to two glued faces that does not intersect  $D$ , contradicting that  $M$  is a fine neighbourhood of  $D$ .

By Corollary 4.10, formula (83) and the induction hypothesis, the rescaled state sum for  $M$  is

$$\mathcal{Z}'(M, l_{\partial M}, b) = \sum_l \sum_{\text{Hom}_g} \prod_{e \in E_g} \dim l(e) \text{ev}(P') \text{6j}(t), \quad (88)$$

where

- $\text{ev}(P')$  denotes the cyclic evaluation of the corresponding polygon diagram for  $M'$ ,
- $E_g$  is the set of internal edges in  $M$  that correspond to boundary edges of  $t$  and  $M'$ ,
- the sum  $\sum_l$  runs over all labelings of edges in  $E_g$  with simple objects in the chosen sets of representatives,
- the sum  $\sum_{\text{Hom}_g}$  runs over bases of the morphism spaces for glued faces of  $t$  and  $M'$ .

We compute the sum in (88) depending on the number of glued faces of  $t$ :

(i) If  $t$  is glued to  $M'$  along a single face  $f$ , then  $E_g = \emptyset$ . Identity (66) implies that the sum in (88) is given by

$$\mathcal{Z}'(M, l_{\partial M}, b) = \sum_{\text{Hom}_g} \text{ev}(P') \text{6j}(t) \stackrel{(66)}{=} \text{ev}(P).$$

(ii) If  $t$  is glued to  $M'$  along two faces  $f, f'$  that share an edge  $e$ , then  $E_g = \{e\}$  and  $e$  intersects  $D$ . Otherwise,  $t$  would have to intersect  $D$  in four edges, as in Figure 2 (b). As the intersections of the defect disc in  $t$  with  $f$  and  $f'$  are both glued to the boundary of the defect disc in  $M'$ , the defect surface  $D$  could not be a disc.

We apply identity (66) to glue  $t$  on  $M'$  along  $f$ . This yields a polygon diagram  $P''$  with the morphisms for  $f'$  assigned to adjacent sides of  $P''$  that are separated by a vertex labeled  $l(e)$ . Identity (67) implies that the state sum in (88) is given by

$$\mathcal{Z}'(M, l_{\partial M}, b) = \sum_{l(e)} \sum_{\substack{\text{Hom}(f), \\ \text{Hom}(f')}} \dim l(e) \text{ev}(P') \text{6j}(t) \stackrel{(66)}{=} \sum_{l(e)} \sum_{\text{Hom}(f')} \dim l(e) \text{ev}(P'') \stackrel{(67)}{=} \text{ev}(P).$$

This proves the claim for the case where  $M$  is a fine neighbourhood of the defect disc.

2. Suppose now that  $M$  is obtained from a fine neighbourhood of the defect disc by inverse shellings with tetrahedra that do not intersect  $D$ . We prove the claim by induction over the number  $n$  of tetrahedra in the triangulation that do not intersect  $D$ . If  $n = 0$  the claim holds by 1.

If  $M$  contains  $n + 1$  tetrahedra that do not intersect  $D$ , then  $M$  is obtained by gluing a tetrahedron  $t$  that does not intersect  $D$  to a defect 3-manifold  $M'$  with  $n$  tetrahedra that do not intersect  $D$  and also satisfies

the assumptions. If  $t$  is contained in a region labeled by a spherical fusion category  $\mathcal{C}$ , then by Corollary 4.10 and the induction hypothesis, the rescaled state sum for  $M$  is given by

$$\mathcal{Z}'(M, l_{\partial M}, b) = \sum_l \sum_{\text{Hom}_g} \frac{\prod_{e \in E_g} \dim l(e)}{\dim \mathcal{C}^{v_g}} \text{ev}(P') \text{6j}(t), \quad (89)$$

where the notation is as in (88) and  $v_g \in \{0, 1\}$  is the number of internal vertices in  $M$  that correspond to boundary vertices of  $t$  and  $M'$ . We compute the sum in (89) depending on the number of glued faces of  $t$ :

(i) If  $t$  is glued to  $M'$  along a single face  $f$ , then  $E_g = \emptyset$  and  $v_g = 0$ . Identity (69) then implies that the state sum in (89) is given by

$$\mathcal{Z}'(M, l_{\partial M}, b) = \sum_{\text{Hom}_g} \text{ev}(P') \text{6j}(t) \stackrel{(69)}{=} \text{ev}(P).$$

(ii) If  $t$  is glued to  $M'$  along two faces  $f, f'$  that share an edge  $e$ , then  $E_g = \{e\}$  and  $v_g = 0$ . We use identity (69) to insert the 6j symbol for  $t$  into the diagram  $P'$ . This yields a polygon diagram  $P''$  with the morphisms for  $f'$  assigned to vertices in the interior that are connected by an edge labeled  $l(e)$ . Applying the second identity in (60) then yields

$$\mathcal{Z}'(M, l_{\partial M}, b) = \sum_{l(e)} \sum_{\substack{\text{Hom}(f), \\ \text{Hom}(f')}} \dim l(e) \text{ev}(P') \text{6j}(t) \stackrel{(69)}{=} \sum_{l(e)} \sum_{\text{Hom}(f')} \dim l(e) \text{ev}(P'') \stackrel{(60)}{=} \text{ev}(P).$$

(iii) If  $t$  is glued to  $M'$  along three faces  $f, f', f''$ , then they share three edges  $e = f \cap f'$ ,  $e' = f \cap f''$  and  $e'' = f' \cap f''$ , and there is exactly one vertex  $v$  in  $t$  that becomes internal after the gluing. Thus we have  $E_g = \{e, e', e''\}$  and  $v_g = 1$ . We first glue  $t$  to  $M'$  along  $f$  with identity (69). This eliminates the summation over  $\text{Hom}(f)$  in (89) and yields a polygon  $P''$  with the morphisms for  $f'$  assigned to adjacent vertices in the interior that are connected by an edge labeled  $l(e)$ . Applying the second identity in (60) then eliminates the summation over  $l(e)$  and  $\text{Hom}(f')$  and the factor  $\dim l(e)$  in (89), as in (ii). This yields a polygon diagram  $P'''$  that differs from  $P$  only in a disc in its interior, where one has

$$\begin{array}{ccc} P''' & & P \\ \begin{array}{c} \text{---} i \\ \gamma \uparrow \\ \text{---} l(e') \text{---} \text{---} l(e'') \text{---} \\ \gamma \downarrow \\ \text{---} i \end{array} & & \begin{array}{c} | \\ i \end{array} \end{array} \quad (90)$$

with  $\gamma \in \text{Hom}(f'')$  and  $i \in I_{\mathcal{C}}$  labeling the remaining edge of  $f''$ . Multiplying  $\text{ev}(P''')$  by  $\dim l(e') \dim l(e'') \dim \mathcal{C}^{-1}$  and summing over  $l(e'), l(e'') \in I_{\mathcal{C}}$  and over  $\gamma \in \text{Hom}(f'')$  then yields

$$\mathcal{Z}'(M, l_{\partial M}, b) = \dim \mathcal{C}^{-1} \sum_{\gamma, l(e'), l(e'')} \dim l(e') \dim l(e'') \text{ev}(P''') \stackrel{(65)}{=} \text{ev}(P).$$

□

Note that the evaluation of the diagram obtained by projecting the dual of the boundary triangulation on  $M$  to the defect surface  $D$  does not depend on the choice of the underlying PL homeomorphism  $\phi : M \rightarrow [0, 1] \times D$ . By Lemma 5.10 different choices of  $\phi$  yield isotopic projection maps. Diagrams for spherical fusion categories that are related by PL isotopies have the same evaluation. This is well-known and can be viewed as a special case of [JS91, Th. 1.12], [BMS12, Th. 2.12] for 2-category diagrams and [BMS12, Th. 3.9] for planar 2-category diagrams, see also the paragraphs after Example 2.1 and Definition 2.2. Together with identities (39) to (43) this ensures that the evaluation of the resulting diagram is independent of  $\phi$ .

As the evaluation of the polygon diagram in Proposition 5.11 depends only on the triangulation and labeling of  $\partial M$  and on the defect data, we obtain

**Corollary 5.12.** *Let  $M, M'$  be triangulated 3-manifolds with defect data that satisfy the assumptions of Proposition 5.11 and whose boundary triangulations coincide. Then for all labelings  $l_{\partial M}$  of the boundary one has  $\mathcal{Z}(M, l_{\partial M}) = \mathcal{Z}(M', l_{\partial M})$ .*

In particular, this implies that the state sum of any generic transversal triangulated 3-manifold with defect data is invariant under generic transversal bistellar moves. This follows with Corollary 4.10, as the tetrahedra in such moves define triangulations of a 3-ball that satisfy the assumptions of Proposition 5.11 and agree on its boundary.

**Corollary 5.13.** *Let  $M$  be a generic and transversal triangulated 3-manifold with defect data and  $l_{\partial M}$  a labeling of its boundary. Then the state sum  $\mathcal{Z}(M, l_{\partial M})$  from Definition 4.7 is invariant under generic transversal bistellar moves in the interior of  $M$ .*

All generic transversal bistellar moves for tetrahedra with defect surfaces are shown in Figure 8. The moves for tetrahedra that also involve defect lines and defect vertices are analogous, but with the additional conditions that defect vertices must not lie on faces and defect edges must not intersect edges of the tetrahedra.

The bistellar invariance of state sums for 3-manifolds with defect surfaces has a similar interpretation to the one for Turaev-Viro-Barrett-Westbury state sums outlined at the end of Section 5.1. The moves in Figure 8 (c) to (f) encode the pentagon relation (6) for the structure isomorphisms  $c_{i,j,m} : (i \otimes j) \triangleright m \rightarrow i \triangleright (j \triangleright m)$  for a  $\mathcal{C}$ -module category and equivalent relations obtained from it by taking inverses. The moves in Figure 8 (g) to (i) encode the pentagon relation (10) and the invertibility of the structure isomorphisms  $b_{c,m,d} : (c \triangleright m) \triangleleft d \rightarrow c \triangleright (m \triangleleft d)$  in a  $(\mathcal{C}, \mathcal{D})$ -bimodule category. The corresponding moves for surfaces with line and point defects combine these pentagon relations with the pentagon relations (13), (15) for  $\mathcal{C}$ -module and  $\mathcal{D}$ -right module functors and the hexagon relation (17) for  $(\mathcal{C}, \mathcal{D})$ -bimodule functors.

As for a spherical fusion category, the bistellar invariance for manifolds with defects can be formulated as generalised Biedenharn-Elliott and orthogonality relations for 6j symbols, which generalise the diagrammatic identities (86) and (87). However, it becomes cumbersome to list all of these relations.

## 5.4 Triangulation independence

In this section we show that any two generic transversal triangulations of a 3-manifold with defect data yield the same state sum if they agree at its boundary. Note that this does not follow directly from Corollary 5.13, because it is not guaranteed a priori that such triangulations are related by *generic transversal* bistellar moves. As a first step, we derive a counterpart of Proposition 5.11 for general defect surfaces.

We again consider 3-manifolds  $M$  that shell to fine neighbourhoods of a defect surface  $D$  and project the dual of the boundary triangulation on  $\partial M$  to  $D$  as in Definition 5.9 with an orientation preserving PL homeomorphism  $\phi : M \rightarrow [0, 1] \times D$ . The only difference to Proposition 5.11 is that  $D$  is no longer a disc and the resulting diagram on  $D$  must be cut along the triangulation to obtain a polygon diagram.

**Proposition 5.14.** *Let  $M$  be a triangulated 3-manifold with defect data that shells to a fine neighbourhood of a defect surface  $D$  by shellings of tetrahedra that do not intersect  $D$ . Let  $P$  be a polygon diagram obtained by projecting the dual of the triangulation on  $\partial M$  to  $D$  and cutting  $D$  along the triangulation to a disc. Then*

$$\mathcal{Z}'(M, l_{\partial M}, b) = \sum_l \sum_{\text{Hom}(\Delta_i)} \text{ev}(P) \prod_{e \in E_i} \dim l(e),$$

where

- $E_i$  and  $\Delta_i$  are the sets of internal edges and triangles of  $M$  that correspond to boundary vertices and edges in  $P$ ,
- the sum is over all assignments of simple objects to edges in  $E_i$  and bases of the morphism spaces of triangles in  $\Delta_i$ .

*Proof.* The claim follows by induction over the number  $n$  of tetrahedra in  $M$  that do not intersect  $D$ .

1. For  $n = 0$ ,  $M$  is a fine neighbourhood of  $D$ . Cutting  $D$  along the triangulation to a disc corresponds to cutting  $M$  to a 3-ball  $B$  that is a fine neighbourhood of a defect disc. Edges in  $E_i$  correspond to boundary edges of  $B$  and elements of  $\Delta_i$  to boundary triangles in  $B$ . Every labeling of internal edges in  $M$  defines a labeling  $l$  of  $E_i$  and a labeling  $l'$  of the internal edges of  $B$ .

The state sum for  $M$  is given by formula (81). By Proposition 5.11, summing over the labeling  $l'$  and the labelings of internal triangles of  $B$  yields the state sum for  $B$ , which is the evaluation of  $P$ . As every edge in

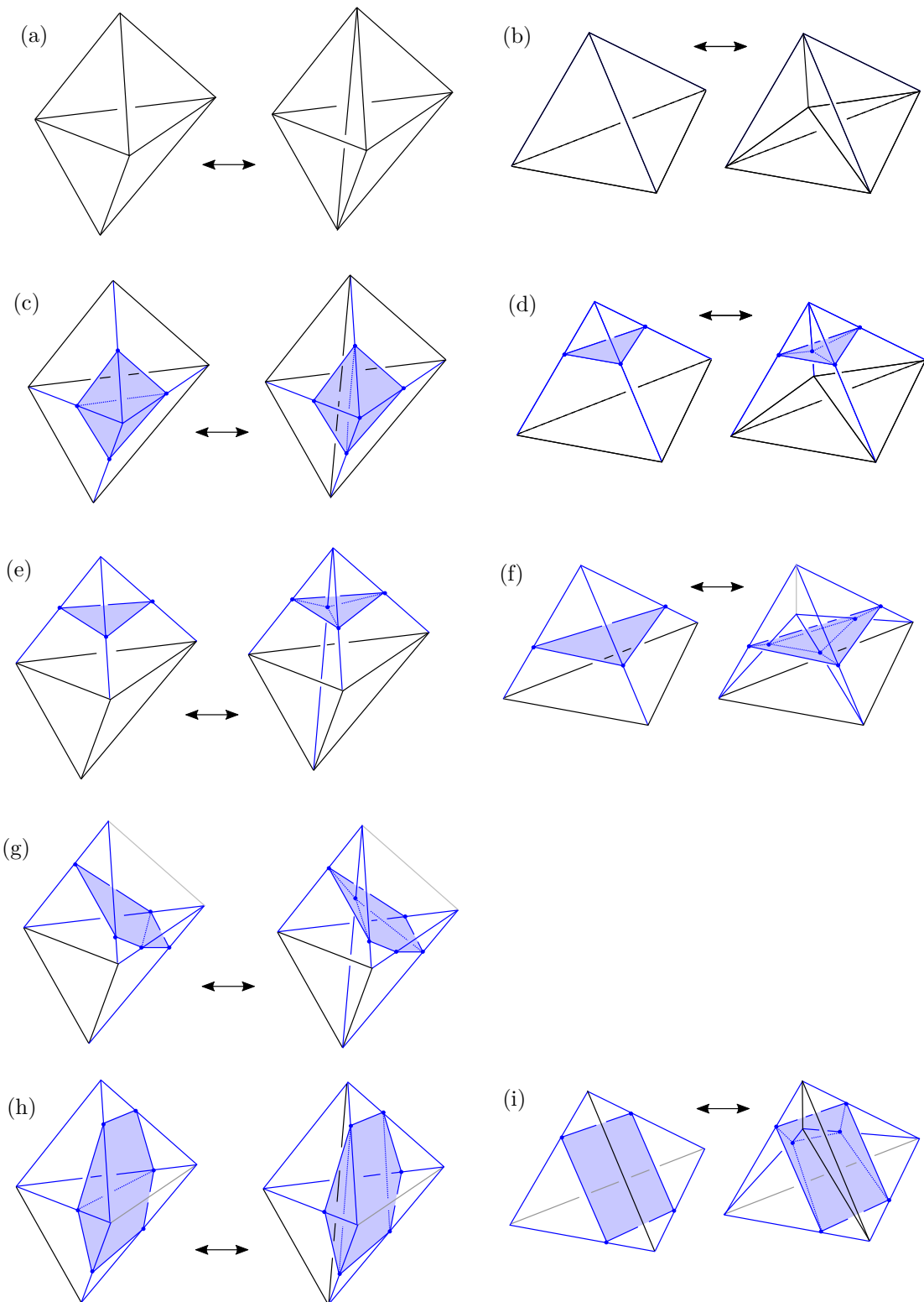


Figure 8: bistellar moves for tetrahedra without and with defect discs:  
 (a),(b): encoding the associator of a spherical fusion category  $\mathcal{C}$ ,  
 (c)-(f): encoding the natural isomorphism  $c$  for a  $\mathcal{C}$ -module category  $\mathcal{M}$ ,  
 (g)-(i): encoding the natural isomorphism  $b$  for a  $(\mathcal{C}, \mathcal{D})$ -bimodule category  $\mathcal{M}$ .

$E_i$  is internal in  $M$ , but in the boundary of  $B$ , the state sum for  $M$  is obtained by multiplying this expression with  $\prod_{e \in E_i} \dim l(e)$  and summing over the labelings of edges in  $E_i$  and morphism spaces for triangles in  $\Delta_i$ .

2. Suppose that  $M$  contains  $n+1$  tetrahedra that do not intersect  $D$ . As  $M$  shells to a fine neighbourhood of  $D$ , it is obtained by gluing a tetrahedron  $t$  that does not intersect  $D$  to triangulated manifold  $M'$  that also satisfies the assumptions and has  $n$  tetrahedra that do not intersect  $D$ . If  $t$  is contained in the region labeled by a spherical fusion category  $\mathcal{C}$ , then by the induction hypothesis and Corollary 4.10 the state sum of  $M$  is given by formula (89) in the proof of Proposition 5.11.

It remains to show that (89) yields  $\text{ev}(P)$ . If  $t$  is glued to  $M'$  along a single face, this follows as in 2.(i) in the proof of Proposition 5.11. If  $t$  is glued to  $M'$  along two faces  $f, f'$  that share an edge  $e = f \cap f'$  or along three faces  $f, f', f''$  that share edges  $e = f \cap f', e' = f \cap f''$  and  $e'' = f' \cap f''$ , we can assume without loss of generality that the edges in the polygon diagram  $P'$  for  $M'$  that correspond to  $e, e', e''$  do not intersect  $\partial P'$ . This is possible, because the assumptions imply that they do not intersect a side of  $P'$  that is contained in  $\partial D$ . If they intersect sides of  $P'$  that are in the interior of  $D$ , we can apply identity (66) to cut  $P'$ , glue it back together in such a way that these edges do not intersect  $\partial P'$  and reverse this transformation after the gluing of  $t$ . The claim then follows as in 2.(ii) and 2.(iii) in the proof of Proposition 5.11.  $\square$

After summation over the objects and morphisms at its boundary, the evaluation of the polygon diagram in Proposition 5.14 is again independent of the choice of the PL homeomorphism  $\phi : M \rightarrow [0, 1] \times D$  that defines the projection of the boundary graph on  $D$ . Lemma 5.10 ensures that different choices for  $\phi$  yield PL isotopic projection maps and hence diagrams for spherical fusion categories with the same evaluations. Together with identities (39) to (43) and identities (66) and (67) this ensures the polygon evaluations for different choice of  $\phi$  are equal. As the latter are precisely the cutting and gluing identities that relate different polygon presentations of surfaces, see for instance [L, Ch. 6] and [ST, Ch. 6.38 and 6.40], it also follows that all ways of cutting the surface in Proposition 5.14 yield the same value for the state sum.

Note also that Proposition 5.14 allows one to drop the requirement that a fine triangulation is generic in the interior of  $M$ . For a triangulation that is non-generic in the interior of  $M$ , a small displacement of the defect surfaces, defect lines and defect vertices yields a generic triangulation. As the cyclic evaluations of the associated polygon diagrams coincide, all such displacements have the same state sum.

It remains to show that the state sum from Proposition 5.14 does not depend on the choice of the triangulation in the interior of  $M$ . This follows again from identities (66) and (67).

**Lemma 5.15.** *Let  $M, M'$  be triangulated 3-manifolds with defect data that shell to fine neighbourhoods of a defect surface  $D$  with shellings by tetrahedra that do not intersect  $D$ . Suppose that the triangulations of  $M, M'$  coincide on the boundary. Then for all labelings  $l_{\partial M}$  and  $b$*

$$\mathcal{Z}(M, l_{\partial M}, b) = \mathcal{Z}(M', l_{\partial M}, b).$$

*Proof.* By Proposition 5.14 the rescaled state sums for  $M, M'$  are obtained by projecting the dual graph of the boundary triangulation on  $\partial M$  to  $D$ , cutting  $D$  along the triangulations to discs and evaluating the resulting polygon diagrams  $P, P'$ . With identities (66) and (67) we can cut the polygon diagrams  $P, P'$  into smaller pieces that are the intersections of  $P, P'$  with the tetrahedra in the two triangulations.

More precisely, one obtains embedded graphs  $\Gamma, \Gamma'$  on  $D$ , whose vertices, edges and faces are the intersections of  $D$  with the edges, triangles and tetrahedra in the triangulations. We denote by the same letters the associated graphs on  $P, P'$  and call vertices or edges of  $\Gamma, \Gamma'$  internal, if they are not contained in  $\partial D$  and boundary otherwise. By adjusting the triangulations, we can assume that  $\Gamma, \Gamma'$  are *generic*, meaning that (i) defect vertices and vertices labeled by spherical fusion categories are in the interior of faces of  $\Gamma, \Gamma'$ , (ii) defect edges and edges labeled by spherical fusion categories intersect the edges of  $\Gamma, \Gamma'$  transversally in the interior.

With the labelings of the defects and the triangulations every face of  $\Gamma$  and  $\Gamma'$  becomes a polygon diagram. By Proposition 5.14, (66) and (67), the rescaled state sums for  $M, M'$  are obtained by multiplying the evaluations of these polygon diagrams for  $\Gamma, \Gamma'$ , rescaling with the dimensions of the simple objects at internal vertices and summing over all labelings of internal vertices and over bases of the morphism spaces at internal edges.

Using again identities (66) and (67), we cut these polygon diagrams into smaller pieces that correspond to a common subdivision of  $\Gamma$  and  $\Gamma'$ . By slightly displacing the vertices of  $M, M'$  one can achieve that the graphs  $\Gamma, \Gamma'$  remain generic and that every point  $v'' \in (\Gamma \cap \Gamma') \setminus \partial D$  is a transversal intersection point of an edge  $e$  of  $\Gamma$  and an edge  $e'$  of  $\Gamma'$ , while all boundary edges and vertices of  $\Gamma, \Gamma'$  remain fixed. If the



displacements of vertices are sufficiently small, this does not change the evaluations of the polygon diagrams for  $\Gamma, \Gamma'$  and hence preserves the state sums.

Let  $\Gamma''$  be the embedded graph on  $D$  obtained by superimposing  $\Gamma$  and  $\Gamma'$  and inserting a new four-valent vertex at each intersection point  $v'' = e \cap e'$ . Then every edge of  $\Gamma''$  is either on an edge of  $\Gamma$  or of  $\Gamma'$ . Every vertex of  $\Gamma''$  is either a vertex of  $\Gamma$ , of  $\Gamma'$  or an intersection point of an edge of  $\Gamma$  and an edge of  $\Gamma'$ . Summing the product of polygon evaluations for  $\Gamma''$  over the labelings at those internal edges and vertices that lie on  $\Gamma'$  yields the corresponding product of polygon evaluations for  $\Gamma$ . Summing it instead over the labelings at the internal edges and vertices that lie on  $\Gamma$  gives the corresponding product of polygon evaluations for  $\Gamma'$ . By combining these two summations one obtains that the state sums are equal.  $\square$

By combining Lemma 5.15 with the triangulation independence of Turaev-Viro-Barrett-Westbury state sums for spherical fusion categories, we can now show that the state sums for two generic transversal triangulations of a 3-manifold  $M$  with defect data coincide, whenever their triangulations coincide at the boundary.

**Theorem 5.16.** *Let  $T, T'$  be generic transversal triangulations of a 3-manifold  $M$  with defect data that coincide on  $\partial M$ . Then for all boundary labelings  $l_{\partial M}$  and  $b$  the state sums for  $T$  and  $T'$  are equal:*

$$\mathcal{Z}(M, l_{\partial M}, b, T) = \mathcal{Z}(M, l_{\partial M}, b, T').$$

*Proof.* By Lemma 5.7 there are finite sequences of bistellar moves between generic transversal tetrahedra that transform the triangulations  $T, T'$  into triangulations  $S, S'$  that satisfy (i)-(iii) in Lemma 5.7. By Corollary 5.13 one has  $\mathcal{Z}(M, l_{\partial M}, b, T) = \mathcal{Z}(M, l_{\partial M}, b, S)$  and  $\mathcal{Z}(M, l_{\partial M}, b, T') = \mathcal{Z}(M, l_{\partial M}, b, S')$ . To show that  $\mathcal{Z}(M, l_{\partial M}, b, S) = \mathcal{Z}(M, l_{\partial M}, b, S')$ , we denote by  $\Sigma_i$  the connected components of the defect manifold  $D = \coprod_{i=1}^n \Sigma_i$  and by  $r_k$  the regions of  $M$ , which are the connected components of  $M \setminus D = \coprod_{k=1}^m r_k$ .

By Lemma 5.7 (ii) gluing all tetrahedra in  $S, S'$  that are contained in a region  $r_k$  yields triangulated 3-manifolds  $R_k, R'_k$  that are PL homeomorphic to  $\bar{r}_k$ . By Lemma 5.7 (ii) gluing all tetrahedra in  $S, S'$  that intersect  $\Sigma_i$  yields fine neighbourhoods  $D_i, D'_i$  of  $\Sigma_i$ . This implies that all boundary triangles in  $D_i, D'_i$  that are internal triangles of  $M$  are glued to boundary triangles in one of the 3-manifolds  $R_k, R'_k$ . More specifically, each connected component of  $\partial D_i \setminus \partial M$  coincides with a unique boundary component of some  $R_k$ , up to the fact that they have opposite orientations. As  $\partial D \subset \partial M$ , all boundary triangles of  $D_i$  and  $D'_i$  that intersect  $\Sigma_i$  are contained in  $\partial M$  and hence coincide.

As  $D_i$  and  $D'_i$  are both PL homeomorphic to  $[0, 1] \times \Sigma_i$ , their boundaries are PL homeomorphic. As their boundary triangulations agree on  $\partial D \subset \partial M$ , this allows one to transform each connected component of  $\partial D'_i \setminus \partial M$  into the corresponding connected component of  $\partial D_i \setminus \partial M$  by a finite number shellings or inverse shellings with tetrahedra that do not intersect any defect surface. Performing the same shellings on the associated boundary component of  $R'_k$  transforms it into the corresponding boundary component of  $R_k$ .

For each labeling of the edges and triangles, performing such a simultaneous shelling or inverse shelling at  $D'_i$  and  $R'_k$  amounts to multiplying or dividing the state sum of  $M'$  by the 6j symbol of a tetrahedron  $t$  labeled by a spherical fusion category, with the 6j symbol of the tetrahedron  $\bar{t}$  with the same labeling, but the opposite orientation, and with dimension factors associated to their edges. The orthogonality relation (87) and identity (55) ensure that this does not change the state sum.

Hence, we can assume without loss of generality that the triangulations of all 3-manifolds  $D'_i$  and  $D_i$  coincide on the boundary and that the same holds for all triangulated 3-manifolds  $R_k$  and  $R'_k$ . Under this assumption, the state sums of  $D_i$  and  $D'_i$  agree by Lemma 5.15 for all labelings. The state sums of  $R_k$  and  $R'_k$  are the usual Turaev-Viro-Barrett-Westbury state sums for a spherical fusion category and are equal by Theorem 5.5. With Corollary 4.10 this yields

$$\begin{aligned} \mathcal{Z}(M, l_{\partial M}, b, S) &= \sum_{l_{\partial}} \sum_{\text{Hom}_{\partial}} \prod_{i=1}^n \mathcal{Z}(D_i, l_{\partial D_i}, b_{\partial D_i}) \prod_{k=1}^m \mathcal{Z}(R_k, l_{\partial R_k}, b_{\partial R_k}) \\ &= \sum_{l_{\partial}} \sum_{\text{Hom}_{\partial}} \prod_{i=1}^n \mathcal{Z}(D'_i, l_{\partial D'_i}, b_{\partial D'_i}) \prod_{k=1}^m \mathcal{Z}(R'_k, l_{\partial R'_k}, b_{\partial R'_k}) = \mathcal{Z}(M, l_{\partial M}, b, S'), \end{aligned}$$

where the sums are over all labelings  $l_{\partial}$  of internal edges in  $M$  that are boundary edges of  $D_i, D'_i$  and over dual bases of the morphism spaces for internal triangles in  $M$  that are boundary triangles of  $D_i, D'_i$ .  $\square$

Theorem 5.16 extends the definition of the state sum for a defect manifold to triangulations that are non-generic or non-transversal in the interior of  $M$ . Together with Proposition 5.14 it shows that slightly perturbing the defect surface, defect lines or defect vertices in the interior of  $M$  does not change the value of the state sum. This allows one to define the state sum of a non-generic triangulation as the state sum of a small generic deformation. Similarly, any triangulation of  $M$  with non-transversal tetrahedra in the interior can be refined by stellar subdivisions to a triangulation that is transversal. One can then perturb the defect surfaces, lines and vertices to make it generic. By Theorem 5.16 all ways of doing so yield the same state sum.

**Definition 5.17.** *Let  $M$  be a 3-manifold with defect data and  $T$  a triangulation of  $M$  whose boundary triangles are transversal and generic. Then for all boundary labelings  $l_{\partial M}, b$  the state sum of  $M$  is defined as*

$$\mathcal{Z}(M, l_{\partial M}, b, T) := \mathcal{Z}(M, l_{\partial M}, b, T'), \quad (91)$$

for any generic transversal triangulation  $T'$  that coincides with  $T$  on  $\partial M$ .

**Corollary 5.18.** *Let  $M$  be a 3-manifold with defect data and  $T, T'$  triangulations of  $M$  that coincide on  $\partial M$  and whose boundary triangles are transversal and generic. Then their state sums coincide for all boundary labelings  $l_{\partial M}, b$ . In particular, if  $M$  is closed, its state sum does not depend on the choice of the triangulation.*

## 6 Examples of state sums

In this section, we compute the state sums for some examples of defect 3-manifolds. We first consider state sums with defect surfaces, but without defect lines or defect vertices. We then show how to recover ribbon invariants from defect lines and vertices on trivial defect surfaces.

### 6.1 State sums with defect surfaces

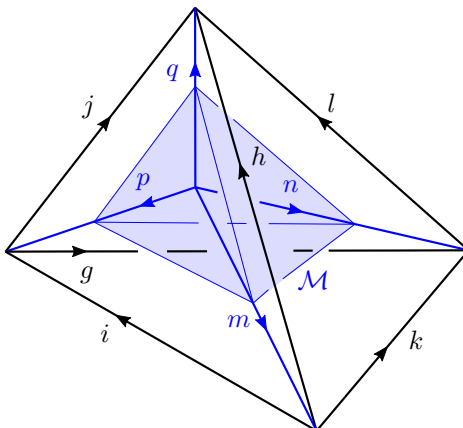
In the following, we assume that all triangulations are generic and transversal at the boundary. Our first example is a defect sphere without defect lines or vertices embedded inside a 3-ball. We suppose that the embedding is *unknotted* in the sense of Zeeman [Ze60]. This means that there is a PL homeomorphism from the 3-ball to itself that sends the defect sphere to the boundary of a tetrahedron, see also Footnote 1 [Ze60].

**Example 6.1.** *Let  $M$  be a 3-ball with an unknotted defect sphere in its interior. Suppose the boundary of  $M$  is labeled by a spherical fusion category  $\mathcal{C}$  and the defect sphere by a  $(\mathcal{C}, \mathcal{D})$ -bimodule category  $\mathcal{M}$  with a bimodule trace. Then for all boundary labelings  $l_{\partial M}, b$  the state sum of  $M$  is*

$$\mathcal{Z}(M, l_{\partial M}, b) = \frac{\dim \mathcal{M}}{\dim \mathcal{D}} \cdot \mathcal{Z}(M', l_{\partial M}, b), \quad (92)$$

where  $M'$  is a triangulated 3-ball labeled by  $\mathcal{C}$  with the same boundary triangulation, but without defects.

*Proof.* As the defect sphere is unknotted, there is a PL homeomorphism from  $M$  to itself that sends  $D$  to the boundary of a tetrahedron. By Theorem 5.16, Corollary 5.18 and because different boundary triangulations are related by elementary shellings and inverse shellings, it is sufficient to prove the claim for the triangulation



We evaluate the state sum by gluing the polygon diagrams for the four tetrahedra in the triangulation. Gluing the bottom tetrahedron to the three tetrahedra above with identity (66) yields for the rescaled state sum

$$\mathcal{Z}'(M, l_{\partial M}, b) = \frac{1}{\dim(\mathcal{D})} \sum_{\alpha, \beta, \gamma}^{m, n, p, q} \dim m \dim n \dim p \dim q$$

Applying identity (67) to eliminate the summation over  $\alpha, p$  yields

$$\mathcal{Z}'(M, l_{\partial M}, b) = \frac{1}{\dim(\mathcal{D})} \sum_{\beta, \gamma}^{m, n, q} \dim m \dim n \dim q$$

and applying identity (67) to eliminate the summation over  $\beta, n$  gives

$$\mathcal{Z}'(M, l_{\partial M}, b) = \frac{1}{\dim(\mathcal{D})} \sum_{m, q, \gamma} \dim m \dim q$$

Applying identity (68) to this diagram yields the result

$$\mathcal{Z}'(M, l_{\partial M}, b) = \frac{\dim \mathcal{M}}{\dim(\mathcal{D})} \left[ \text{Diagram} \right] = \frac{\dim \mathcal{M}}{\dim(\mathcal{D})} \cdot \mathcal{Z}'(M', l_{\partial M}, b).$$

□

Note that Example 6.1 yields the usual Turaev-Viro-Barrett-Westbury invariant for a 3-ball without defects, if one chooses for  $\mathcal{M}$  a spherical fusion category  $\mathcal{C} = \mathcal{D}$  as a bimodule category over itself.

State sums with defect surfaces of genus  $g \geq 1$  are more difficult to compute. We therefore restrict attention to the spherical fusion category  $\mathcal{C} = \text{Vec}_G$  for a finite group  $G$  from Example 1.1, equipped with the a trivial 3-cocycle and the standard spherical structure. The associated Turaev-Viro-Barrett-Westbury state sums are a special case of the Dijkgraaf-Witten models from [DW90], see also Altschuler and Coste [AC93].

By Example 1.1 simple objects in  $\text{Vec}_G$  correspond to group elements  $g \in G$ . For simplicity, we denote them by  $g$  instead of  $\delta^g$  in the following. One has  $\dim(g) = 1$  for all  $g \in G$  and  $\dim(\mathcal{C}) = |G|$  as well as

$$\text{Hom}_{\mathcal{C}}(k, i \otimes j) \cong \text{Hom}_{\mathcal{C}}(i \otimes j, k) \cong \delta_k(ij)\mathbb{C} \quad \forall i, j, k \in G. \quad (93)$$

By Examples 1.7 and 1.16, every finite transitive  $G \times G'^{\text{op}}$ -set  $X$  defines an indecomposable semisimple  $(\text{Vec}_G, \text{Vec}_{G'})$ -bimodule category  $\mathcal{M}$  with a bimodule trace, whose simple objects are in bijection with elements of  $X$ . In the following, we only consider the case, where the cocycle defining  $\psi \in H^2(L, \mathbb{C}^\times)$  from Example 1.7 is trivial. One has  $\dim(x) = 1$  for all  $x \in X$  and  $\dim(\mathcal{M}) = |X|$  as well as

$$\begin{aligned} \text{Hom}_{\mathcal{M}}(x, g \triangleright y) &\cong \text{Hom}_{\mathcal{M}}(g \triangleright y, x) \cong \delta_x(g \triangleright y)\mathbb{C} \\ \text{Hom}_{\mathcal{M}}(x, y \triangleleft g') &\cong \text{Hom}_{\mathcal{M}}(y \triangleleft g', x) \cong \delta_x(y \triangleleft g')\mathbb{C} \quad \forall x, y \in X, g \in G, g' \in G'. \end{aligned} \quad (94)$$

Hence, any 6j symbol vanishes, unless for each triangle with edges labeled by  $x, y \in X$  and by  $g \in G$  or  $g' \in G'$ , the objects  $x$  and  $y$  are related by the action of  $g$  or  $g'$ . Similarly, for any triangle with labeled elements of  $G$  or  $G'$ , the oriented product of the group elements must be trivial by (93). Morphism labels for triangles are just numbers in  $\mathbb{C}$ , and all sums over bases of morphism spaces become trivial.

**Example 6.2.** Let  $\mathcal{C} = \text{Vec}_G$  and  $\mathcal{D} = \text{Vec}_{G'}$  for finite groups  $G, G'$  and  $\mathcal{M}$  the indecomposable  $(\mathcal{C}, \mathcal{D})$ -bimodule category with bimodule trace defined by a finite transitive  $G \times G'^{\text{op}}$ -set  $X$ .

Let  $\Sigma$  be a closed oriented triangulated surface of genus  $g \geq 1$  and  $M = [0, 1] \times \Sigma$  the fine neighbourhood of  $\Sigma$  obtained by replacing each triangle in  $\Sigma$  by a prism as in Figure 9, with a defect surface  $\{\frac{1}{2}\} \times \Sigma$  labeled by  $\mathcal{M}$  and boundary components  $\{1\} \times \Sigma$  and  $\{0\} \times \Sigma$  labeled by  $\mathcal{C}$  and  $\mathcal{D}$ . Suppose that all boundary triangles with non-trivial morphism spaces are labeled with identity morphisms.

Then the rescaled state sum of  $M$  is

$$\mathcal{Z}'(M, l_{\partial M}, b) = \begin{cases} |X^{\rho(\pi_1(\Sigma))}| & \text{if the oriented product of the group elements in each triangle} \\ & \text{on } \{0\} \times \Sigma \text{ and } \{1\} \times \Sigma \text{ is trivial,} \\ 0 & \text{else,} \end{cases}$$

where  $\rho : \pi_1(\Sigma) \rightarrow G \times G'$  is the group homomorphism defined by the labels on  $\{0\} \times \Sigma$  and  $\{1\} \times \Sigma$  and  $X^{\rho(\pi_1(\Sigma))}$  the fixed point set for the induced action of  $\pi_1(\Sigma)$ .

In particular:

- **trivial defect surface:** If  $G = G' = X$  with the standard  $G \times G'^{\text{op}}$ -set structure, then  $\mathcal{Z}'(M, l_{\partial M}, b) = 0$  unless the oriented product of the group elements in each triangle on  $\{0\} \times \Sigma$  and  $\{1\} \times \Sigma$  is trivial and the associated group homomorphisms  $\rho_0, \rho_1 : \pi_1(\Sigma) \rightarrow G$  are conjugated. Then  $\mathcal{Z}'(M, l_{\partial M}, b) = |\text{Stab}(\rho_0)|$ , where  $\text{Stab}(\rho_0)$  is the stabiliser of  $\rho_0$  for the conjugation action of  $G$  on  $\text{Hom}_{\text{Grp}}(\pi_1(\Sigma), G)$ .
- **trivial  $G \times G'^{\text{op}}$ -set:** For a trivial  $G \times G'$ -set  $X = \{\bullet\}$ , one has  $\mathcal{Z}'(M, l_{\partial M}, b) = 1$ , whenever the oriented product of the group elements in each triangle on  $\{0\} \times \Sigma$  and  $\{1\} \times \Sigma$  is trivial.
- **normal subgroup:** If  $X = G \times G'^{\text{op}}/N$  for a normal subgroup  $N \subset G \times G'^{\text{op}}$  one has  $\text{Stab}(m) = \text{Stab}(m') = N$  for all  $m, m' \in X$ . This implies  $\mathcal{Z}'(M, l_{\partial M}, b) = |X|$ , whenever the oriented product of the group elements in each triangle on  $\{0\} \times \Sigma$  and  $\{1\} \times \Sigma$  is trivial and the labelings of  $\{1\} \times \Sigma$  and  $\{0\} \times \Sigma$  define a group homomorphism  $\rho : \pi_1(\Sigma) \rightarrow N$ .

*Proof.* Orient the top and bottom triangle of each prism as the associated triangle of  $\Sigma$ , the vertical edges of each prism according to the orientation of  $\Sigma$ . Subdivide each prism into three tetrahedra as in Figure 9. Label its top and bottom edges with elements of  $G$  and  $G'$  and the vertical edges with elements of  $X$ .

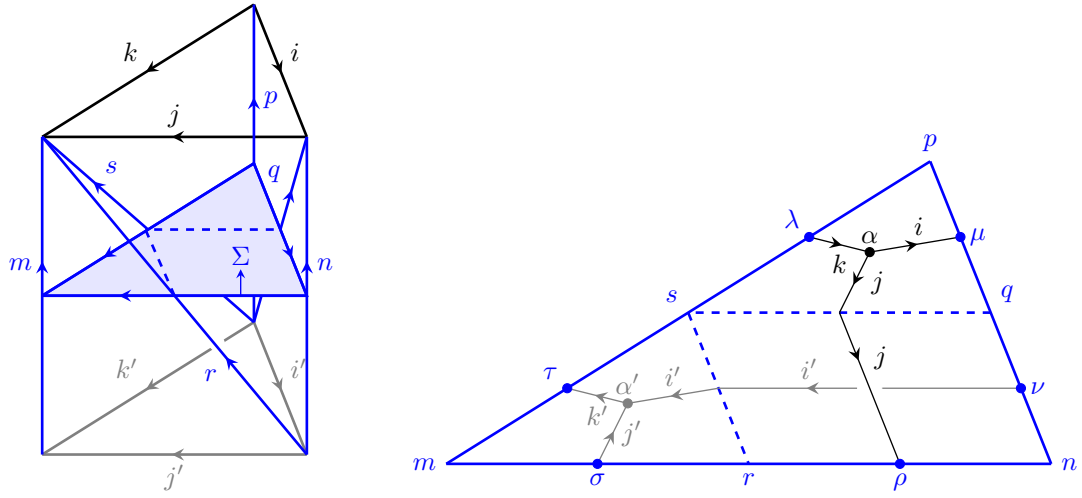


Figure 9: A labeled triangular prism and the associated polygon diagram.

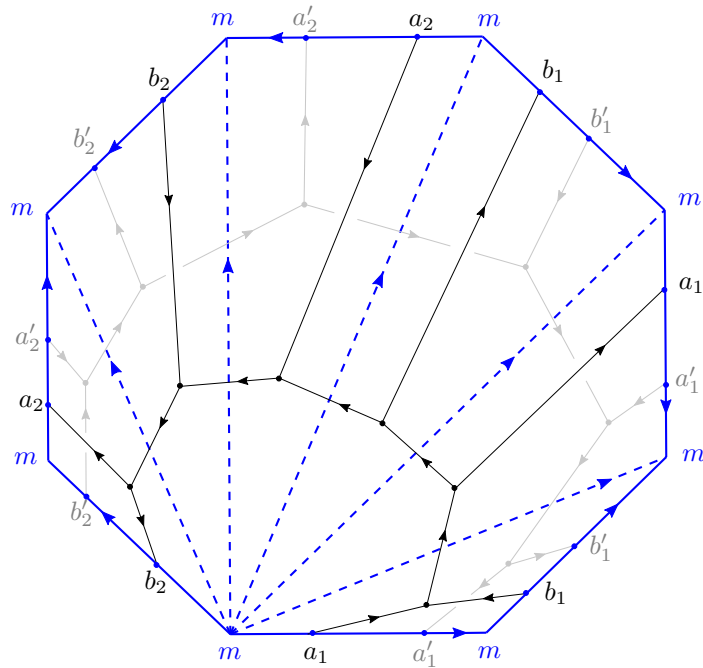


Figure 10: Polygon diagram  $P$  for  $M = [0, 1] \times \Sigma$  for triangulated defect surface  $\Sigma$  of genus 2.

- The orientation of the blue lines indicates the orientation of the triangulation on  $\Sigma$ .
- The group elements on the unlabeled edges are determined by the labels.
- $\text{ev}(P) = 0$  unless  $[a_1, b_1] \cdots [a_g, b_g] = 1$  and  $[a'_1, b'_1] \cdots [a'_g, b'_g] = 1$  and  $(a_i, a'_i), (b_i, b'_i) \in \text{Stab}(m)$  for  $i = 1, 2$ .

By Proposition 5.14 the state sum of each labeled prism is given by the evaluation of the polygon diagram in Figure 9. Also by Proposition 5.14, the state sum for  $M$  is given by the evaluation of any polygon diagram  $P$  obtained by gluing the polygons of the prisms to a disc and summing over the objects at its boundary. We can assume without loss of generality that  $P$  is a  $4g$ -gon with every vertex labeled by  $m \in X$ , as in Figure 10. This yields

$$\mathcal{Z}'(M, l_{\partial M}, b) = \sum_{m \in X} \text{ev}(P).$$

By identity (93), the evaluation of  $P$  vanishes, unless at each vertex of  $P$  that involves only edges labeled by  $G$  or  $G'$ , the oriented product of these group elements is trivial. By choosing maximal trees in the graphs labeled by  $G$  and  $G'$ , one can express the group elements on the trees in terms of the  $2g$  group elements on edges that intersect  $\partial P$ , where  $g$  is the genus of  $\Sigma$ . The labels on these  $2g$  edges then define a group homomorphism  $\rho : \pi_1(\Sigma) \rightarrow G \times G'$ , as shown in Figure 10.

By identity (94) the evaluation  $\text{ev}(P)$  vanishes unless the group elements  $(a_i, a'_i), (b_i, b'_i) \in G \times G'^{op}$  on each side of  $P$  are contained in the stabiliser of  $m \in X$  or, equivalently, the group homomorphism  $\rho$  takes values in  $\text{Stab}(m)$ . In that case, one has  $\text{ev}(P) = 1$ . Summation over all elements  $m \in X$  then yields the result.  $\square$

Example 6.2 gives intuition how the data for the spherical fusion categories interacts with the defect data in state sums of defect 3-manifolds. The next example shows that state sums for defect surfaces in the interior of a 3-ball detect the genus of the defect surface.

**Example 6.3.** Let  $\mathcal{C} = \text{Vec}_G$  and  $\mathcal{D} = \text{Vec}_{G'}$  for finite groups  $G, G'$  and  $\mathcal{M}$  the  $(\mathcal{C}, \mathcal{D})$ -bimodule category with bimodule trace defined by a finite transitive  $G \times G'^{op}$ -set  $X$ . Let  $M$  be the triangulated 3-ball from Figure 11 with an embedded defect surface of genus  $g \geq 1$  in its interior. Then

$$\mathcal{Z}(M, l_{\partial M}, b) = \frac{|X| \cdot |\text{Stab}_G|^g \cdot |\text{Stab}_{G'}|^g}{|G'|} \cdot \mathcal{Z}(M', l_{\partial M}, b), \quad (95)$$

where  $M'$  is the 3-ball with the same boundary triangulation and labeling, but without defects and  $|\text{Stab}_G|, |\text{Stab}_{G'}|$  are the cardinalities of the stabilisers for the  $G$ - and  $G'$ -actions on  $X$ .

*Proof.* The triangulated defect 3-manifold in Figure 11 is constructed as follows:

- take  $2g$  triangular double-pyramids formed by three tetrahedra each, with a cylinder labeled by  $\mathcal{M}$  around the interior edge labeled by  $\mathcal{D}$ ,
- glue them pairwise along adjacent top and bottom faces to form  $g$  rectangular double-pyramids,
- glue the four bottom faces of each rectangular double-pyramid to the four top faces of the next one,
- glue a rectangular pyramid subdivided into four tetrahedra with defect triangles to the top and the bottom of the resulting polyhedron.

If the edges are labeled by group elements as in Figure 11, then the edges labeled  $i, j, k, l, w_s, x_s, y_s, z_s \in G$  for  $s = 1, 2$  are boundary edges. The edges labeled by  $d_r, d'_r \in G'$ , by  $c_r \in G$  for  $r = 1, \dots, g$  and by  $m_s, n_s, p_s, q_s, t, b \in X$  for  $s = 1, \dots, g + 1$  are internal, and their labels are summed over. Conditions (93) and (94) on the morphism spaces imply that the state sum is zero unless the following conditions are met:

- boundary edges of top and bottom pyramid:

$$x_s = y_s \cdot i = w_s \cdot j, \quad z_s = y_s \cdot k = w_s \cdot l \quad s \in \{1, 2\}, \quad (96)$$

- defect edges of top and bottom pyramid:

$$\begin{aligned} m_1 = x_1^{-1} \triangleright t, & \quad n_1 = y_1^{-1} \triangleright t, & \quad p_1 = w_1^{-1} \triangleright t, & \quad q_1 = z_1^{-1} \triangleright t, \\ m_{g+1} = x_2^{-1} \triangleright b, & \quad n_{g+1} = y_2^{-1} \triangleright b, & \quad p_{g+1} = w_2^{-1} \triangleright b, & \quad q_{g+1} = z_2^{-1} \triangleright b, \end{aligned} \quad (97)$$

- double-pyramids: for  $r \in \{1, \dots, g\}$

$$\begin{aligned} n_r = i \triangleright m_r = k \triangleright q_r, \quad p_r = c_r \triangleright n_r = j \triangleright m_r = l \triangleright q_r, \\ m_{r+1} = m_r \triangleleft d_r, \quad n_{r+1} = n_r \triangleleft d_r = n_r \triangleleft d'_r, \quad p_{r+1} = p_r \triangleleft d_r = p_r \triangleleft d'_r, \quad q_{r+1} = q_r \triangleleft d_r = q_r \triangleleft d'_r. \end{aligned} \quad (98)$$

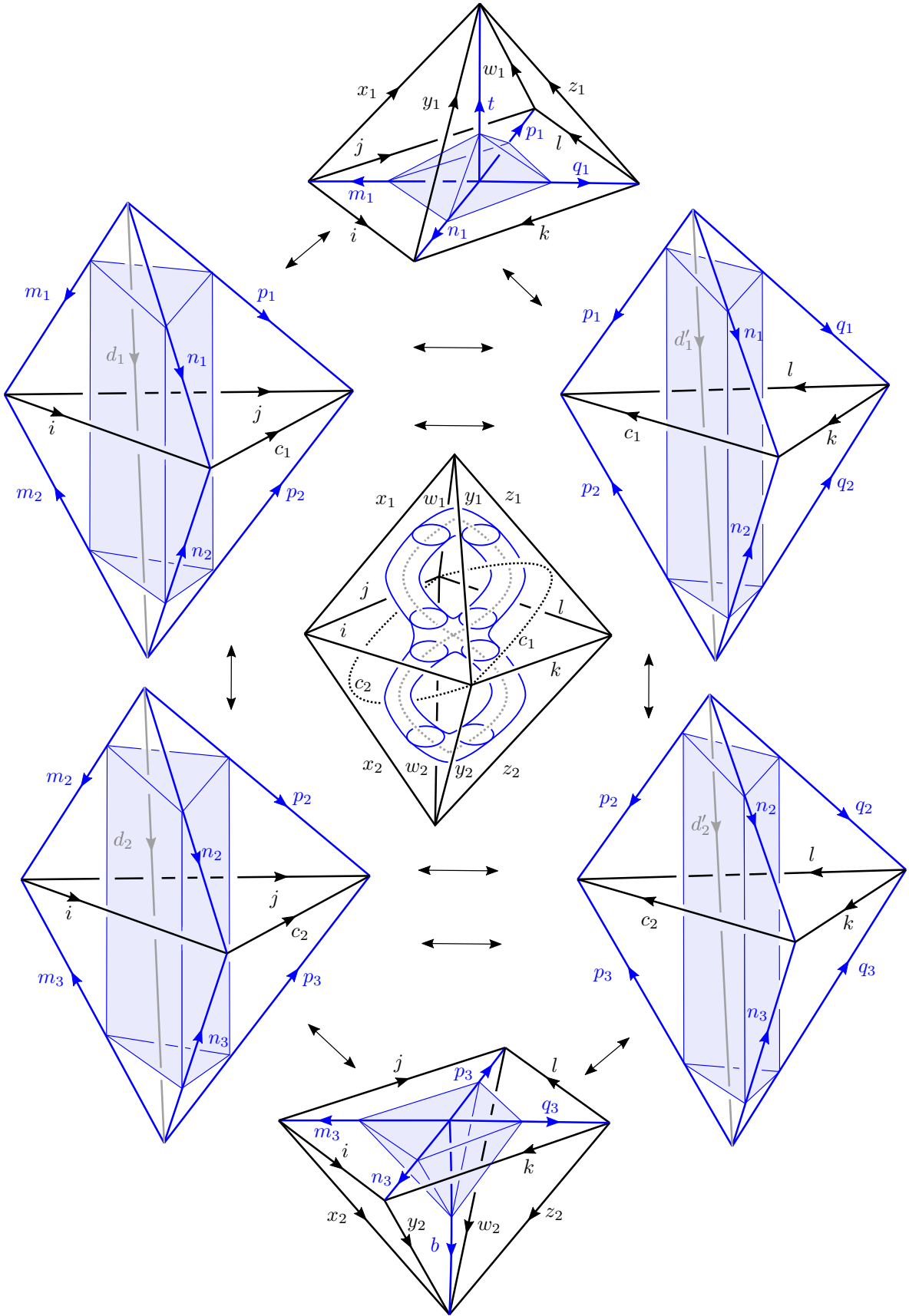


Figure 11: Gluing a surface of genus  $g = 2$  inside a 3-ball.

Condition (96) just states that the state sum is zero, unless the oriented product over the group elements of each boundary triangle is trivial. The first condition in (97) and the second condition in (98) imply

$$\begin{aligned} m_{r+1} &= x_1^{-1} \triangleright t \triangleleft d_1 \cdots d_r & q_{r+1} &= w_1^{-1} \triangleright t \triangleleft d'_1 \cdots d'_r \\ n_{r+1} &= y_1^{-1} \triangleright t \triangleleft d_1 \cdots d_r = y_1^{-1} \triangleright t \triangleleft d'_1 \cdots d'_r & p_{r+1} &= z_1^{-1} \triangleright t \triangleleft d_1 \cdots d_r = z_1^{-1} \triangleright t \triangleleft d'_1 \cdots d'_r. \end{aligned} \quad (99)$$

for all  $r \in \{1, \dots, g\}$ . This expresses  $m_s, n_s, p_s, q_s \in X$  as functions of  $t \in X$ ,  $d_1, \dots, d_g, d'_1, \dots, d'_g \in G'$  and of the group elements on the boundary edges and eliminates the summation over  $m_s, n_s, p_s, q_s$ . The equations in the second line of (99) are satisfied simultaneously iff for all  $r \in \{1, \dots, g\}$

$$d'_1 \cdots d'_r d_r^{-1} \cdots d_1^{-1} \in \text{Stab}_{G'}(t) = \{g \in G' \mid t \triangleleft g' = t\}. \quad (100)$$

Combining (99) with the second line in (97) yields

$$b = w_2 w_1^{-1} \triangleright t \triangleleft d_1 \cdots d_r = x_2 x_1^{-1} \triangleright t \triangleleft d_1 \cdots d_r = y_2 y_1^{-1} \triangleright t \triangleleft d_1 \cdots d_r = z_2 z_1^{-1} \triangleright t \triangleleft d_1 \cdots d_r. \quad (101)$$

As (96) implies  $x_2 x_1^{-1} = y_2 y_1^{-1} = w_2 w_1^{-1} = z_2 z_1^{-1}$ , equation (101) just expresses  $b$  in terms of  $t$  and  $d_1, \dots, d_r$  and thus eliminates the summation over  $b$  from the state sum. The first line in (98) is then equivalent to (99), (96) and the additional condition

$$w_1 c_r y_1^{-1} \in \text{Stab}_G(t) = \{g \in G \mid g \triangleright t = t\} \quad \forall r \in \{1, \dots, g\}. \quad (102)$$

For fixed  $t$  and  $d_1, \dots, d_g$ , the summations over  $d'_1, \dots, d'_g$  and  $c_1, \dots, c_g$  contribute factors  $|\text{Stab}_{G'}(t)|^g$  and  $|\text{Stab}_G(t)|^g$ , respectively, to the state sum. As  $X$  is a transitive  $G \times G'^{op}$ -set, all stabilisers have the same cardinality, and the summation over  $t$  contributes a factor  $|X|$ . As each of the  $g+1$  internal vertices with incident edges from  $\mathcal{D}$  contributes a factor  $\dim(\mathcal{D})^{-1} = |G'|^{-1}$  and the summation over  $d_1, \dots, d_g$  yields a factor  $\dim(\mathcal{D})^g = |G'|^g$  we obtain

$$\mathcal{Z}'(M, l_{\partial M}, b) = \frac{|X| |\text{Stab}_G|^g |\text{Stab}_{G'}|^g}{|G'|} C,$$

where  $C$  is a factor that depends only on the labeling of the boundary triangles. For  $\mathcal{M} = \mathcal{C} = \mathcal{D} = \text{Vec}_G$  as a bimodule category over itself, one has  $|X| = |G'| = |G|$ ,  $|\text{Stab}_G| = |\text{Stab}_{G'}| = 1$ .  $\square$

It is instructive to compare Examples 6.1 and 6.3. If one restricts the data in Example 6.1 to the bimodule category given by a finite  $G \times G'^{op}$ -set  $X$  from Example 6.3, then formula (92) for the state sum for a 3-ball with a defect sphere becomes  $\mathcal{Z}(M, l_{\partial M}, b) = |X|/|G'| \cdot \mathcal{Z}(M', l_{\partial M}, b)$ , which is formula (95) for  $g=0$ .

Examples 6.1 to 6.3 show that the state sums detect properties of the bimodule categories labeling a defect surface and properties of the surface. The next example shows that the state sum models with defects depend on the *embeddings* of defect surfaces into the 3-manifold, and not just on their topology.

This is manifest even for very simple non-trivial defect data. By taking a tubular neighbourhood of a knot  $K$  embedded into  $S^3$  and labeling it with the  $\text{Vec}_G$ -module category defined by a trivial  $G$ -set, one obtains a triangulation of the knot complement with trivial data at the boundary. The associated state sum gives the number of conjugacy classes of group homomorphisms  $\rho : \pi_1(S^3 \setminus K) \rightarrow G$  and hence is sensitive to the embedding of the toroidal defect surface.

**Example 6.4.** *Let  $K \subset S^3$  be a knot, realised as a subgraph of the dual cell complex of a triangulation  $T$  of  $S^3$ . Let  $M$  be the triangulated 3-manifold with defect data constructed as follows:*

1. *Refine  $T$  to a triangulation  $T'$  by applying a 1-4 move to each tetrahedron  $t$  in  $T$  with  $t \cap K \neq \emptyset$  and a stellar move to each triangle  $\Delta$  in  $T$  with  $\Delta \cap K \neq \emptyset$ , such that  $K$  connects the midpoints of two faces of  $t$  with the vertex in its interior, as shown in Figure 12.*
2. *Form a tubular neighbourhood of  $K$  by inserting a defect plane as in Figure 2 (b) into each tetrahedron of  $T'$  that contains an edge in  $K$  and a defect plane as in Figure 2 (a) into each tetrahedron of  $T'$  that contains a vertex, but not an edge of  $K$ , as shown in Figure 12.*
3. *Label the region of  $T'$  that does not contain  $K$  with  $\mathcal{C} = \text{Vec}_G$  for a finite group  $G$  and the region containing  $K$  with the spherical fusion category  $\mathcal{D} = \text{Vec}_{\{1\}} = \text{Vect}_{\mathbb{C}}$ . Label the defect surface with the  $(\mathcal{C}, \mathcal{D})$ -bimodule category  $\mathcal{M}$  defined by the trivial  $G$ -set  $X = \{\bullet\}$ .*



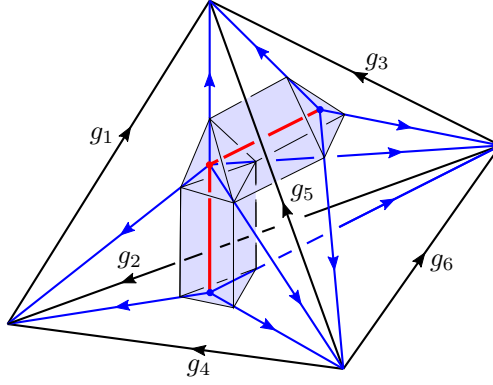


Figure 12: A piece of a knot (red) in the dual complex of a triangulation and the associated defect surface. The state sum vanishes unless  $g_3 = g_1g_2$  and  $g_5 = g_1g_4$ .

Then the state sum of  $M$  is the number of conjugacy classes of group homomorphisms from the fundamental group  $\pi_1(S^3 \setminus K)$  into  $G$

$$\mathcal{Z}(M) = |\text{Hom}_{\text{Grp}}(\pi_1(S^3 \setminus K), G)/G|.$$

*Proof.* Denote by  $r_{\mathcal{C}}$  the region labeled by  $\mathcal{C} = \text{Vec}_G$ . By subdividing the triangulation as in Lemma 5.7, we can assume that each vertex, edge or triangle in  $T'$  that contained in  $r_{\mathcal{C}}$  is part of a tetrahedron contained in  $r_{\mathcal{C}}$ . This does not change the state sum by Theorem 5.16. The union of the tetrahedra in  $r_{\mathcal{C}}$  is then PL homeomorphic to the knot complement  $S^3 \setminus K'$ , where  $K'$  is a solid torus  $S^1 \times D^2$  embedded as a tubular neighbourhood of  $K$ . This defines a triangulation  $T''$  of  $S^3 \setminus K'$  labeled by  $\text{Vec}_G$ .

The remaining tetrahedra are as in Figure 12. By construction, all red edges in Figure 12 are labeled with the simple object  $\mathbb{C}$  of  $\text{Vect}_{\mathcal{C}}$ , all blue edges by the simple object  $\bullet$  in  $\mathcal{M}$ , while the black edges are labeled with elements of  $G$ . Each triangle  $\Delta$  with  $\Delta \cap t \neq \emptyset$  has two edges labeled by  $\bullet$ , one edge labeled by a group element  $g \in G$  and is assigned the morphism space  $\text{Hom}(\bullet, \bullet) \cong \mathbb{C}$  for any  $g \in G$ . The triangles  $\Delta$  in Figure 12 with  $\Delta \cap D = \emptyset$  are part of tetrahedra contained in  $r_{\mathcal{C}}$ . Their labeling is determined by the labeling of  $T''$ , and their morphism spaces are  $\text{Hom}(\Delta) \cong \mathbb{C}$  if the oriented product of the group elements on their edges is trivial and  $\text{Hom}(\Delta) \cong \{0\}$  else.

Let  $l : E'' \rightarrow G$  be a labeling of the oriented edges of  $T''$  with elements of  $G$ . As each triangle in  $T'$  occurs in exactly two tetrahedra and all morphism spaces are zero- or one-dimensional, the product of all generalised 6j symbols in  $T'$  is one if the oriented product of the group elements on each triangle  $\Delta$  in  $T''$  vanishes and zero else. It follows that the state sum is proportional to the number of labelings  $l$  that satisfy this condition

$$\mathcal{Z}(M) = \frac{|\{l : E'' \rightarrow G \mid \prod_{e \in \Delta} l(e) = 1 \ \forall \Delta \in \Delta''\}|}{|G|^{|V''|}}, \quad (103)$$

where  $V''$ ,  $E''$  and  $\Delta''$  are the sets of vertices, edges and triangles of  $T''$ .

Every such labeling  $l$  defines a group homomorphism  $\rho_l : \pi_1(S^3 \setminus K) \rightarrow G$ , and every group homomorphism  $\rho : \pi_1(S^3 \setminus K) \rightarrow G$  is obtained from such a labeling. The group homomorphisms  $\rho_l, \rho_{l'}$  for two labelings  $l, l' : E'' \rightarrow G$  are conjugate iff there is a map  $f : V'' \rightarrow G$ ,  $v \mapsto g_v$  such that  $l'(e) = g_{t(e)} \cdot l(e) \cdot g_{s(e)}$  for all  $e \in E''$ , where  $s(e)$  and  $t(e)$  denote the starting and target vertex of  $e$ . This shows that  $\mathcal{Z}(M)$  is the number of conjugacy classes of group homomorphisms  $\rho : \pi_1(S^3 \setminus K) \rightarrow G$ .  $\square$

Although the data in Example 6.4 is quite trivial, it shows that the state sum with defects can distinguish non-isotopic embeddings of surfaces. It would be interesting to investigate this further and to see if it can distinguish knotted embeddings of spheres.

## 6.2 Ribbon invariants from line defects

In this section we show how defect lines on trivial defect surfaces give rise to ribbon invariants. These surfaces are labeled by a spherical fusion category  $\mathcal{C}$  as a  $(\mathcal{C}, \mathcal{C})$ -bimodule category. As  $\mathcal{C}$  is a spherical fusion category, its center  $\mathcal{Z}(\mathcal{C})$  is a ribbon category, see for instance [TV10, Lemma 10.1]. By Example 1.10, the monoidal category  $\text{End}_{\mathcal{C}}(\mathcal{C})$  is canonically monoidally equivalent to  $\mathcal{Z}(\mathcal{C})$ . Under this monoidal equivalence, an object  $(a, \sigma_{-,a})$  of  $\mathcal{Z}(\mathcal{C})$  corresponds to the  $(\mathcal{C}, \mathcal{C})$ -bimodule functor  $F = a \otimes - : \mathcal{C} \rightarrow \mathcal{C}$  with coherence data

$$\begin{aligned} s_{c,c'}^F &= a_{c,a,c'} \circ (\sigma_{c,a}^{-1} \otimes 1_{c'}) \circ a_{a,c,c'}^{-1} : a \otimes (c \otimes c') \rightarrow (a \otimes c) \otimes c' \rightarrow (c \otimes a) \otimes c' \rightarrow c \otimes (a \otimes c'), \\ t_{c,c'}^F &= a_{a,c,c'} : (a \otimes c) \otimes c' \rightarrow a \otimes (c \otimes c') \end{aligned} \quad (104)$$

and a morphism  $\alpha : a \rightarrow b$  in  $\mathcal{Z}(\mathcal{C})$  to the  $(\mathcal{C}, \mathcal{C})$ -bimodule natural transformation  $\nu = \alpha \otimes - : a \otimes - \Rightarrow b \otimes -$  from Example 1.10.

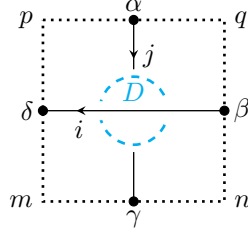
Any diagram representing a ribbon tangle for  $\mathcal{Z}(\mathcal{C})$  can be realised as a defect graph on a trivial defect disc. This amounts to replacing over- and undercrossings in the diagram with defect vertices labeled by (inverse) braidings and maxima and minima by defect vertices labeled with the (co)evaluations in  $\mathcal{Z}(\mathcal{C})$ . Every diagram  $D$  for a  $(0, 0)$ -ribbon tangle then defines a morphism  $\alpha \in \text{End}_{\mathcal{Z}(\mathcal{C})}(e)$  and a bimodule natural transformation  $\nu = \alpha \otimes - : \text{id}_{\mathcal{C}} \Rightarrow \text{id}_{\mathcal{C}}$  with  $\nu_x = \text{tr}(\alpha)1_x = \text{ev}(D)1_x : x \rightarrow x$  for every  $x \in I_{\mathcal{C}}$ .

**Example 6.5.** Let  $\mathcal{C}$  be a spherical fusion category and  $t$  a tetrahedron as in Figure 2 (b) with a trivial defect surface that contains a diagram  $D$  for a  $(0, 0)$ -ribbon tangle labeled with  $\mathcal{Z}(\mathcal{C})$ . Then one has

$$\mathcal{Z}'(t) = \text{ev}(D) \cdot 6j(t'),$$

where  $t'$  is the tetrahedron with the same labels and without the defects and  $\text{ev}(D) \in \mathbb{C}$  the evaluation of  $D$ .

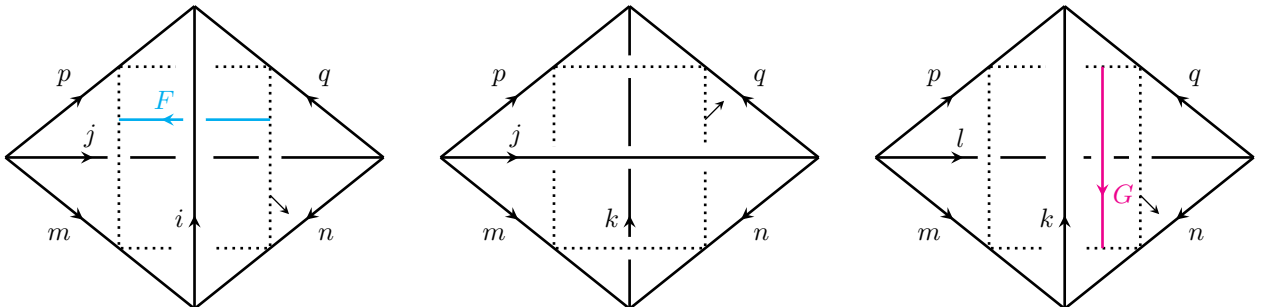
*Proof.* The  $6j$  symbol of the defect tetrahedron  $t$  is obtained from the associated polygon diagram



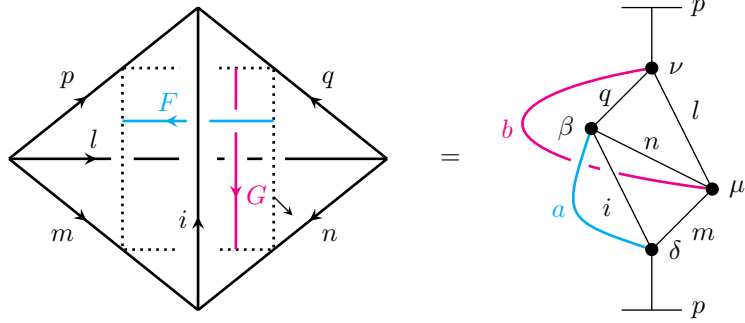
where the dashed circle labeled  $D$  contains the diagram  $D$ . This diagram superimposes the  $6j$  symbol for  $t'$  and the diagram  $D$ . By (104), overcrossings of the line labeled  $i$  over lines in  $D$  correspond to half-braidings  $\sigma_{i,a}^{\pm 1}$ , while overcrossings of lines in  $D$  over  $j$  correspond to associators in  $\mathcal{C}$ . The line labeled  $i$  describes the functor  $i \otimes - : \mathcal{C} \rightarrow \mathcal{C}$  and the line labeled  $j$  the functor  $- \otimes j : \mathcal{C} \rightarrow \mathcal{C}$ . Identities (39) to (43) allow one to separate the two diagrams and yield the result.  $\square$

Example 6.5 shows that ribbon invariants can be realised as line and point defects on a trivial defect plane. However, this involves ribbon diagrams rather than ribbons in three-dimensional space, and the braidings are external input, namely defect data labeling vertices. We now show how ribbon invariants are obtained from line defects in a 3-ball that are not confined to a plane and where the braidings arise from the state sum.

**Example 6.6.** Let  $\mathcal{C}$  be spherical fusion category as a  $(\mathcal{C}, \mathcal{C})$ -bimodule category and  $F = a \otimes - : \mathcal{C} \rightarrow \mathcal{C}$  and  $G = b \otimes - : \mathcal{C} \rightarrow \mathcal{C}$  the bimodule functors for  $(a, \sigma_{-,a}), (b, \sigma_{-,b}) \in \text{Ob}\mathcal{Z}(\mathcal{C})$  with coherence data as in (104). We consider the following three tetrahedra labeled with objects in  $I_{\mathcal{C}}$ :

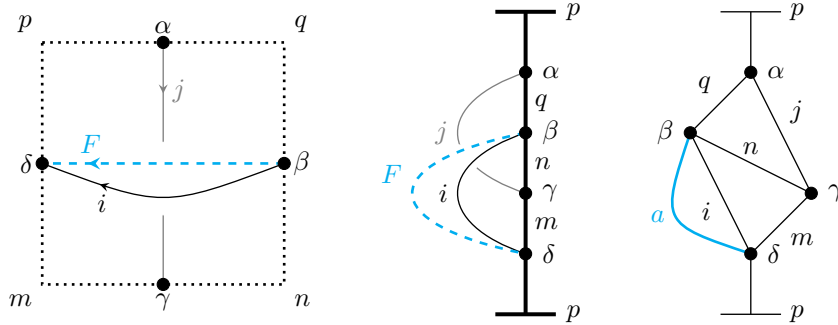


Glue the first tetrahedron to the second along the two faces labeled with  $j, m, n$  and  $j, p, q$  and the second to the third along the two faces labeled with  $k, m, p$  and  $k, n, q$ . This yields a triangulated 3-ball  $M$  with a one-holed torus as a trivial defect surface. Then the rescaled state sum  $Z'(M)$  is the  $6j$  symbol of the tetrahedron



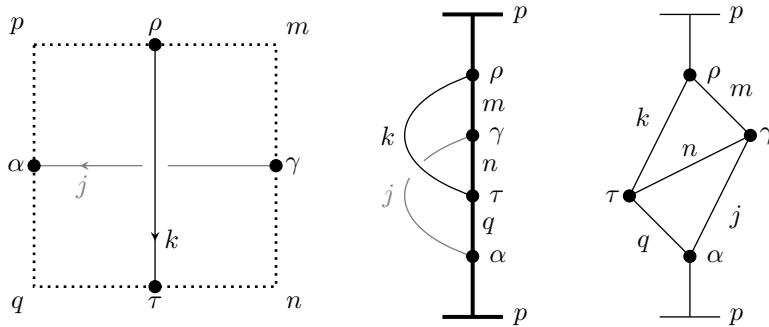
where the crossing of the lines labeled  $F$  and  $G$  on the defect surface is assigned the  $(\mathcal{C}, \mathcal{C})$ -bimodule natural transformation  $\nu = \sigma_{a,b}^{-1} \otimes - : (b \otimes a) \triangleright - \Rightarrow (a \otimes b) \triangleright -$ .

*Proof.* The polygon diagram and the associated  $6j$  symbols for the first tetrahedron are given by



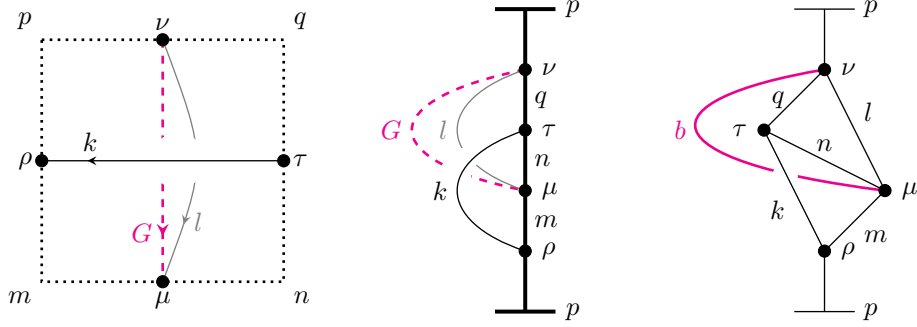
where the first diagram for the  $6j$  symbol is in the diagrammatic notation of the previous sections and the second the usual diagram for a spherical fusion category as in [TV92, BW96], with the objects from  $\mathcal{Z}(\mathcal{C})$  highlighted in colour. It is obtained from the second diagram by inserting the functor  $- \otimes j : \mathcal{C} \rightarrow \mathcal{C}$  for the line labeled  $j$  and the functor  $F(i \otimes -) = a \otimes (i \otimes -) : \mathcal{C} \rightarrow \mathcal{C}$  for the lines with  $F$  and  $i$ .

The polygon diagram and  $6j$  symbols for the second tetrahedron are given by



Note that here the polygon diagram is viewed from the back, not the front, since the trivial defect plane is oriented in the opposite direction. Again, the second diagram for the  $6j$  symbol is the standard diagram for a spherical fusion category obtained by inserting the functors  $k \otimes - : \mathcal{C} \rightarrow \mathcal{C}$  and  $- \otimes j : \mathcal{C} \rightarrow \mathcal{C}$  for the black line labeled  $k$  and the grey line labeled  $j$  in the second diagram.

The polygon diagram and the 6j symbols for the third tetrahedron are given by



Here, the second 6j symbol is obtained from the first by inserting the functor  $k \otimes - : \mathcal{C} \rightarrow \mathcal{C}$  for the black line labeled  $k$  and the functor  $G(- \otimes l) = b \otimes (- \otimes l) : \mathcal{C} \rightarrow \mathcal{C}$  for the lines labeled  $G$  and  $l$ . The crossing in the second 6j symbol stands for the morphism  $\sigma_{k,b}^{-1} : b \otimes k \rightarrow k \otimes b$  associated with  $b$ .

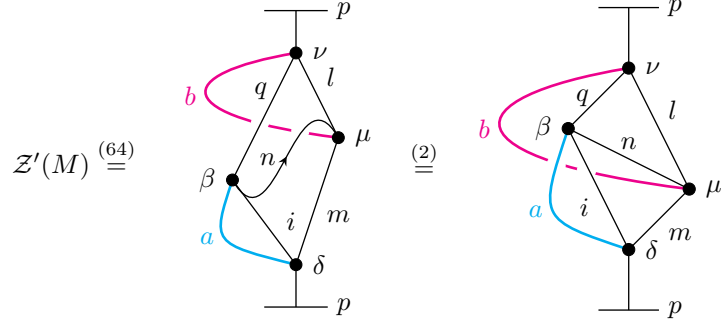
The rescaled state sum is obtained by multiplying the three 6j symbols and the dimensions of the internal edges, summing over the labels  $j, k \in I_{\mathcal{C}}$  and over the morphisms  $\alpha, \gamma, \rho, \tau$  assigned to the glued faces

$$\mathcal{Z}'(M) = \sum_{\alpha, \gamma, \rho, \tau} \sum_{j, k} \dim(j) \dim(k)$$

To compute this state sum we first use (66) to glue the polygon diagrams along the faces labeled by the objects  $k, m, p$  and  $q, j, p$  and the morphisms  $\rho$  and  $\alpha$ . We then simplify the resulting expressions with (64) and apply (2) together with the naturality of the half-braiding. This gives

$$\mathcal{Z}'(M) \stackrel{(66)}{=} \sum_{\gamma, \tau} \sum_{j, k} \frac{\dim(j)}{\dim(k)} \text{ (diagram)} \stackrel{(64)}{=} \sum_{k, \tau} \dim(k) \text{ (diagram)} \stackrel{(2)}{=} \sum_{k, \tau} \dim(k) \text{ (diagram)}$$

Applying again identities (64) and (2) together with the naturality of the half-braiding yields

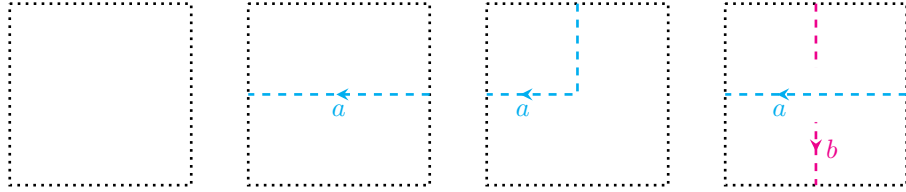


□

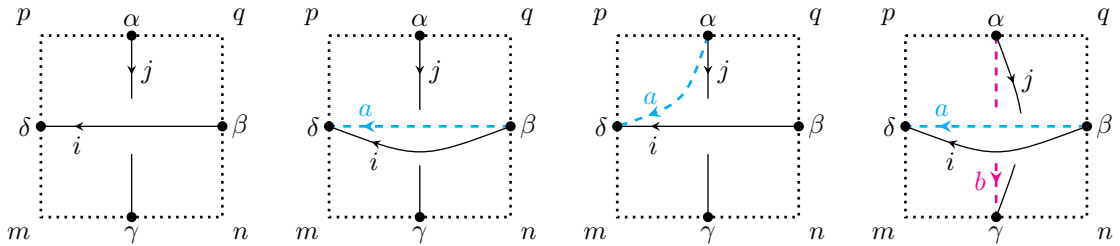
Example 6.6 allows one to construct any ribbon link invariant for the centre  $\mathcal{Z}(\mathcal{C})$  of a spherical fusion category  $\mathcal{C}$  from state sums that involve only defect surfaces and defect lines. This is achieved by considering a ribbon diagram and realising each crossing as in Example 6.6.

**Example 6.7.** Let  $\mathcal{C}$  be a spherical fusion category with center  $\mathcal{Z}(\mathcal{C})$  and  $L$  a ribbon link whose connected components are labeled by objects of  $\mathcal{Z}(\mathcal{C})$ . Let  $M$  be the following triangulated 3-manifold with defect data:

1. Realise a ribbon diagram  $D_L$  for  $L$  as a PL diagram that is the horizontal and vertical composite of the following squares and the ones obtained by rotating them, reversing orientation in the third square and replacing an over- by an undercrossing in the last square



2. Assign to a dashed line with label  $(a, \sigma_{-,a})$  in  $\mathcal{Z}(\mathcal{C})$  the  $(\mathcal{C}, \mathcal{C})$ -bimodule functor  $F_a = a \otimes - : \mathcal{C} \rightarrow \mathcal{C}$  with coherence data as in (104), to a crossing with labels  $a, b$  the bimodule natural transformation given by  $\sigma_{a,b}^{\pm 1}$ , as in Example 6.6, and to the midpoint of the second and third diagram either the identity or the (co)units of the adjunction  $F_a^l \dashv F_a$ .
3. Draw solid vertical and horizontal lines in each square that connect the midpoints of the boundary edges and end to the left of the dashed lines, viewed in the direction of their orientation. Let the vertical line cross under and the horizontal line over all other lines of the diagram.
4. Label each vertex of the square and each solid line by a simple object of  $\mathcal{C}$ , such that the labels match at the vertices and edges where the squares are glued to form the diagram  $D_L$ . Label each endpoint of lines at the boundary by a morphism in the appropriate morphism space in  $\mathcal{C}$



5. Assign to each square in 4. a defect tetrahedron for the  $(\mathcal{C}, \mathcal{C})$ -bimodule category  $\mathcal{C}$  whose 6j symbol is the polygon diagram in 4. , as in Figure 13. Construct the last defect tetrahedron in Figure 13 as in Example 6.6 by gluing three tetrahedra with defect planes without crossings.

6. The polygon diagrams glue to a diagram that superimposes  $D_L$  with additional edges labeled by objects of  $\mathcal{C}$ , whose endpoints are labeled by morphisms in  $\mathcal{C}$ . This defines a gluing pattern for the associated tetrahedra, as in Figure 14, that yields a triangulated 3-ball  $M$  with a ribbon link  $L'$  in the interior.

The state sum of  $M$  is

$$\mathcal{Z}(M, l_{\partial M}, b) = \text{ev}(D_L) \cdot \mathcal{Z}(M', l_{\partial M}, b),$$

where  $\mathcal{Z}(M', l_{\partial M}, b)$  is the the state sum of the 3-ball  $M'$  with the same labels, but without defects.

*Proof.* As the dimension factors for boundary edges and vertices coincide for  $M$  and  $M'$ , it is sufficient to consider the rescaled state sums. By Proposition 5.11 and Example 6.6, the rescaled state sum for  $M$  is the evaluation of the polygon diagram obtained by gluing all defect squares. This is the ribbon diagram  $D_L$ , superimposed with a graph labeled by  $\mathcal{C}$ , which is the dual of the triangulation on  $\partial M$ .

The evaluation of this polygon diagram is computed as in Example 6.5. By (104) overcrossings of solid lines over lines in  $T$  correspond to half-braidings of objects of  $\mathcal{Z}(\mathcal{C})$  with objects in  $\mathcal{C}$ , while undercrossings correspond to associators in  $\mathcal{C}$ . As all vertices involve only solid lines, one can use identities (39) to (43) to separate the graph labeled by  $\mathcal{C}$  and the diagram  $D_L$ . This yields the product of the rescaled state sum  $\mathcal{Z}'(M', l_{\partial M}, b)$  and the evaluation of  $D_L$ .  $\square$

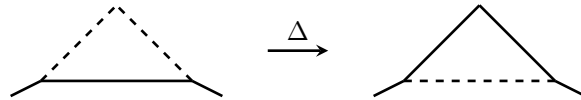
Example 6.7 constructs a specific example of a triangulated 3-ball with a ribbon link as a defect. An analogous factorisation of the state sum is obtained for any ribbon link labeled by  $\mathcal{Z}(\mathcal{C})$  in any triangulated 3-ball labeled by  $\mathcal{C}$ . This follows from the triangulation independence of the state sum and the fact that it is invariant under  $\Delta$ -moves, which encode ambient isotopies of ribbon links.

**Proposition 6.8.** *Let  $M$  be a triangulated 3-ball labeled by a spherical fusion category  $\mathcal{C}$ . Let  $L$  be a ribbon link in the interior of  $M$  that is blackboard-framed with respect to a disc bisecting  $M$  and labeled by  $\mathcal{Z}(\mathcal{C})$ . Then the state sum is given by*

$$\mathcal{Z}(M, l_{\partial M}, b) = \mathcal{Z}(M', l_{\partial M}, b) \cdot \text{ev}(D_L),$$

where  $\mathcal{Z}(M', l_{\partial M}, b)$  is the state sum of the 3-ball  $M'$  with the same labels, but without the link, and  $D_L$  a ribbon diagram obtained by projecting  $L$  on the disc.

*Proof.* 1. We first show that the state sum is invariant under PL ambient isotopy of the ribbon link. By a result of Graeb [G], see also Burde and Zieschang [BZ, Prop. 1.10] and Yetter [Y, Sec. 2.2], two PL links in a 3-ball are ambient isotopic iff they are related by a finite sequence of  $\Delta$ -moves. A  $\Delta$ -move places a triangle on the link that intersects it only in one side and replaces this side by the other two sides of the triangle.



An analogous result holds for ambient isotopies of blackboard-framed ribbon links if one restricts attention to  $\Delta$ -moves that respect the framing, that is, keep the links blackboard framed and can be realised without introducing kinks, see for instance [Y, Sec. 2.2]. Thus it is sufficient to show that the state sum is invariant under  $\Delta$ -moves that respect the blackboard framing of  $L$ .

Consider a blackboard framed  $\Delta$ -move with a triangle  $\Delta$ . By Corollary 5.13 and Lemma 5.7, suppose without loss of generality that the tetrahedra intersecting  $\Delta$  form a fine neighbourhood of  $\Delta$  and that gluing all tetrahedra that intersect  $\Delta$  yields a triangulated 3-ball  $B$  bisected by a defect plane that extends  $\Delta$ .

By Proposition 5.11 the state sums for  $B$  before and after the  $\Delta$ -move are obtained by projecting the dual of its boundary triangulation on the defect plane and evaluating the resulting polygon diagram. This yields ribbon diagrams that superimpose a ribbon segment labeled by  $\mathcal{Z}(\mathcal{C})$  with the boundary diagrams labeled by  $\mathcal{C}$ . The polygon diagrams before and after the  $\Delta$ -move are related by a  $\Delta$ -move on the ribbon segment in the polygon. Identities (39) to (42) imply that the evaluations of these polygon diagram are equal. As  $M \setminus B$  is not affected by the  $\Delta$ -move, the state sum of  $M$  is invariant under the  $\Delta$ -move by Corollary 4.10.

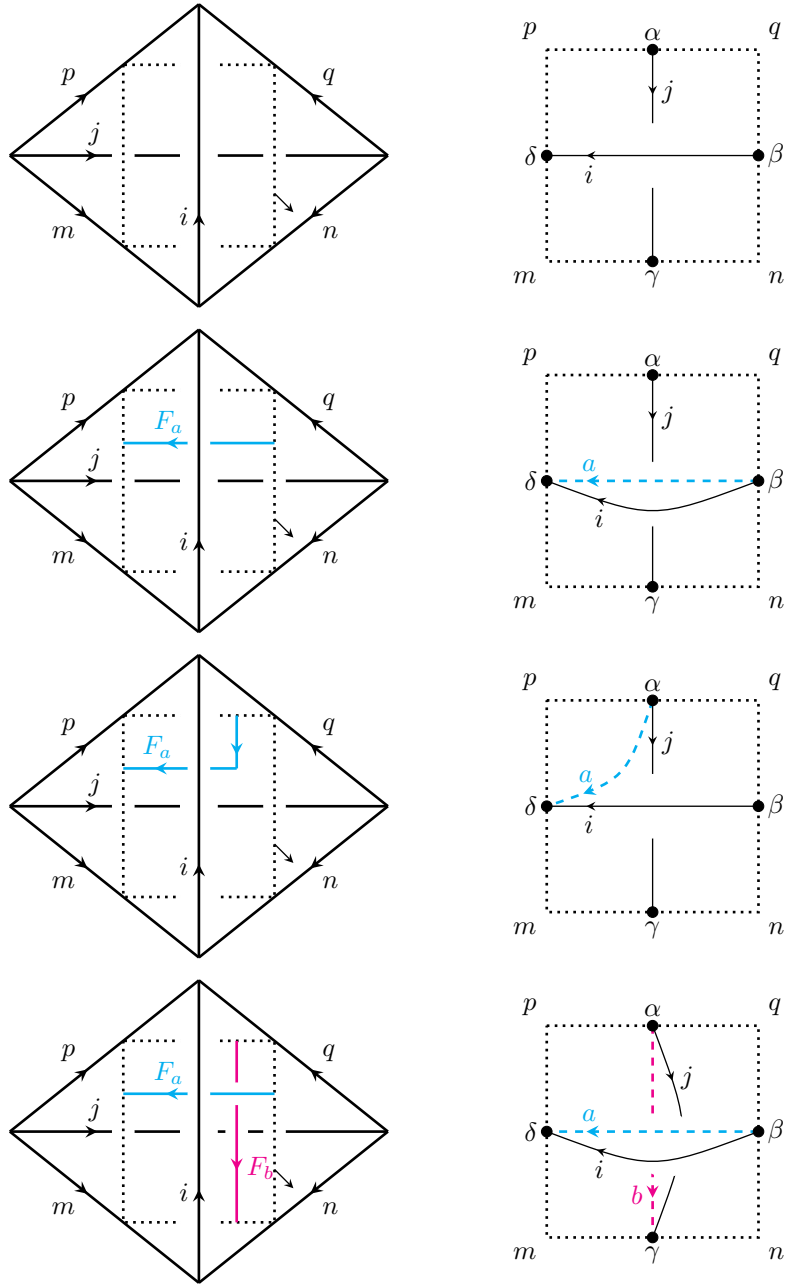


Figure 13: Defect tetrahedra assigned to the square diagrams from Example 6.7. The last tetrahedron is obtained by gluing three tetrahedra without crossings as in Example 6.6.

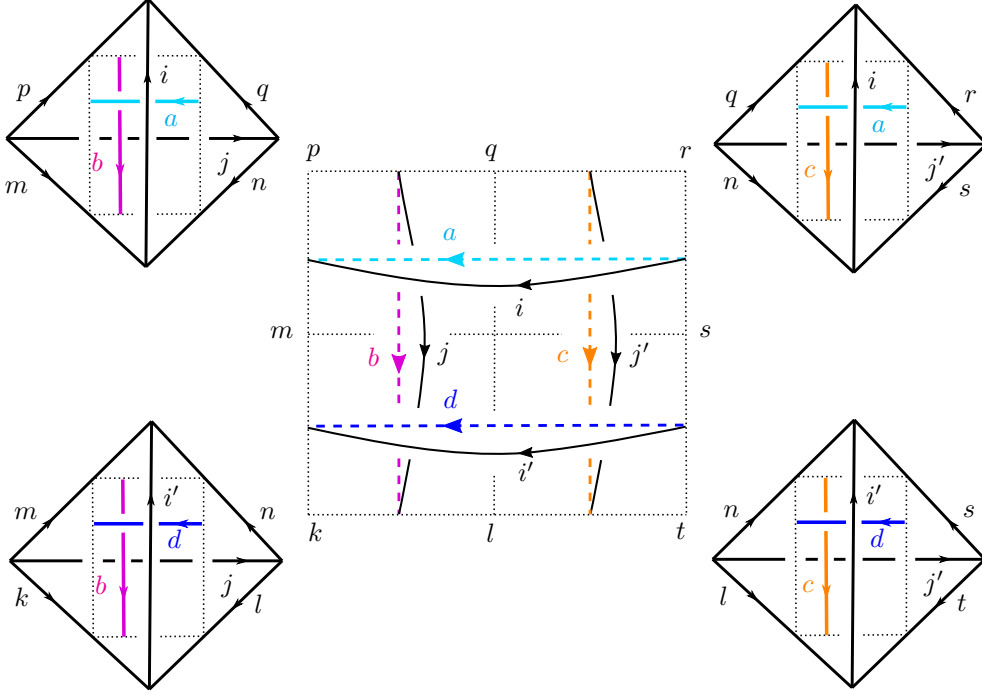


Figure 14: Gluing four defect tetrahedra and the associated polygon diagram.

2. By applying 2d isotopies to the ribbon diagram  $D_L$ , one can transform it into a diagram  $D'$  as in Example 6.7 and construct a triangulated 3-ball  $N$  with a ribbon link  $L'$  in the interior that projects to  $D' = D_{L'}$ . By Example 6.7 one has  $\mathcal{Z}(N, l_{\partial N}, b) = \mathcal{Z}(N', l_{\partial N}, b) \cdot \text{ev}(D_{L'})$ , where  $N'$  is the 3-ball without  $L'$ .

As the boundary triangulations of  $M$  and  $N$  are related by elementary shellings and inverse shellings with tetrahedra that do not intersect  $L$  and  $L'$ , it is sufficient to show that  $\mathcal{Z}(M, l_{\partial N}, b) = \mathcal{Z}(N, l_{\partial N}, b)$ , if the labeled boundary triangulations for  $M$  and  $N$  agree. As the link diagrams  $D_L$  and  $D_{L'}$  are isotopic, one has  $\text{ev}(D_L) = \text{ev}(D_{L'})$  and the links  $L$  and  $L'$  that project to  $D_L$  and  $D_{L'}$  are ambient isotopic. This allows one to transform  $L$  into  $L'$  by a finite sequence of  $\Delta$ -moves. The first part of the proof implies that this does not affect the state sum. By the triangulation independence of the usual Turaev-Viro-Barrett-Westbury state sum, one has  $\mathcal{Z}(M', l_{\partial M}, b) = \mathcal{Z}(N', l_{\partial N}, b)$ , and with Theorem 5.16 this yields

$$\mathcal{Z}(M, l_{\partial N}, b) \stackrel{1}{=} \mathcal{Z}(N, l_{\partial N}, b) \stackrel{6,7}{=} \text{ev}(D_{L'}) \cdot \mathcal{Z}(N', l_{\partial N}, b) \stackrel{5,16}{=} \text{ev}(D_L) \cdot \mathcal{Z}(M', l_{\partial N}, b).$$

□

Proposition 6.8 can be generalised to ribbon tangles realised as defect graphs on trivial defect surfaces. One can also generalise it to ribbon links embedded in more general 3-manifolds. Embedding a ribbon link  $L$  labeled by  $\mathcal{Z}(\mathcal{C})$  in a single tetrahedron labeled by  $\mathcal{C}$  and gluing it to the tetrahedron with the opposite orientation along all four faces yields the state sum for a 3-sphere  $L$  in the interior

$$\mathcal{Z}(S^3, L) = \frac{\text{ev}(D_L)}{\dim \mathcal{C}}.$$

This coincides with Turaev and Virelizier's state sum graph TQFT for a 3-sphere containing a ribbon link in [TV17, Th. 16.1]. In fact, we expect that our state sums with defect lines and vertices on trivial defect surfaces always coincide with the corresponding graph TQFTs with ribbons from [TV17, Ch. 16] and [TV10]. It would be nice to show this in full generality and to compare with the results by Balsam and Kirillov in [KB10, B10] that also involve ribbons labeled by  $\mathcal{Z}(\mathcal{C})$ .

We also expect that our state sum is related to the modular functor constructed from bimodule categories over finite tensor categories by Fuchs et al. [FSS19] if one restricts the latter to our categorical data. However, it is not clear to us how our construction is related to the work [LY20] by Lee and Yetter, which also constructs



triangulation independent state sums with defect surfaces. However, the defect surfaces in [LY20] are labeled with different categorical data, namely bicategories equipped with spherical duals and certain 2-functors. They should be thought of as defects with additional structure, according to the authors. We believe that this is a different type of defect that cannot be related directly to our construction.

The examples in this section show that the state sum models with defects give relevant information about defect surfaces and are easy to compute for simple categorical data. It would be feasible to investigate further examples that involve defect lines and points on non-trivial defect surfaces, at least for spherical fusion categories  $\mathcal{C} = \text{Vec}_G$  and  $\mathcal{D} = \text{Vec}_{G'}$  and bimodule categories defined by finite transitive  $G \times G'^{\text{op}}$ -sets. In this case, the categorical defect data for defect lines and defect points can be worked out explicitly to describe defects of all codimensions for Dijkgraaf-Witten theory [DW90]. It would also be interesting to investigate knotted defect surfaces beyond the torus and with less trivial categorical data.

With the results by Balsam and Kirillov [BK12, Kr11] on the relation between Turaev-Viro-Barrett-Westbury state sums, Levin-Wen models [LW05] and Kitaev's quantum double models [Ki03], it should also be possible to apply our state sums with defects to those models and to make contact with the work [KK12] by Kitaev and Kong. In the long run it would be desirable to determine if our state sum model with defects defines a defect TQFT in the sense of the works [CMS20, CRS19] by Carqueville et al. and to relate it to the works [CRS18, KMRS21] by Carqueville et al. and by Koppen et al. on defects and domain walls in the context of Reshetikhin-Turaev TQFTs. We leave these questions for future work.

## Acknowledgements

This article originated from discussions with John W. Barrett. We had originally planned to work on this project together, but this became impossible due to the Covid-19 pandemic and its impact on research and teaching. I am extremely grateful to him for helpful discussions, encouragement and comments on drafts of this article. I am also grateful to Gregor Schaumann for remarks and discussions on bimodule categories and bimodule traces and to Andreas Knauf for discussions and comments on drafts of this article.

## References

- [AC93] Daniel Altschuler and Antoine Coste. Invariants of three-manifolds from finite group cohomology. *Journal of Geometry and Physics*, 11(1):191–203, 1993.
- [B10] Balsam, B. (2010). Turaev-Viro invariants as an extended TQFT III. arXiv preprint arXiv:1012.0560.
- [BK12] Balsam, B., & Kirillov Jr, A. (2012). Kitaev's lattice model and Turaev-Viro TQFTs. arXiv preprint arXiv:1206.2308.
- [BMG07] Barrett, J. W., Faria Martins, J., & García-Islas, J. M. (2007). Observables in the Turaev-Viro and Crane-Yetter models. *Journal of Mathematical Physics*, 48(9), 093508.
- [BMS12] Barrett, J. W., Meusburger, C., & Schaumann, G. (2012). Gray categories with duals and their diagrams. arXiv preprint arXiv:1211.0529.
- [BW96] Barrett, J., & Westbury, B. (1996). Invariants of piecewise-linear 3-manifolds. *Transactions of the American Mathematical Society*, 348(10), 3997-4022.
- [BZ] Burde, G., & Zieschang, H. (2008, August). Knots. In *Knots*. de Gruyter.
- [CMS20] Carqueville, N., Meusburger, C., & Schaumann, G. (2020). 3-dimensional defect TQFTs and their tricategories. *Advances in Mathematics*, 364, 107024.
- [CRS18] Carqueville, N., Runkel, I., & Schaumann, G. (2018). Line and surface defects in Reshetikhin-Turaev TQFT. *Quantum Topology*, 10(3), 399-439.
- [CRS19] Carqueville, N., Runkel, I., & Schaumann, G. (2019). Orbifolds of n-dimensional defect TQFTs. *Geometry & Topology*, 23(2), 781-864.
- [C95] Casali, M. R. (1995). A note about bistellar operations on PL-manifolds with boundary. *Geometriae Dedicata*, 56(3), 257-262.
- [DSS20] Douglas, C., Schommer-Pries, C., & Snyder, N. (2020). Dualizable tensor categories (Vol. 268, No. 1308). American Mathematical Society.

- [DW90] Dijkgraaf, R., & Witten, E. (1990). Topological gauge theories and group cohomology. *Communications in Mathematical Physics*, 129(2), 393-429.
- [EGNO] Etingof, P., Gelaki, S., Nikshych, D., & Ostrik, V. (2016). *Tensor categories* (Vol. 205). American Mathematical Soc.
- [ENO05] Etingof, P., Nikshych, D., & Ostrik, V. (2005). On fusion categories. *Annals of Mathematics*, 581-642.
- [E66] Epstein, D. B. (1966). Curves on 2-manifolds and isotopies. *Acta Mathematica*, 115, 83-107.
- [FSS19] Fuchs, J., Schaumann, G., & Schweigert, C. (2019). A modular functor from state sums for finite tensor categories and their bimodules. arXiv preprint arXiv:1911.06214.
- [G] Graeb, W. (1950). Die semilinearen Abbildungen. In *Die semilinearen Abbildungen* (pp. 3–70). Springer, Berlin, Heidelberg.
- [JS91] Joyal, A., & Street, R. (1991). The geometry of tensor calculus, I. *Advances in mathematics*, 88(1), 55-112.
- [KS93] Karowski, M., & Schrader, R. (1993). A combinatorial approach to topological quantum field theories and invariants of graphs. *Communications in mathematical physics*, 151(2), 355-402.
- [KB10] Kirillov Jr, A., & Balsam, B. (2010). Turaev-Viro invariants as an extended TQFT. arXiv preprint arXiv:1004.1533
- [Kr11] Kirillov Jr, A. (2011). String-net model of Turaev-Viro invariants. arXiv preprint arXiv:1106.6033.
- [Ki03] Kitaev, A. Y. (2003). Fault-tolerant quantum computation by anyons. *Annals of Physics*, 303(1), 2-30.
- [KK12] Kitaev, A., & Kong, L. (2012). Models for gapped boundaries and domain walls. *Communications in Mathematical Physics*, 313(2), 351-373.
- [KMRS21] Koppen, V., Mulevicius, V., Runkel, I., & Schweigert, C. (2021). Domain walls between 3d phases of Reshetikhin-Turaev TQFTs. arXiv preprint arXiv:2105.04613.
- [L] Lee, J. (2010). *Introduction to topological manifolds* (Vol. 202). Springer Science & Business Media.
- [LY20] Lee, I. J., & Yetter, D. N. (2020). Bicategories for TQFTs with Defects with Structure. arXiv preprint arXiv:2003.06538.
- [Li99] Lickorish, W. B. R. (1999). Simplicial moves on complexes and manifolds. *Geometry and Topology Monographs*, 2(299-320), 314.
- [LW05] Levin, M. A., & Wen, X. G. (2005). String-net condensation: A physical mechanism for topological phases. *Physical Review B*, 71(4), 045110.
- [N26] Newman, M. H. A. (1926). On the foundations of combinatorial analysis situs. In *Proc. Royal Acad. Amsterdam* (Vol. 29, pp. 610-641).
- [Mu03] Mueger, M. From subfactors to categories and topology. I: Frobenius algebras in and Morita equivalence of tensor categories. *J. Pure Appl. Algebra*, 180(1-2):81–157, 2003.
- [P91] Pachner, U. (1991). PL homeomorphic manifolds are equivalent by elementary shellings. *European journal of Combinatorics*, 12(2), 129-145.
- [P90] Pachner, U. (1990). Shellings of simplicial balls and pl manifolds with boundary. *Discrete mathematics*, 81(1), 37-47.
- [RS] Rourke, C. P., & Sanderson, B. J. (2012). *Introduction to piecewise-linear topology*. Springer Science & Business Media.
- [Sa57] Sanderson, D. E. (1957). Isotopy in 3-Manifolds I. Isotopic Deformations of 2-Cells and 3-Cells. *Proceedings of the American Mathematical Society*, 8(5), 912-922.
- [S13] Schaumann, G. (2013). Traces on module categories over fusion categories. *Journal of Algebra*, 379, 382-425.
- [S15] Schaumann, G. (2015). Pivotal tricategories and a categorification of inner-product modules. *Algebras and Representation Theory*, 18(6), 1407-1479.
- [ST] Birman, J. S., & Eisner, J. (1980). *Seifert and Threlfall, A Textbook of Topology*. Academic Press.
- [T] Turaev, V. G. (2020). *Quantum invariants of knots and 3-manifolds* (Vol. 18). Walter de Gruyter GmbH & Co KG.
- [TV10] Turaev, V., & Virelizier, A. (2010). On two approaches to 3-dimensional TQFTs. arXiv preprint arXiv:1006.3501.

- [TV17] Turaev, V., & Virelizier, A. (2017). *Monoidal categories and topological field theory* (Vol. 322, pp. xii+523). Basel: Birkhäuser.
- [TV92] Turaev, V. G., & Viro, O. Y. (1992). State sum invariants of 3-manifolds and quantum 6j-symbols. *Topology*, 31(4), 865-902.
- [Y] Yetter, D. N. (2001). *Functorial Knot Theory: Categories of Tangles, Coherence, Categorical Deformations and Topological Invariants* (Vol. 26). World Scientific.
- [Ze60] Zeeman, E. C. (1960). Unknotting spheres. *Annals of Mathematics*, 350-361.
- [Zi98] Ziegler, G. M. (1998). Shelling polyhedral 3-balls and 4-polytopes. *Discrete & Computational Geometry*, 19(2), 159-174.